

令和2年度博士学位論文

寒冷気候におけるコンクリート橋梁の耐久性の改善

**Improvement of Durability for Concrete Bridges in Cold  
Climate**

八戸工業大学大学院工学研究科

博士後期課程 社会基盤工学専攻

張

萌

**2021 Dissertation for Degree of Doctor in Engineering**

**Improvement of Durability for Concrete Bridges  
in Cold Climate**

**Hachinohe Institute of Technology**

**Graduate School of Engineering**

**Doctor of Science Program in Civil Engineering and Architecture**

**D18301      Zhang Meng**

**Supervisor: Professor Minoru Aba, Chair**

**Associate Professor Yuki Sakoi**

**Professor Yoichi Tsukinaga**

This thesis is dedicated to my beloved wife **Jianqing Cao**.

---

## ACKNOWLEDGEMENT

Time flies, three years will soon be over, and there is an indescribable feeling in my heart: nostalgia, gratitude, excitement and anticipation. I am deeply indebted to many individuals without whose help I never could have finished this formidable task.

First of all, I wish to express my profound gratitude to Prof. Minoru Aba, my thesis advisor, for his constant guidance, encouragement and patience throughout this whole process. Together, we went to the construction site to sample, to practice bridge construction, and to participate in my first JCI conference in Kobe, Japan. The many experiences with Prof. Aba in the past three years have made me familiar with this country, this city (Hachinohe City). In any case, I am very grateful to you Prof. Aba.

I would like to express my sincere gratitude to Professor Yoichi Tsukinaga. A fluent, mellow and full English, and sometimes speaking Chinese, giving people a cordial feeling. Encouraging eyes and a smile always give people strength. Every time I see you, I feel full of energy. Thank you for your help and care in the laboratory.

I would like to express my sincere gratitude to Associate Prof. Yuki Sakoi. In the past three years, I have communicated with you the most. Thank you for your generous donation and help. I have learned a lot of knowledge from you. I feel that every time I encounter difficulties, I can get the answer from you (omnipotent), and always give me guidance with great patience. Remember when I visited my family for the first time, it was also Tokyo where you accompanied me. The gratitude to you is beyond words, anyway, thank you.

I would like to express my sincere gratitude to Prof. Watanabe and Associate Prof. Yamamoto, thanks to the great help in Japanese learning, Japanese translation, cultural exchange, life and so on.

I would like to express my sincere gratitude to Prof. Hasegawa, although Prof. Hasegawa is so busy, but he has given me a lot of help and care in studies and life, Thank you, Prof. Hasegawa.

I would like to extent my appreciation to other professors and staff in the Department

---

for offering me help and advice and to my friends for your companion.

Thanks to Mr. Sasada, Mr. Ebina, Mr. Natusaka, Mr. Kimura, Mr. Nakamura, Miss Akasaka, etc.

Thanks to the graduate and undergraduate students: Sakamoto, Jutani, Yamazaki, Shimomukai, Takashima, Ito, Suzuki, etc.

Finally, thank you to my parents and wife for their love, support and sacrifice!

---

## CONTENTS

<b>CHAPTER 1 INTRODUCTION.....</b>	<b>- 1 -</b>
1.1 PROBLEM STATEMENT AND OBJECTIVE .....	- 1 -
1.2 SCOPE AND SIGNIFICANCES OF THIS STUDY .....	- 7 -
1.3 THESIS ORGANIZATION .....	- 8 -
1.4 REFERENCE .....	- 9 -
<b>CHAPTER 2 INVESTIGATION OF EXISTING SUBSTRUCTURES OF RC BRIDGES AND DEICING SALT SCALING RESISTANCE .....</b>	<b>- 10 -</b>
2.1 GENERAL .....	- 10 -
2.2 INTRODUCTION .....	- 10 -
2.3 DETAIL OF SURVEY AND EXPERIMENT.....	- 13 -
2.3.1 <i>Survey of existing RC structures</i> .....	- 13 -
2.3.2 <i>Experimental outline</i> .....	- 15 -
2.4 RESULTS AND DISCUSSIONS .....	- 17 -
2.4.1 <i>Evaluation of the effect of additional curing after demolding</i> .....	- 17 -
2.4.2 <i>Evaluation of effect of using permeability formwork</i> .....	- 19 -
2.4.3 <i>Influence of curing condition on surface quality in laboratory</i> .....	- 21 -
2.4.4 <i>Expectation of curing period based on deicing salt scaling resistance</i> .....	- 23 -
2.5 SUMMARY .....	- 24 -
2.6 REFERENCE .....	- 25 -
<b>CHAPTER 3 DURABILITY FOR RC SLAB OF BRIDGE.....</b>	<b>- 28 -</b>
3.1 GENERAL .....	- 28 -

---

3.2	INTRODUCTION .....	- 28 -
3.3	MATERIALS AND METHOD .....	- 29 -
3.3.1	<i>Deicing salt scaling resistance</i> .....	- 31 -
3.3.2	<i>Alkali-silica reaction</i> .....	- 31 -
3.3.3	<i>Drying shrinkage and mass loss</i> .....	- 33 -
3.3.4	<i>Uniaxial restrained and free shrinkage</i> .....	- 33 -
3.4	LABORATORY STUDY OF CONCRETE DURABILITY WITH DIFFERENT W/B RATIOS AND CEMENT TYPES - 33 -	
3.4.1	<i>Deicing salt scaling resistance</i> .....	- 33 -
3.4.2	<i>Alkali-silica reaction</i> .....	- 35 -
3.4.3	<i>Drying shrinkage and mass loss</i> .....	- 37 -
3.4.4	<i>Uniaxial restrained and free shrinkage</i> .....	- 40 -
3.5	FIELD STUDY OF CONCRETE DURABILITY .....	- 42 -
3.5.1	<i>Effect of construction execution process on deicing salt resistance of concrete</i> .....	- 42 -
3.5.2	<i>Restrained shrinkage of actual RC slab on construction site</i> .....	- 43 -
3.6	SUMMARY .....	- 46 -
3.7	REFERENCE .....	- 47 -
<b>CHAPTER 4 AIR VOID SYSTEM FOR RC SLAB OF BRIDGE .....</b>		<b>- 48 -</b>
4.1	GENERAL .....	- 48 -
4.2	INTRODUCTION .....	- 49 -
4.3	RC SLAB OF MOUNT AOBUNA No. 1 BRIDGE.....	- 51 -
4.3.1	<i>Materials and mix proportion</i> .....	- 51 -

---

4.3.2	<i>Method</i> .....	- 52 -
4.3.3	<i>Results and discussions</i> .....	- 54 -
4.4	RC SLAB OF SHINYANAGIBUCHI BRIDGE .....	- 61 -
4.4.1	<i>Materials and method</i> .....	- 61 -
4.4.2	<i>Results and discussions</i> .....	- 63 -
4.5	SUMMARY .....	- 69 -
4.6	REFERENCE .....	- 71 -
<b>CHAPTER 5 SHRINKAGE FOR RC SLAB OF BRIDGE USING SUPERABSORBENT POLYMERS (SAP) INTERNAL CURING</b> .....		<b>- 73 -</b>
5.1	GENERAL .....	- 73 -
5.2	INTRODUCTION .....	- 73 -
5.3	MATERIALS AND CURING CONDITIONS .....	- 77 -
5.3.1	<i>Materials</i> .....	- 77 -
5.3.2	<i>Curing conditions</i> .....	- 80 -
5.4	INTERNAL CURING MORTAR WITH SAP .....	- 80 -
5.4.1	<i>Mixture proportions and mixing procedure</i> .....	- 80 -
5.4.2	<i>Testing methods</i> .....	- 81 -
5.4.3	<i>Effect of individual and hybrid addition of SAP and KEA on the length and mass change</i> .....	- 83 -
5.4.4	<i>Pores distribution characteristics</i> .....	- 89 -
5.4.5	<i>Compressive strength</i> .....	- 91 -
5.4.6	<i>Effect of pore structure on the drying shrinkage, mass loss and the compressive strength</i> .....	- 92 -
5.5	INTERNAL CURING CONCRETE WITH SAP .....	- 95 -

---

5.5.1	<i>Mixture proportions</i> .....	- 95 -
5.5.2	<i>Testing methods</i> .....	- 96 -
5.5.3	<i>Influence of incorporation methods of SAP on internal curing effect</i> .....	- 97 -
5.5.4	<i>Effect of incorporation methods of SAP on length and mass change</i> .....	- 100 -
5.5.5	<i>Pores distribution characteristics</i> .....	- 101 -
5.5.6	<i>Effect of incorporation methods of SAP on compressive strength</i> .....	- 104 -
5.6	SUMMARY .....	- 105 -
5.7	REFERENCE .....	- 107 -
<b>CHAPTER 6 RECOMMENDATION OF FABRICATING DURABLE BRIDGES CONCRETE IN COLD CLIMATE</b> .....		<b>- 114 -</b>
<b>CHAPTER 7 CONCLUSIONS</b> .....		<b>- 121 -</b>
7.1	GENERAL .....	- 121 -
7.2	MAJOR CONCLUSIONS .....	- 121 -

---

## LIST OF FIGURES

Figure 1.1. Deteriorated RC bridge structures: a ASR, b Granulated concrete.....	- 1 -
Figure 1.2. Deteriorated RC bridge structures (Mainly frost damage).....	- 2 -
Figure 1.3. Distribution of deicing salt spread on roads and average temperature in winter.	- 4 -
Figure 1.4. Early-age shrinkage cracking of RC structures.....	- 5 -
Figure 1.5. Thesis road map. ....	- 6 -
Figure 2.1. Visual rating of the existing concrete structures surface micro cracks. ....	- 14 -
Figure 2.2. Test set-up for the deicing salt test and Torrent method.....	- 14 -
Figure 2.3. Effect of the additional curing on the surface air permeability of existing structures.....	- 17 -
Figure 2.4. Relationship between the surface air permeability coefficient and curing period. ....	- 19 -
Figure 2.5. Effect of the permeability formwork on the surface air permeability of structure. ....	- 20 -
Figure 2.6. Scaling amount after 60 cycles of freezing-thawing action.....	- 22 -
Figure 2.7. Relationship between curing period and the scaling amount after 60 cycles of freezing-thawing action. ....	- 24 -
Figure 3.1. Using SWW method to test ASR expansion in concrete. ....	- 30 -
Figure 3.2. Concrete drying shrinkage experiment. ....	- 31 -
Figure 3.3. Uniaxial restrained and free shrinkage.....	- 32 -

---

Figure 3.4. Restrained expansion and drying shrinkage.....	- 32 -
Figure 3.5. Cumulative scaled materials of concrete surface after 60 cycles of freeze-thaw cycles: (a) Ordinary Portland cement; (b) Fly ash cement; (c) Blast furnace slag cement. ....	- 34 -
Figure 3.6. Cumulative scaled materials of concrete surface after 60 cycles of freeze-thaw cycles: (a) W/B=0.35; (b) W/B=0.40; (c) W/B=0.45; W/B=0.50.....	- 35 -
Figure 3.7. Expansion of concrete with (a) Ordinary Portland cement, (b) Fly ash cement, and (c) Blast furnace slag cement at different W/B ratios. ....	- 36 -
Figure 3.8. Influence of cement types and W/B ratios on drying shrinkage of concrete. .-	37 -
Figure 3.9. Influence of cement types and W/B ratios on mass loss of concrete. ....	- 38 -
Figure 3.10. Relationship between mass loss and drying shrinkage. ....	- 39 -
Figure 3.11. Uniaxial restrained shrinkage of concrete. ....	- 40 -
Figure 3.12. Uniaxial free shrinkage of concrete. ....	- 40 -
Figure 3.13. Restrained expansion and drying shrinkage of concrete.....	- 41 -
Figure 3.14. Cumulative scaled materials of concrete surface after 60 cycles of freeze-thaw cycles: (a) mock slab; (b) actual slab. ....	- 43 -
Figure 3.15. Restrained shrinkage and temperature history of actual RC slab. ....	- 44 -
Figure 3 16. Cracks appear at the bottom surface of the RC slab (2019.08.06).....	- 45 -
Figure 4.1. Size of samples for observation of air void.....	- 52 -
Figure 4.2. RC mock slab specimen. ....	- 52 -
Figure 4.3. Distribution characteristics of air void. ....	- 55 -
Figure 4.4. Measurement of laboratory. ....	- 56 -

---

Figure 4.5. Distribution characteristics (mock slab).....	- 58 -
Figure 4.6. Measurement of mock slab. ....	- 58 -
Figure 4.7. Distribution characteristics (actual construction).....	- 59 -
Figure 4.8. Measurement of actual construction. ....	- 59 -
Figure 4.9. Air content of the diameter 0-500 $\mu$ m. Figure 4.10. Air content of the diameter 0-200 $\mu$ m.....	- 60 -
Figure 4.11. Void frequency of the diameter 0-500 $\mu$ m. Figure 4.12. Void frequency of the diameter 0-200 $\mu$ m.....	- 60 -
Figure 4.13. Polypropylene fiber.....	- 62 -
Figure 4.14. RC bridge slab: (a) Mock RC slab and (b) Actual RC slab. ....	- 63 -
Figure 4.15. Non-destructive testing on site (NDT): (a) Surface water absorption test (SWAT) and (b) Torrent method. ....	- 63 -
Figure 4.16. Scaling resistance of different dosages of the EA.....	- 64 -
Figure 4.17. Scaling resistance of the RC slab (Concrete specimens obtained from execution process).....	- 64 -
Figure 4.18. Distribution characteristics of air void (Concrete specimens obtained from execution process).....	- 65 -
Figure 4.19. Distribution of void frequency. (Concrete specimens obtained from execution process.) .....	- 65 -
Figure 4 20. Void frequency of the diameter 0-500 $\mu$ m. Figure 4 21. Void frequency of the diameter 0-200 $\mu$ m.....	- 68 -
Figure 5.1. Micro-cracks appear on RC bridge slab.....	- 76 -
Figure 5.2. SAP sample and sorption capacity of the SAP powder.....	- 79 -
Figure 5.3. Mixing procedure of mortar incorporated SAP.....	- 79 -

---

Figure 5.4. Specimen and hand-held strain comparator. ....	- 80 -
Figure 5.5. Effect of the individual addition of SAP on length and mass. ....	- 82 -
Figure 5.6. Effect of the hybrid addition of SAP and KEA on length and mass. ....	- 82 -
Figure 5.7. Relative shrinkage and relative mass loss under drying condition. (After 28 days.).....	- 85 -
Figure 5.8. Relationship between length and mass change under the drying condition (from day 7 to 91). ....	- 86 -
Figure 5.9. Pore distribution characteristics with individual addition of SAP. ....	- 88 -
Figure 5.10. Pore distribution characteristics with hybrid addition of SAP and KEA... -	- 89 -
Figure 5.11. Compressive strength with different SAP dosages and with/without KEA. -	- 92 -
Figure 5.12. The relationship among the SAP content, the drying shrinkage, the mass loss, and the pore volume<100 nm diameter. (a) Relationship between SAP content and pore volume<100 nm diameter. (b) Correlation between the drying shrinkage and pore volume<100 nm diameter. (c) Correlation between the mass loss and pore volume<100 nm diameter. (d) Pore volume distribution with 100 nm as boundary at 28 d. ....	- 94 -
Figure 5.13. The relationship between the compressive strength and the pore volume>50 nm diameter.....	- 95 -
Figure 5.14. Concrete specimens for measuring changes in length and mass.....	- 97 -
Figure 5.15. Distribution characteristics of SAP in hardened concrete.....	- 97 -
Figure 5.16. The phenomenon on the surface of hardened concrete. ....	- 98 -
Figure 5.17. Range of concrete affected by internal curing. ....	- 98 -
Figure 5.18. Estimate the residual internal curing volume.....	- 99 -
Figure 5.19. Effect of the incorporation methods of SAP on length and mass (KEA20). ....	- 100 -

---

Figure 5.20. Effect of the incorporation methods of SAP on length and mass (KEA30). ..... - 100 -

Figure 5.21. Effect of incorporation methods and contents of SAP on the pore distribution characteristics. (KEA20)..... - 102 -

Figure 5.22. Effect of incorporation methods and contents of SAP on the pore distribution characteristics. (KEA30)..... - 103 -

Figure 5.23. Compressive strength of concrete with different incorporation methods, SAP and KEA contents. .... - 104 -

Figure 6.1. Cumulative scaled materials of concrete surface after 60 cycles of freeze-thaw. - 119 -

Figure 6.2. Comparison of the size of the peeled scales of various samples after salt freezing damage. .... - 119 -

---

## LIST OF TABLES

Table 2.1. List of surveyed existing structures. ....	- 12 -
Table 2.2. Mix proportion of concrete (Unit content: kg/m <sup>3</sup> ). ....	- 15 -
Table 2.3. Experimental conditions. ....	- 15 -
Table 2.4. The surface air permeability coefficient ( $\times 10^{-16} \text{m}^2$ ). ....	- 20 -
Table 3.1. Mix proportions. ....	- 30 -
Table 3.2. Curing methods of concrete. ....	- 32 -
Table 4.1. Mix proportions of concrete. ....	- 51 -
Table 4.2. Parameters of air void in laboratory. ....	- 53 -
Table 4.3. Parameters of air void on site. ....	- 53 -
Table 4.4. Mix proportions of concrete. ....	- 62 -
Table 4.5. Parameters of air void on mock slab. ....	- 67 -
Table 4.6. Parameters of air void on actual slab. ....	- 67 -
Table 4.7. The results of the NDT test in-situ. ....	- 68 -
Table 5.1. Chemical compositions of blast furnace slag cement (BB) and expansion agent (KEA) (wt %). ....	- 78 -
Table 5.2. Physical properties of blast furnace slag cement (BB) and expansion agent (KEA). ....	- 78 -

---

Table 5.3. Mix proportions and slump flow after 15 jolts of mortar. Unit: kg/m<sup>3</sup>..... - 79 -

Table 5.4. Mix proportions, slump and air content of concrete..... - 96 -

---

## ABSTRACT

Concrete, because of its good plasticity, versatility, and low cost is widely used in the construction of all kinds of infrastructures such as roads, bridges, dams, and tunnels. However, the durability of concrete structures in cold climates has always been the focus of attention. In the cold region of Japan, many existing reinforced concrete (RC) structures currently are suffering from multiple deteriorations such as frost damage, the chloride ion attack, alkali-silica reaction (ASR), and granulated concrete due to severe environment and climates, which seriously restricted its service life and function.

As we all know, in cold regions, road and bridge deterioration is a common phenomenon main related to frost attack. Deicing salt is widely used to ensure the driving safety of vehicles in winter. When the average temperature less than  $-3^{\circ}\text{C}$  in winter and the deicing salt was sprayed approximately 20 t/km per year according to the report in the Tohoku region of Japan. For this reason, the Tohoku Regional development bureau has published the manual for the countermeasure to frost damage of concrete structures under spreading deicing salt. This manual was proposed to increase the target air content of fresh concrete on site. That is to cover the decreasing of air content while the execution process of construction and to attain air content in hardened concrete. In the case of concrete structures under the most severe environment on frost damage risk, the W/B less than 45% and the target air content of 6% were requested. However, study on the deicing salt scaling resistance and the distribution characteristics of air voids during the entire construction execution phase are not clear yet.

Furthermore, maintenance management for extending the service life of the existing RC structures becomes particularly critical in recent years. Nevertheless, the increase in maintenance management will inevitably lead to an increase in maintenance costs, which seriously restricts the development of the modern social economy. In the Tohoku region of Japan, over 40% of bridges will reach a service life of more than 50 years by 2025, which means a large number of bridges would have potential risks on its performance, according to the Ministry of Land. In other words, the great majority of existing RC bridge structures

---

are about to or have entered a large-scale rehabilitation and reconstruction period. Therefore, the fabrication of durable concrete is of great significance to green and sustainable development. This thesis focuses on improving the concrete durability for bridge structures in cold climate via the survey of surface air permeability of existing RC bridge substructures (Non-destructive testing, NDT), laboratory tests, tests of concrete frost resistance at various stages of the actual construction process, and a novel exploration of curing method. Around this subject, the main research contents and conclusions are as follows:

- (1) The influence of the initial curing on air permeability and the deicing salt scaling resistance of surface concrete were investigated. These results showed that concrete curing with sheet or permeability formwork was better than curing in air with increased of duration. Especially, utilizing the form of permeable sheet is greatly effective for the attainment of high surface quality and durable concrete. Simultaneously, focus on cold weather concreting, could evaluate the appropriate curing period including additional curing from combining with the surface air permeability and the deicing salt scaling resistance of concrete. It is also decided that the concrete has better deicing salt frost resistance, when the surface air permeability coefficient is less than  $1 \times 10^{-16} \text{ m}^2$ .
- (2) To obtain high-durability concrete suitable for cold climates, the deicing salt scaling resistance, alkali-silica reaction (ASR), restrained and free shrinkage, and the visual evaluation of RC bridge slab surface cracks were conducted in the laboratory and field. These results indicated that concrete with FB cement has a better deicing salt scaling resistance, however, it has little difference in terms of deicing salt scaling resistance regardless of cement types and W/B ratios, when the air content of fresh concrete reaches 6%. Concrete (especially for low W/B ratios) with BB cement has better resistance for ASR expansion, autogenous/drying shrinkage under restrained/free conditions, and cracking.
- (3) The air void system of RC bridge slabs of Mount Aobuna No. 1 Bridge and Shinyanagibuchi Bridge were studied. The results revealed that the air void frequency increase with W/B ratio decrease, especially the diameter 0 - 200  $\mu\text{m}$ . Confirming the air void in the range of 0 - 200  $\mu\text{m}$  was one of the significant factors for featuring the distribution of air void and the spacing factor. Moreover, the dosage of the expansive agent has little influence on deicing salt scaling resistance of concrete. PP fiber can improve the anti-scaling performance of concrete surfaces, however, the curing methods of fiber concrete

---

would be one of the significant factors to determine the surface scaling resistance. It is proved that wet curing is helpful to the frost resistance of PP fiber concrete.

- (4) The effects of the individual or hybrid addition of superabsorbent polymers (SAP) with varying dosages (0.1%, 0.2%, 0.3%, and 0.6%) and the lime-type expansive agent (KEA) on the length and mass change, compressive strength, and pore structures (MIP) of mortars were investigated. The results showed that the incorporation of SAP can effectively mitigate its autogenous shrinkage and the length change value of the mortar with SAP smaller than Ref until 49 d, regardless of the presence of KEA. The hybrid addition of SAP and KEA increase the initial expansion of the specimens as compared with individual addition of SAP, which is a beneficial effect on compensating for the shrinkage of the mortar under drying conditions. Moreover, the addition of SAP seems to delay cement hydration and increase the volume of macropores (greater than 100 nm), thereby reducing the compressive strength of the mortars. The introduction of KEA slightly promoted the formation of micropores, resulting in a slight increase in compressive strength compared with the samples without KEA. Furthermore, in our view, it promotes pore refinement, so as to reduce moisture evaporation.
- (5) The influence of different SAP incorporation methods and different SAP and KEA contents on internal curing effect the shrinkage behavior and compressive strength of concrete were studied. The results showed that the concrete with pre-soaked SAP, due to the clustering of pre-soaked SAP in the fresh concrete, it is difficult to uniformly distribute in the concrete matrix, resulting in the formation of larger pores in the hardened concrete. However, the existence of these larger pores did not adversely affect the compressive strength of concrete. In addition, when the surface of concrete was exposed for 63 days under drying conditions, the wet residue range of the concrete samples with pre-soaked SAP was larger than that of the concrete samples with dry SAP powder. The combined effect of SAP and KEA is beneficial to mitigate the autogenous shrinkage of concrete and delay the drying shrinkage, regardless of the incorporation methods of SAP. The voids created by SAP and air-entraining agent have a negative impact on the compressive strength of concrete. The compressive strength decreases with the increase of SAP contents, regardless of the incorporation methods of SAP. In addition, when the SAP content is 0.3%, its compressive strength is greater than or close to the concrete samples with 5% air content.

---

To sum up, this work has tried to improve the durability of concrete in cold areas through laboratory and field research, thereby extending the service life of the RC structures and reducing subsequent maintenance costs. The research results and recommendations provide a little technical contribution for casting durable concrete in cold climate.

---

## 要 旨

コンクリートは、その優れた可塑性、汎用性、および低コストのために、道路、橋、ダム、トンネルなどのあらゆる種類のインフラストラクチャーの建設に広く使用されている。しかし、寒冷地でのコンクリート構造物の耐久性は常に注目されてきた。日本の寒冷地では、現在、多くの既存の鉄筋コンクリート（RC）構造物が、厳しい供用環境や気候のために、凍害、塩害、アルカリシリカ反応（ASR）、砂利化などの複合劣化が顕在化している。そのため、その性能・機能や耐用年数の低下が課題となっている。

ご存知のように、寒冷地では主に凍害に起因する橋梁やトンネルの劣化が一般的な現象である。1990年代初頭から、冬の車両の安全運転を確保するために凍結防止剤（塩化物）が広く使用されている。日本の東北地方の報告によると、冬の平均気温が $-3^{\circ}\text{C}$ 未満で、凍結防止剤が年間約 $20\text{t}/\text{km}$ 散布されている。このため、国土交通省東北地方整備局では、凍結防止剤が散布されるコンクリート橋梁の凍害対策マニュアルを発行している。このマニュアルは、現場でのフレッシュコンクリートの目標空気量を増やすために提案されている。それは、建設の施工段階での空気量の減少をカバーし、硬化コンクリートの空気量を確保することを目的としている。凍害リスクが最も厳しい環境下のコンクリート構造物の場合、W/Bが45%未満で、目標空気量が6%であることが要求されている。しかし、実際の施工段階におけるソルトスケーリング抵抗と気泡の分布特性に関する研究はまだ明確ではない。

さらに、近年では既存のRC構造物の長寿命化を目的とした維持管理が特に重要になっている。それにも関わらず、管理構造物の増大は必然的に維持費の増加につながり、それは現代の社会経済の発展に深刻な影響を及ぼすことが懸念される。国土省によると、日本の東北地方では、40%以上橋梁が2025年までに供用開始から50年以上に達するため、多くの橋梁がその性能に潜在的なリスクを抱えている。言い換えれば、既存のRC橋梁の大部分は、大規模なリハビリと更新の時期に差し掛かっている。したがって、耐久性のあるコンクリート構造物の整備は、グリーンで持続可能な地域社会にとって非常に重要といえる。この論文は、既存のRC橋梁の表層透気係数の調査（非破壊検査、NDT）、実験室試験、実際の現場フィールド

---

のさまざまな段階でのコンクリートの耐凍害性の試験を通じて、寒冷気候におけるコンクリート橋梁の耐久性の改善を目指したものである。主な研究内容と得られた成果を以下に示す。

(1) 表層部コンクリートの透気性とソルトスケーリング抵抗性に及ぼす初期養生の影響を調査した。これらの結果は、シートまたは透水型枠を使用したコンクリート養生は、養生時間が長くなる気中での養生よりも優れていることを示した。特に透水型枠を利用することは、高い表層品質と耐久性のあるコンクリートの確保に非常に効果的である。同時に、寒冷地コンクリートに焦点を当て、表層部コンクリートの透気性とソルトスケーリング抵抗性との組合せによって、追加養生を含む適切な養生期間を評価することができることを明らかにした。また、表層透気係数が  $1 \times 10^{-16} \text{ m}^2$  未満の場合、コンクリートのスケーリング抵抗性が優れていると判断される。

(2) 寒冷地に適した耐久性の高いコンクリートを得るために、ソルトスケーリング抵抗性、アルカリシリカ反応 (ASR)、抑制および乾燥収縮、RC 橋床版の表面ひび割れの目視評価を実験室および現場で実施した。これらの結果より、FB セメントを使用したコンクリートのソルトスケーリング抵抗が優れていることを示した。一方、フレッシュコンクリートの空気量が 6% に達すると、セメントの種類や W/B 比に関係なく、ソルトスケーリング抵抗性に大きな差は認められなかった。BB セメントを使用したコンクリート (特に低 W/B 比の場合) は、ASR の膨張、拘束あるいは無拘束下での自己・乾燥収縮、およびひび割れに対する抵抗性が優れていることが分かった。

(3) 青ぶな山 1 号橋 (青森県) と新柳渕橋 (岩手県) の高耐久 RC 床版の気泡組織を評価した。その結果、W/B が減少すると、特に直径  $0 \sim 200 \mu\text{m}$  の気泡分布が増加することを明らかにした。 $0 \sim 200 \mu\text{m}$  の範囲の気泡を確認することは、気泡分布と気泡間隔係数を特徴づけるための重要な要因の一つである。さらに、膨張材の使用は、コンクリートのソルトスケーリング抵抗にほとんど影響を与えないことが示された。ポリプロピレン繊維は、コンクリート表面のスケーリング抵抗性を向

---

上させることができるが、その場合であってもコンクリートの養生方法は、表面のスケーリング抵抗性を決定する重要な要因となる。湿潤養生はポリプロピレン繊維コンクリートの耐凍害性に役立つことが検証された。

(4) さまざまな使用量(0.1%, 0.2%, 0.3%, および 0.6%)の超吸収性ポリマー(SAP)と石灰型膨張材(KEA)の個別またはハイブリッド添加が、モルタルの長さや質量の変化、圧縮強およびモ細孔構造(MIP)及びその影響を調査した。結果は、SAPを組み込むことで、KEAの存在に関係なく、材齢49日までのSAPを使用したモルタルの自己収縮とモルタルの長さ変化を効果的に軽減できることを示した。SAPとKEAのハイブリッド添加は、SAPの個別添加と比較して、試験片の初期膨張を増加させる。これは、乾燥条件下でのモルタルの収縮を補償する上で有益な効果となる。さらに、SAPを追加すると、セメントの水和が遅れ、マクロポアの体積が増加し(100nmを超える)、それによってモルタルの圧縮強度が低下する傾向にある。KEAの導入により、微細孔の形成がわずかに促進され、KEAを含まないサンプルと比較して圧縮強度がわずかに増加した。さらに、水分の逸散を抑制するために細孔の微細化を促進する。

(5) コンクリートの収縮挙動と圧縮強度に及ぼす内部養生効果に関するさまざまなSAP混入方法とさまざまなSAPおよびKEA含有量の影響を研究した。その結果、SAPを事前に水に浸して使用したコンクリートは、SAPを事前に水に浸したため、フレッシュコンクリート中のマトリックスに均一に分布させることが難しく、硬化したコンクリートに大きな空隙が形成されることが分かった。ただし、これらの大きな空隙の存在は、コンクリートの圧縮強度への悪影響は確認されなかった。さらに、コンクリートの表面を乾燥条件下で63日間暴露した場合、SAPを事前に水に浸漬したコンクリートサンプルの湿った残留物の範囲は、乾燥したSAP粉末を含むコンクリートサンプルのそれよりも大きかった。SAPとKEAの複合効果は、SAPの混入方法に関係なく、コンクリートの自己収縮を緩和し、乾燥収縮を遅らせるのに寄与した。SAPと空気連行剤によって作成された気泡は、コンクリートの圧縮強度に悪影響を及ぼす。SAPの混入方法に関係なく、SAPの含有量が増え

---

ると圧縮強度が低下する。さらに，SAP 含有量が 0.3% の場合，その圧縮強度は 5% の空気量のコンクリートサンプルよりも大きいか，それに近いことを明らかにした。要約すると，この論文は寒冷地でのコンクリート橋梁の長寿命化を目的としたものであり，実験室およびフィールド調査を通じてコンクリートの耐久性の改善を実現した。これらの研究成果は，寒冷地域でのコンクリート橋梁の耐用年数の延長に寄与し，将来のメンテナンスコストの削減が期待される。

## CHAPTER 1 INTRODUCTION

### 1.1 Problem statement and objective

Concrete, because of its good plasticity, versatility, and low cost is widely used in the construction for all kinds of infrastructures such as road, bridge, dam, and tunnel for nearly a century. However, with the passage of time, most of the existing reinforced concrete (RC) structures have been difficult to meet the needs of social and economic development in terms of function and service life. In addition, it can be noticed that many existing RC structures currently are suffering from deterioration due to severe environment and climates such as frost damage, the chloride ion attack, alkali-silica reaction (ASR), and granulated concrete (see Figure 1.1 and 1.2), which seriously restricted its service life and function. This deterioration of concrete that affects the performance of concrete and causes the risk of RC structures security directly.

In general, the development of concrete deterioration is a gradual process from the surface to the inside. Initially, these degenerations may occur on the concrete surface and reduced the compactness of the concrete surface as well as cause cracking, which increased



a



b

Figure 1.1. Deteriorated RC bridge structures: a ASR, b Granulated concrete.



Figure 1.2. Deteriorated RC bridge structures (Mainly frost damage).

permeability of concrete surface. As the degree of deterioration deepens, water, gas, and ions from the surrounding environment will penetrate the RC structures through a variety of transport mechanisms, resulting in accelerated degradation for the mechanical properties of the RC structures such as corrosion of steel bars and reduction of concrete strength.

Maintenance management for extending the service life of the existing RC structures becomes particularly critical in recent years. Nevertheless, the increase in maintenance management will inevitably lead to an increase in maintenance costs, which seriously restricts the development of the modern social economy. In the Tohoku region of Japan, over 40% of bridges will reach a service life of more than 50 years by 2025, which means a large number of bridges would have potential risks on its performance (see Figure 1.2), according to the Ministry of Land (Ministry of Land, 2017). In other words, the great majority of existing RC bridge structures are about to or have entered a large-scale rehabilitation and reconstruction period. Thus, there is increasing concern on durable RC structures, which not only can resist the effects of a severe environment but prolong the service life and reduce the maintenance costs.

As we all know, in cold regions, road and bridge deterioration is a common phenomenon mainly related to frost attack. Deicing salt is widely used to ensure the driving safety of vehicles in winter. When the average temperature is less than  $-3^{\circ}\text{C}$  in winter and the deicing salt was sprayed approximately 20 t/km per year according to the report in the Tohoku region of Japan (see Figure 1.3). For this reason, the Tohoku Regional development bureau has published the manual for countermeasure to frost damage of concrete structures under

spreading deicing salt (Bureau, 2017). This manual was proposed to increase the target air content at the loading of freshly mixed concrete on site. That is to cover the decreasing of air content while the execution process of construction and to attain air content in hardened concrete. In the case of concrete structures under the most severe environment on frost damage risk, the W/B less than 45% and the target air content of 6% were requested. However, research on the deicing salt scaling resistance and the distribution characteristics of air void during the entire construction execution phase were relatively few.

In addition, the reduction of environmental pollution and sustainable use of resources are the main concerns of the scientific community. “Green, sustainable and smart” is proposed as a new requirement to achieve the coordinated development of environment and economy, among which, the industrial by-product materials such as ground granulated blast furnace slag (GGBFS) and fly ash (FA) replacing conventional Portland cement were employed for fabricating concrete, which not only provides a “Green, sustainable” solution for

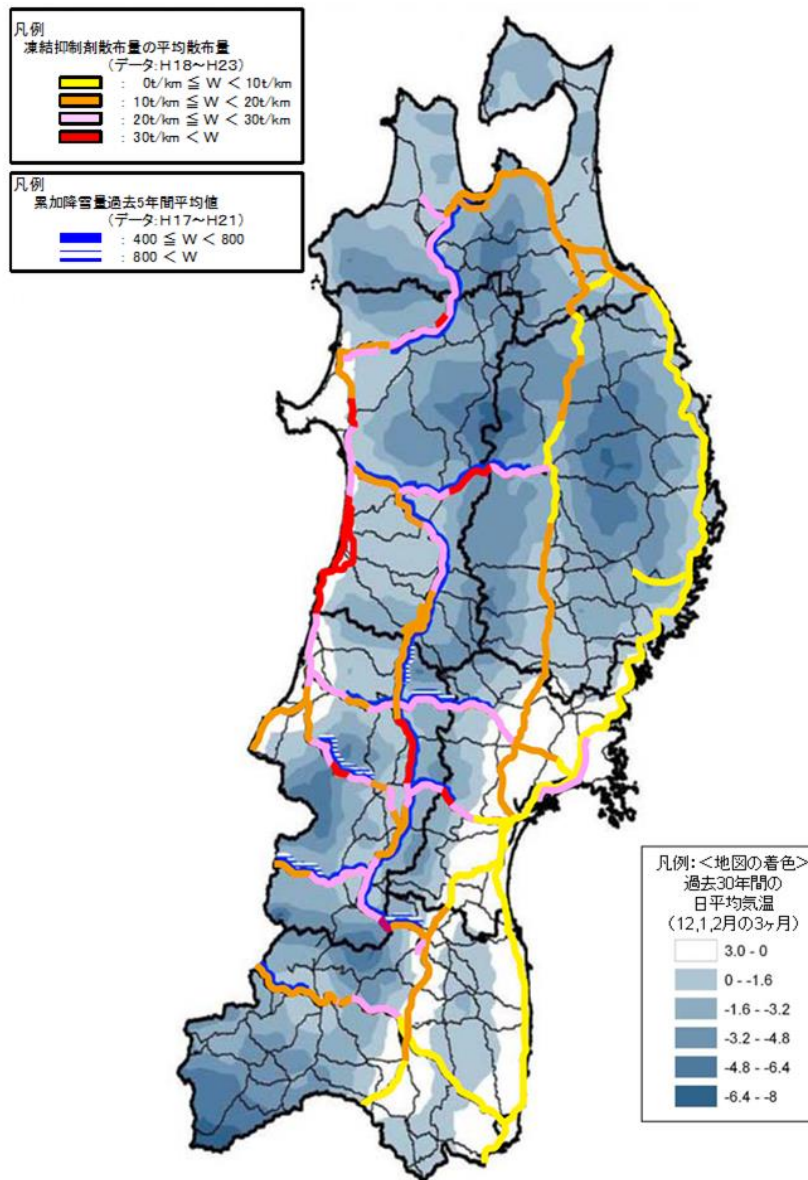


Figure 1.3. Distribution of deicing salt spread on roads and average temperature in winter.



Figure 1.4. Early-age shrinkage cracking of RC structures.

mitigating the emissions of carbon dioxide but also potential to improved durability of concrete. Furthermore, internal curing with superabsorbent polymers (SAP) was proposed as one method to reduce the potential for early-age shrinkage cracking (see Figure 1.4) and may provide long-term self-curing for concrete in the later period, reflecting the “smart”.

Accordingly, some basic policies of lifetime improvement of concrete structures served in cold climate were proposed. For example:

For the frost attack, (1) using the additional curing to ensure the quality of the concrete cover; (2) properly increase the air content of fresh concrete and ensure the air content and quality of hardened concrete.

For the chloride attack, (1) External use GGBFS or FA to replace ordinary Portland cement as an admixture; (2) for the internal protection of steel bars, anti-corrosion steel bars are used instead of ordinary steel bars.

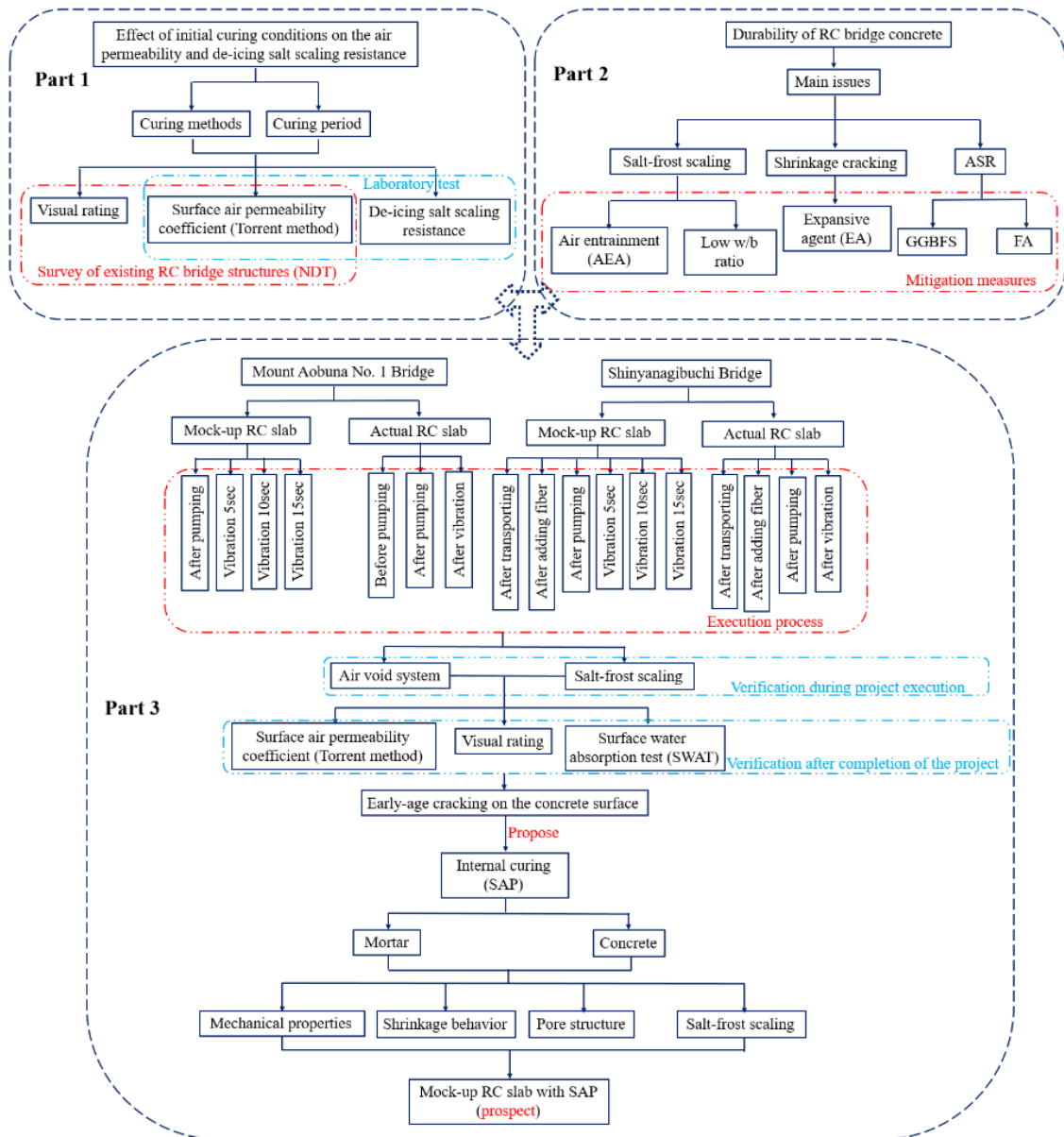


Figure 1.5. Thesis road map.

For the alkali-silica reaction (ASR), (1) using the aggregate not induced ASR under chloride condition; (2) effective use of GGBFS or FA to replace ordinary Portland cement as an admixture.

For the early-age shrinkage cracking, (1) individual addition of expansive agent; (2) individual addition of SAP; (3) hybrid addition of expansive agent and SAP.

Although these countermeasures have been proved to be effective by many researchers, there are still differences in the application of actual engineering under different geographical and climatic environmental conditions. Thus, some countermeasures need to be verified both in laboratory and field.

To sum up, as it can be seen that the concrete surface layer plays an extremely important role in preventing the deterioration of RC structures. Indeed, enhancing the performance of the deicing salt scaling resistance and reducing the potential for early-age shrinkage cracking (thanks to autogenous and drying shrinkage) of surface concrete may be an effective way to delay the deterioration and extend the service life of RC structures in cold regions, but it is usually difficult to ensure the consistency of concrete durability in laboratory and field, which serves as one of the major motivations for this work.

## **1.2 Scope and significances of this study**

This thesis focuses on improving the concrete durability for bridge structures in cold climate via the survey of existing RC bridge structures (Non-destructive testing, NDT), laboratory tests, the whole process of field construction tests, and a novel exploration of curing method.

The primary route of this research are shown in Figure 1.5 and the scope and significances can be summarized below:

- Investigating the effect of initial curing conditions on the air permeability of concrete surface through a survey of existing RC bridge structures;
- Identifying the effect of initial curing conditions on the air permeability of the concrete surface and deicing salt scaling resistance under simulating winter concrete construction in the laboratory;
- Evaluating and selecting durable bridge concrete suitable for the cold climate via deicing salt scaling resistance, ASR, shrinkage behavior;
- Substantiating air void distribution characteristics of concrete associated with construction execution process and laboratory;
- Exploring the potential of reducing for early-age shrinkage of mortar and concrete by using superabsorbent polymers (SAP) as an internal curing admixture;

- Assessing the influence of individual/hybrid addition of SAP and KEA for improving early-age shrinkage of mortar and concrete, which provides insight for the field application in preparing durable concrete mixes.

The purpose of this work, its essence is a process of the ongoing improvement of concrete durability through laboratory and field investigation. To provide a reference for gradually establishing the correlation between the concrete performance of the laboratory and the actual construction.

### 1.3 Thesis organization

Chapter 1: This chapter presents a general background, the problem statement and the research objective of this dissertation. It also gives the significances and road map of this work.

Chapter 2: This chapter presents the effect of initial curing conditions on the air permeability and deicing salt scaling resistance of surface concrete via the field inspection (NDT) and laboratory testing. The significance of initial curing conditions/methods for improving the surface quality of concrete is explained.

Chapter 3: This chapter presents a detailed evaluation of RC bridge concrete durable with the various cement types, water-cement ratios, and execution process by deicing salt scaling resistance, alkali-silica reaction (ASR) and shrinkage behavior. After testing in the laboratory, the appropriate concrete is selected for the actual bridge slab and its application effect is evaluated.

Chapter 4: This chapter presents air void characteristics of concrete that mainly include the air void system of Mount Aobuna No. 1 Bridge and Shinyanagibuchi Bridge.

Chapter 5: This chapter proposes the internally cured concrete with superabsorbent polymers (SAP) for mitigating early-age cracking. Investigating the combined effect of SAP contents and expansive agent (KEA) on mechanical properties, shrinkage behavior, and pore structure of mortar and concrete.

Chapter 6: This chapter puts forward the recommendations of fabricating durable concrete in cold climate.

Chapter 7: This chapter gives the major findings and results of the work presented in this thesis.

## 1.4 Reference

Bureau, T. R. D. (2017). The manual for counterplan to frost damage of concrete structures under spreading deicing salt (in Japanese).

Ministry of Land, I. T. a. T. R. B. (2017, 10 October 2017). Road annual report. Retrieved from [http://www.mlit.go.jp/road/sisaku/yobohozen/yobohozen\\_maint\\_h28.html](http://www.mlit.go.jp/road/sisaku/yobohozen/yobohozen_maint_h28.html)

## CHAPTER 2 INVESTIGATION OF EXISTING SUBSTRUCTURES OF RC BRIDGES AND DEICING SALT SCALING RESISTANCE

### 2.1 General

Enhancing the surface quality of concrete is a key to improve the durability of reinforced concrete, which can protect steel bars from corrosion due to the migration of gas, water and ion from the surrounding environment. Therefore, the influence of the initial curing on air permeability and the deicing salt scaling resistance of surface concrete were investigated during this study. Firstly, existing bridge structures in the cold region of Japan were surveyed by visual rating and non-destructive test (NDT) for the surface quality of concrete. Secondly, the concrete specimens were prepared for different curing conditions and methods (Conditions: in cold weather concreting, heat-supply curing, and non-heat-supply curing. Methods: extension demold period, and water-retention sheet). These results showed that concrete curing with sheet or permeability formwork was better than curing in air with increased of duration. Especially, utilizing the form of permeable sheet is greatly effective for the attainment of high surface quality and durable concrete. Simultaneously, focus on cold weather concreting, could evaluate the appropriate curing period including additional curing from combining with the surface air permeability and the deicing salt scaling resistance of concrete. It is also decided that the concrete has better deicing salt frost resistance, when the surface air permeability coefficient is less than  $1 \times 10^{-16} \text{ m}^2$ .

### 2.2 Introduction

One of the most significant issues for concrete structures is to ensure long-term durability in severe conditions of the actual environment. Therefore, the surface quality of concrete cover has to be critical to attaining the durability of a concrete structure.

In the cold region of Japan, the deicing agent has been used on the roads since early 1990s when using spike-tires on a car was banned, in order to secure the driving safety of the car in the winter season. The main component of the deicing agent is sodium chloride, potassium chloride, calcium chloride magnesium chloride. The excessive spreading of these agents induced the acceleration of multiple deterioration (such as frozen deterioration of the concrete cover, corrosion of reinforcement due to chloride ion, and the alkali silica reaction of aggregates) (Caspeele, Taerwe, & Frangopol, 2018) of concrete structures. The concrete cover has the function as mitigating layer for some deterioration factors (water, ion, gas and so on) that can be penetrate the concrete surface from the surrounding environment (Cady, Weyers, & aggregates, 1983; L. Yu, François, Dang, L'Hostis, & Gagné, 2015). Therefore, if severe deterioration occurs on the cover concrete, the durability of concrete structures is probably affected by the degree of deterioration. Thus, it is important for concrete structures to ensure and improve the quality of the surface concrete. The initial curing of concrete is the greatest factor to ensure the quality of the concrete cover, which can make concrete obtain a sufficient heat of hydration and improve the strength (Al-Khaiat, Haque, & Research, 1998; Z. Zhang & Qian, 2017). The drying of cementation materials due to poor curing, particularly at the concrete surface, leads to restricted hydration in the surface layers and thus to higher porosity and permeability (Elkedrouci, Diao, Pang, & Li, 2018; Güneysi, Özturan, & Gesog˘lu, 2007; Mangat, Limbachiya, & Research, 1999; Patel, Parrott, Martin, Killoh, & research, 1985).

Table 2.1. List of surveyed existing structures.

Structures	Members	Ready-mixed concrete	Period of construction (Y. M)	Date of survey (Y. M)	Standard curing period (during formwork keeping)	Additional curing after demolding	Permeability formwork
Bridge A	A1, A2	24-8-25 BB	2014.01-2014.02	2014.06	14 days, 7 days	-(non)	—
Bridge B	A1, A2	24-8-25 BB	2010.06-2010.07	2013.11	10 days	-(non)	—
Box culvert B	Side wall	24-8-25 BB	2014.05-2014.06	2015.06	7 days	-(non)	—
Bridge C	P2	27-8-25 BB	2009.12-2010.02	2013.11	5 days	-(non)	—
Bridge D	P1, P2	24-8-25 BB	2014.01-2014.02	2015.01	P1: 8 days P2: 9 days	Sheet curing P1: 15 days P2: 11 days	—
Box culvert D	Side wall	24-8-25 BB	2014.06	2014.10	14 days, 7 days	-(non)	—
Bridge E	A1, A2	24-8-25 BB	2013.04	2014.11	A1: 10 days A2: 8 days	Curing agent	—
Box culvert E	Slab	24-8-25-BB	2016.06	2016.09	1 day	Water-supply curing (6-36 days)	—
Bridge F	P2, P3, P4	24-12-25 BB	2015.01-2015.04	2015.07	7 days	Sheet curing	○
Bridge G	A1	24-8-25 BB	2014.01	2015.06	7 days	-(non)	—
Bridge H	A1	24-8-25 BB	2015.04	2015.08	60 days	-(non)	—
Bridge I	A2, P2	24-8-25 BB	2017.03-2017.04	2017.08	A2: 9 days P2: 5 days	Sheet curing A2: 27 days P2: 68 days	—
Bridge J	A1, P1	24-8-25 BB	2016.12-2017.06	2017.08	A1: 9 days P1: 7 days	Sheet curing A1: -(non) P1: 25 days	—

※Ready-mixed concrete: design strength-slump value-maximum size of coarse aggregate / Blast furnace slag cement (BB). Pier: P1, P2, P3, P4; Abutment: A1, A2. (Y. M): (Year. Month).

In addition, deicing salt scaling resistance is another feature influenced by the surface quality of concrete. Research and surveys of the past showed that the spraying of deicing salt on a concrete surface led to gradual deterioration from the surface into the inner part (Şahin, Taşdemir, Gül, & Çelik, 2010). The higher and looser porosity of the surface concrete tended to markedly reduce the deicing salt scaling resistance (M Pigeon, Talbot, Marchand, Hornain, & Research, 1996). Thus, attainment of high surface quality is essential to make the durable concrete in a severe environment. However, the initial curing period of concrete which is necessary to attain the surface quality and the deicing salt scaling resistance of concrete, would be not be clear enough, and has not been specifically indicated even in the standard specifications for the construction of concrete structures (Kawabe, ABA, Sutoh, & Ohmori, 2015).

The purpose of this paper is to investigate the influence of some curing methods and mold-types on surface quality of concrete structures through a survey of existing RC structures using NDT (testing of surface air permeability and water content) in cold regions. After the survey, concrete specimens were used for simulated cold weather concreting, the influence of a curing temperature, curing methods and additional curing or not on the surface quality of concrete was experimentally examined, and the durability of its concrete, especially freezing-thawing resistance with a sodium chloride solution (scaling resistance) was also evaluated via laboratory test.

## **2.3 Detail of survey and experiment**

### **2.3.1 Survey of existing RC structures**

Evaluating the effects of some experiments, in an attempt to ensure and improve the surface quality of concrete was conducted, existing concrete structures in Aomori and Iwate Prefecture in the northern part of mainland of Japan were targeted. The mold types, the additional curing methods, and the additional curing period were set as the parameters to survey the targeted structures with the surface air permeability test (Torrent method see Figure 2.2a)

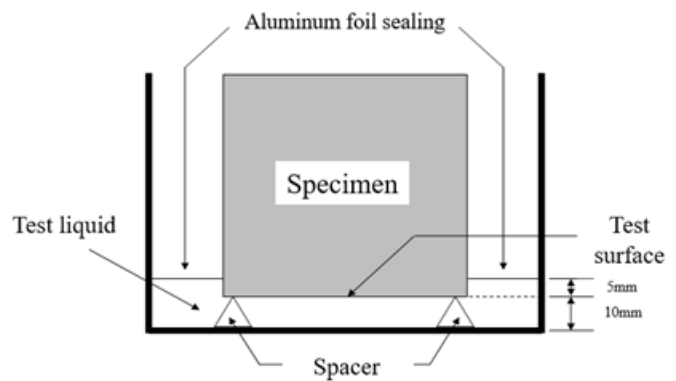
(Neves et al., 2015; Torrent & Structures, 1992). Table 2.1 shows the information of the surveyed structures. The W/C used for these surveyed structures were in the range of 50 ~ 55%. Blast furnace slag cement (BB) was used for such structures. Simultaneously, the visual rating of the existing concrete structures surface micro cracks were also conducted in the surveying with Figure 2.1 (Aba, Sakoi, Kanehama, & Otomichi, 2016; Kawabe et al., 2015), which will be presented in the results and discussion as follows.

Visual rating of surface micro cracks				
Rating grade	4(AAA)	3(AA)	2(A)	1(B)
<b>Observation method:</b> 1. Polishing the surface lightly with sandpaper to remove dirt. 2. Wiping with a cloth of being impregnated with acetone. 3. Evaluating the micro cracks of surface concrete, when acetone is completely absorbed into concrete.				
	Almost no micro cracks on surface concrete of survey-area.	Appearing slight micro cracks on surface concrete of survey-area.	Appearing moderate number of micro cracks on surface concrete of survey-area.	Appearing severe number of micro cracks on surface concrete of survey-area.

Figure 2.1. Visual rating of the existing concrete structures surface micro cracks.



a Surface air permeability test



b Specimen of deicing salt scaling test

Figure 2.2. Test set-up for the deicing salt test and Torrent method.

Table 2.2. Mix proportion of concrete (Unit content: kg/m<sup>3</sup>).

Types	W/B (%)	Air (%)	s/a (%)	Cement	Water	S1	S2	G	AE
N	54	6	45	288	156	620	270	1086	2.59
BB	54	6	44	281	152	605	262	1121	2.53

※ S1: Normal sand; S2: Limestone crushed sand; AE: Air entraining admixture.

Table 2.3. Experimental conditions.

Curing conditions	Age of demold	Additional curing period	Additional curing	N		BB	
				Normal mold	Permeability form-work	Normal mold	Permeability form-work
Heat-supply curing (15°C)	N: 3 days, BB:5 days		Extending demold period	•	—	•	—
				•	—	•	—
				•	•	•	•
Heat-supply curing (5°C)	N: 5 days, BB:7 days	7 days 21 days	Water-retention sheet	•	—	•	—
			Air (room condition)	•	—	•	—
			•	•	•	•	
Non-heat-supply curing(+8~-2°C)	N: 3 days, BB:5 days		Extending demold period	•	—	•	—
			Water-retention sheet	•	—	•	—
			High-adiabatic sheet①	•	—	•	—
			High-adiabatic sheet②	•	—	•	—

### 2.3.2 Experimental outline

#### *Preparation of materials and specimens*

The mix proportions of the concrete were listed in Table 2.2. The ready-mixed concrete (24-12-25, target air content:  $5.0 \pm 0.5\%$ .) with two types of cements (ordinary Portland cement (N) and blast furnace slag cement (BB)) were adopted in this experiment. N was used for reference specimens. The replacement ratio of blast furnace slag is 42% and its chemical composition is set according to JIS R 5211. The fine aggregates and the coarse aggregates used for the test were pit sand and crushed limestone respectively. Prism specimens of  $150 \times 150 \times 530$  mm were produced in a laboratory that assumed cold weather concreting in a temporary snow covered enclosure under the temperature controlling (Temperature: 10°C, and Relative humidity: 60%).

#### *Procedure*

The curing conditions, additional curing methods, additional curing period and the application of a permeability formwork were set as experimental parameters, which are presented in Table 2.3. A heat-supply curing technique was used in this study, the curing temperature of concrete in cold weather conditions was exposed to be maintained at 5°C or higher until the compressive strength reaches the values given in the JSCE Guidelines for Concrete structures (Maruyama, 2010). Thus, the curing temperature at 5°C was selected for entire the curing conditions until demolding of the specimens. After the demolding of the specimens, the heat-supply curing (15°C), the heat-supply curing (5°C) and the non-heat-supply curing (simulating an actual outside condition in winter: +8 ⇔ -2°C) were executed as additional curing (extending demold period, wrapping with water-retention sheet, and in air conditions). After the additional curing period, specimens were kept in an air conditioned room (20°C, 60%) for 63 days, and then the surface air permeability test was conducted to confirm the quality of the surface concrete with NDT (Torrent method). Measuring six positions on the two other surfaces except the casting surface side were done on every specimen (150 × 150 × 530 mm).

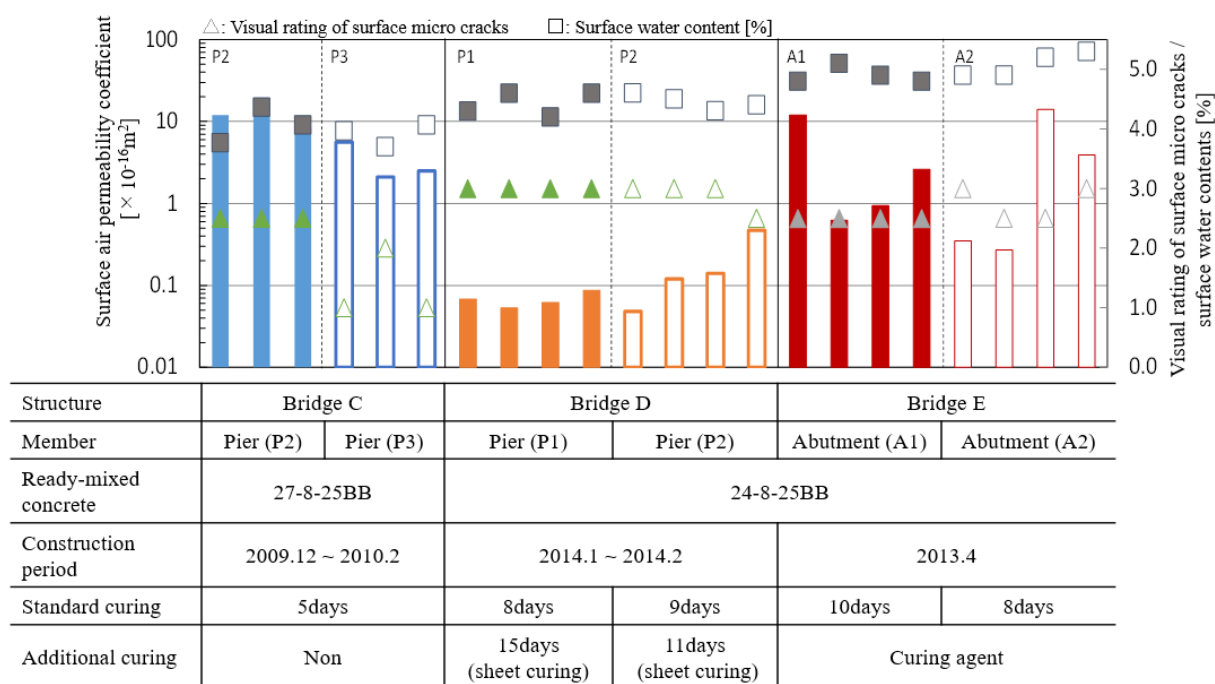
Specimens with dimensions of 150 × 150 × 150 mm were cut from a prism specimen that came from measuring surface air permeability, then the deicing salt scaling resistance test was conducted in accordance to JSCE-K 572 (6.10) (see Fig.2b). The testing surface of a specimen was the side surface perpendicular to the casting direction. The specimens were sealed on their surface except for the testing surface, and after the capillary suction period, they are kept for seven days at a temperature of 20 ± 2°C with 3% Na Cl solution. Then, the specimens were exposed to freezing-thawing conditions (Temperature: 20 ⇔ -20°C, two cycles a day) (ASTM, 2012; Setzer, Fagerlund, Janssen, & structures, 1996). The scaling amount of a specimen was measured every 6 cycles up to 60 cycles.

## 2.4 Results and discussions

### 2.4.1 Evaluation of the effect of additional curing after demolding

The results of the surface air permeability coefficient, the surface water contents and the visual rating of surface micro cracks are shown in Figure 2.3. Different methods of the additional curing after demolding were utilized. Bridge C is the case of a non-additional curing, Bridge D is the case of a heat-and-moisture retention curing via polyethylene sheet after demolding and Bridge E is the case of using the curing-agent (low drying shrinkage type) after demolding. Testing the air permeability coefficient requires the water contents of a concrete surface to be at a lower level (Neves et al., 2015; Torrent & Structures, 1992). From this figure, the water contents of all of the measurements are under 5.5%.

From these results, it is observed that the surface air permeability coefficient of Bridge D is lower than Bridge C and Bridge E. The surface air permeability of Bridge C indicated the range from  $2.9 \sim 14 \times 10^{-16} \text{ m}^2$  and Bridge E has a range from  $0.3 \sim 1.2 \times 10^{-16} \text{ m}^2$ . The



※Ready-mixed concrete: design strength-s slump value-maximum size of coarse aggregate / Blast furnace slag cement (BB)

Figure 2.3. Effect of the additional curing on the surface air permeability of existing structures.

results are little different between Bridge C and Bridge E, although additional curing has not been conducted on Bridge C. On the other hand, the coefficient of surface air permeability of Bridge D indicated almost  $0.1 \times 10^{-16} \text{ m}^2$ . The reason of this is considered that it is due to the effect of heat and moisture-retention by being sealed immediately after demolding with polyethylene sheet, and is due to the result of the improved surface quality of concrete by its positive effect. In addition, compared with the result of the case of another curing method, Bridge E has some fluctuation range of data in the same structural member. It may be due to non-uniform spray of the curing-agent on the surface of concrete.

Moreover, the results of visual rating of surface micro cracks are also shown in Figure 2.3. It is showed that the visual rating of Bridge C and Bridge E have larger fluctuations in the same structural member. However, the visual rating and the surface air permeability coefficient of Bridge D are relatively stable. Thus, the entirety of the concrete structures can obtain better quality via the sheet curing method.

Figure 2.4 indicates the relationship between the surface air permeability and the entire curing period (including an additional curing period). This figure includes all data from the survey, which includes the results of the survey other than the structures described above, together (see Table 1). The data shown in this figure are (a) Cement type: Blast furnace slag cement (type B), (b) W/C: 50 - 55%, and (c) Mold types: ordinary mold (wooden type), and the additional curing methods are a case of sealed curing (extension of a demolded period, or using a water-retention sheet).

From this result, it was found that the surface air permeability decreased with the extension of the curing period which included an additional curing period. Especially, in the case of a curing period less than 10 days, the surface air coefficient change in a range from  $0.024 \times 10^{-16} \text{ m}^2$  to  $19 \times 10^{-16} \text{ m}^2$ . A trend was recognized that has a large variation. It was considered that the reason was the density of surface concrete was decreased because the cement hydration stopped, and during drying of the concrete surface after demolding, some micro cracks appeared. In the case that the curing period was longer than 14 days, the surface air coefficient change was in the range from  $0.007 \times 10^{-16} \text{ m}^2$  to  $1 \times 10^{-16} \text{ m}^2$ . A trend was

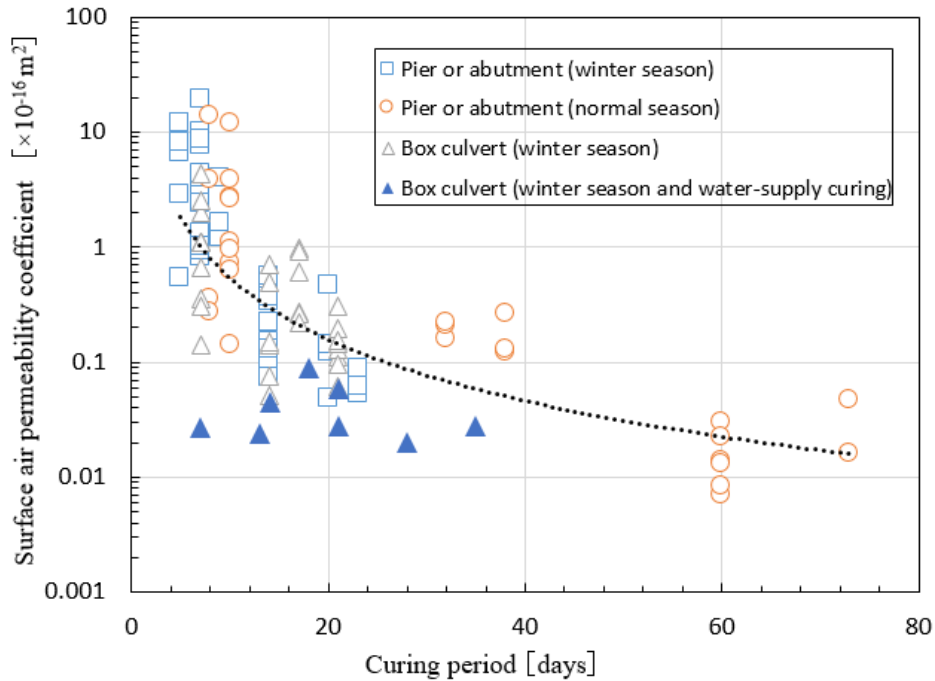
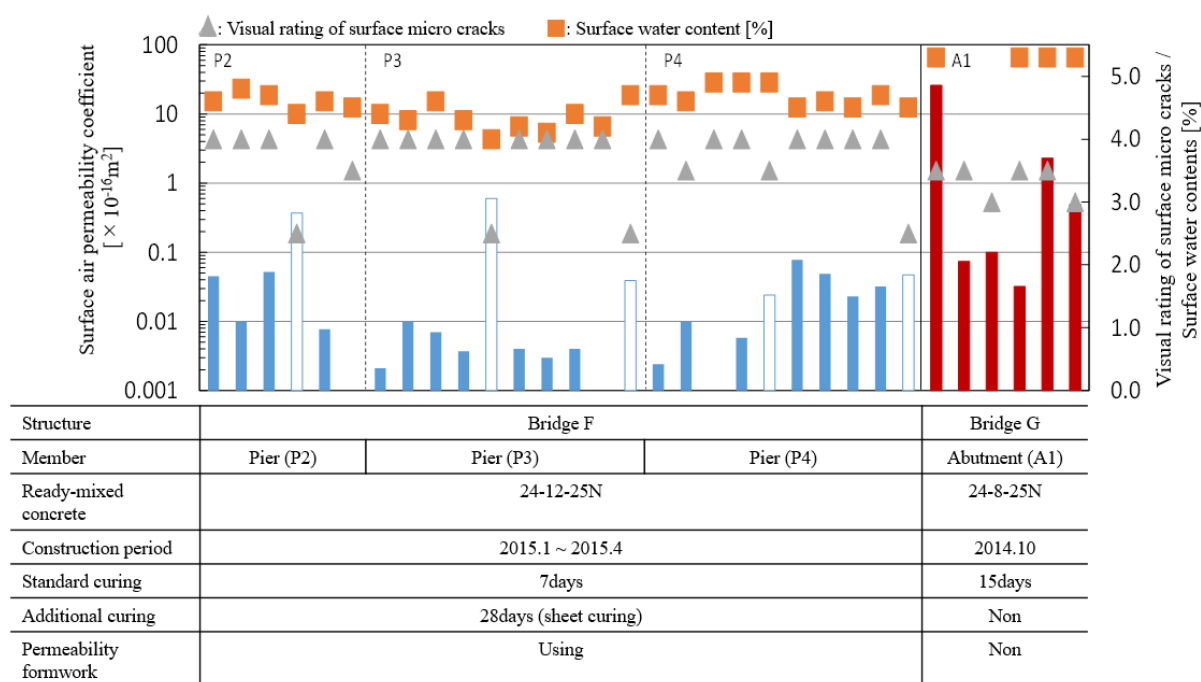


Figure 2.4. Relationship between the surface air permeability coefficient and curing period.

recognized that has less variation, and the coefficient varied within a certain range. Moreover, it was observed that the method of water-supply curing could improve the air permeability of concrete better than others in winter.

#### 2.4.2 Evaluation of effect of using permeability formwork

The development of a unique type of permeable formwork was proposed by researchers as a replacement for the conventional formwork used since 1987 in Japan (K. Tanaka & Ikeda, 1987). Permeability formwork is the setting a permeability sheet on the face of the mold, and using this formwork, it was expected that the quality of surface concrete was improved by draining extra water and/or by reducing surface air void. Figure 2.5 indicates whether the surface air permeability of structures (Bridge F, G) used the formwork with a permeable sheet or not. The pier of Bridge F is an elliptical shape, and the measuring results in the curved position shown with the white color bars in the figure, and the characteristics of this pier construction as follows:



※Ready-mixed concrete: design strength-slump value-maximum size of coarse aggregate / Blast furnace slag cement (BB)

Figure 2.5. Effect of the permeability formwork on the surface air permeability of structure.

Table 2.4. The surface air permeability coefficient ( $\times 10^{-16} \text{ m}^2$ ).

Curing conditions	Additional curing	Ce-ment		N		BB					
		Mold	Normal mold	Permeability form-work		Normal mold	Permeability form-work				
				7d	21d			7d	21d	7d	21d
Heat-supply curing (15°C)	Extending demold period	Period	1.60	1.45	—	—	2.90	1.70	—	—	
			1.90	0.80	—	—	1.77	0.87	—	—	
			2.05	3.40	1.80	1.75	5.00	4.80	0.68	1.86	
Heat-supply curing (5°C)	Water-retention sheet		1.43	1.15	—	—	3.25	2.95	—	—	
		Air (room condition)		1.50	1.21	—	—	3.25	1.18	—	—
				3.05	3.00	2.45	1.85	7.05	9.05	1.06	1.21
Non-heat-supply curing(+8~-2°C)	Extending demold period		1.35	2.20	—	—	2.65	4.45	—	—	
		Water-retention sheet		1.90	2.00	—	—	2.55	6.05	—	—
		High-adiabatic sheet①		1.70	1.50	—	—	2.40	1.60	—	—
		High-adiabatic sheet②		2.35	1.40	—	—	2.05	0.88	—	—

(a) Large amount of bleeding water occurred during construction.

(b) It was not only using a permeability formwork but also conducting a sealed curing with a water-retention sheet for about 1 month.

A comparison of results between Bridge G and Bridge F revealed that the surface air permeability coefficient of Bridge F (about  $0.1 \sim 0.01 \times 10^{-16} \text{ m}^2$ ) was lower than Bridge G (about  $0.1 \sim 10 \times 10^{-16} \text{ m}^2$ ). Therefore, the effectiveness of utilizing permeability formwork was confirmed and indicated. Then, comparing the coefficient of different measuring positions, it can be seen that the surface air permeability coefficient in the straight position (blue bar less than  $0.1 \times 10^{-16} \text{ m}^2$ ) is lower than the curved position (white bar more than  $0.1 \times 10^{-16} \text{ m}^2$ ) on Bridge F. In addition, there were also some straight positions that showed a remarkable low coefficient (less than  $0.001 \times 10^{-16} \text{ m}^2$ ). This reason may be considered that is the influence of the excessive bleeding amount that was gathered the near surface of concrete in a curved position of the pier and lead to an increase in water to cement ratio.

Moreover, in the case of Bridge F, the results of visual rating of surface micro cracks were indicated that the visual rating increases with the decrease of the surface air permeability coefficient.

### **2.4.3 Influence of curing condition on surface quality in laboratory**

From the results of the survey targeting existing concrete structures, the importance of curing conditions for the improvement of surface quality was found. Therefore, the objective of this section is to evaluate the influence of curing conditions on surface quality of concrete, assuming the cold weather concreting, and the experimental programs were planned.

Results of the surface air permeability coefficient for all conditions are listed in Table 2.4. The moisture content was 4.2 ~ 5.1% at the time of measuring the surface air permeability. From Table 4, in the case of non-heat-supply curing, it was confirmed that the surface air permeability was decreased due to heat-protection curing with high-adiabatic sheet. Simultaneously, it was found that the surface air permeability was decreased with the extension

of the additional curing period at the same temperature. Moreover, focus on the difference in mold types (normal mold/permeability formwork), it was found that the surface air permeability for the specimen which used the permeability formwork was a lower value.

Figure 2.6a~c presents the scaling amount after 60 cycles of freezing-thawing action. From these figures, for the specimen assuming heat-supply curing ( $15^{\circ}\text{C}$  and  $5^{\circ}\text{C}$ ), it was found that the scaling amount of specimen conducting air curing indicated the trend that

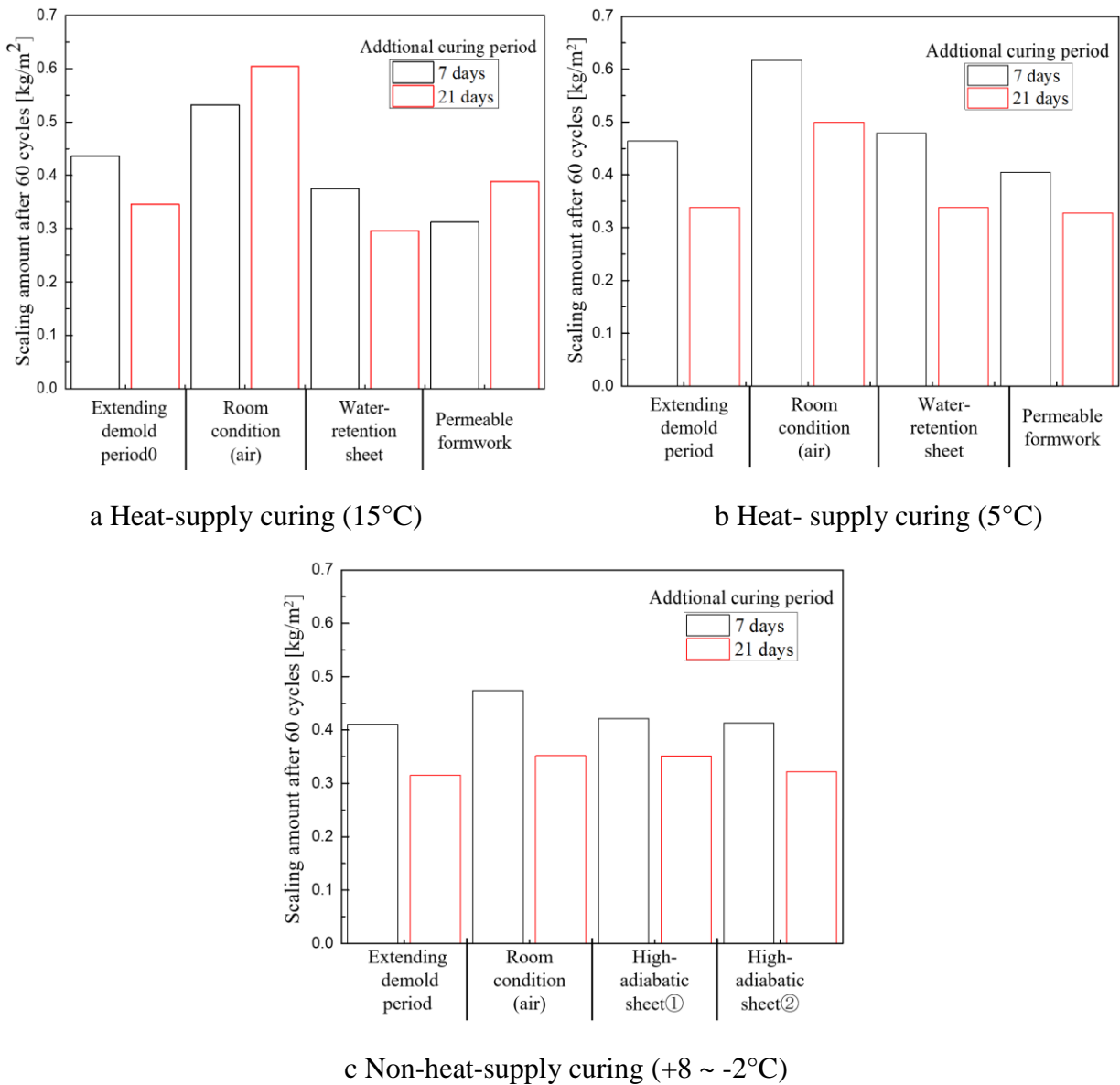


Figure 2.6. Scaling amount after 60 cycles of freezing-thawing action.

large scaling amount occurred compared with that of specimens under other curing conditions. On the other hand, in the case of keeping the mold setting, using a permeability formwork or using a water-retention sheet, it was confirmed that the scaling amount was reduced. The influence of additional curing period revealed that the scaling amount was decreased with the increase of an additional curing period, except in some cases. For the case of no-heat-supply curing (+8 ~ -2°C), the influence of the additional curing method on scaling amount was less, and it was found that the scaling amount was decreased with the increase of the additional curing period regardless of the difference in an additional curing method. Therefore, it was considered that the heat-retaining curing was enough to ensure the surface quality and the deicing salt scaling resistance of concrete. It was not necessary to conduct heat-supply curing in cold weather concreting when the outside temperature was above -2°C, as the test result showed.

#### **2.4.4 Expectation of curing period based on deicing salt scaling resistance**

Construction of concrete structures in actual engineering is not only to ensure the progress of the project, but also to provide better quality to ensure durability. The curing period of concrete is closely related to the progress of the project. Scaling amount is one of the parameters to evaluate the durability of concrete. Figure 2.7 is the relationship between the surface air permeability coefficient with the scaling amount after 60 freezing-thawing cycles and a curing period including additional curing. The object of this figure is to play a guiding role to help the decision-makers of construction to select an appropriate initial curing period by combining with the results of the on-site surveys and the laboratory experiments.

From this result, it was found that the surface air permeability coefficient decreases with the increase of the curing period, and the scaling amount decreases with the decrease of the surface air permeability coefficient, regardless of curing temperature and curing method. In addition, it can be found that the range of the surface air permeability coefficient changes from large to small. In other words, the surface air permeability coefficient tended

towards stability with the increase of the curing period (the surface quality of concrete is improving).

Furthermore, it is possible to consider an appropriate initial curing period according to the low scaling amount and surface air permeability coefficient in Figure 2.7. From this figure, when an example of the scaling amount is  $0.3 \text{ kg/m}^2$ , the safety curing period would need at least three weeks and the surface air permeability coefficient is about  $1 \times 10^{-16} \text{ m}^2$ . It was decided that the concrete has better deicing salt frost resistance, when the surface air permeability coefficient is less than  $1 \times 10^{-16} \text{ m}^2$  or the initial curing period is more than three weeks. Therefore, using NDT to test the surface air permeability of concrete is promising as an effective method for confirming the deicing salt frost resistance of concrete.

### 2.5 Summary

In this investigation, the aim was to assess the surface quality of concrete through initial curing conditions and deicing salt scaling resistance in field surveys and laboratory examinations. The following summary may be drawn:

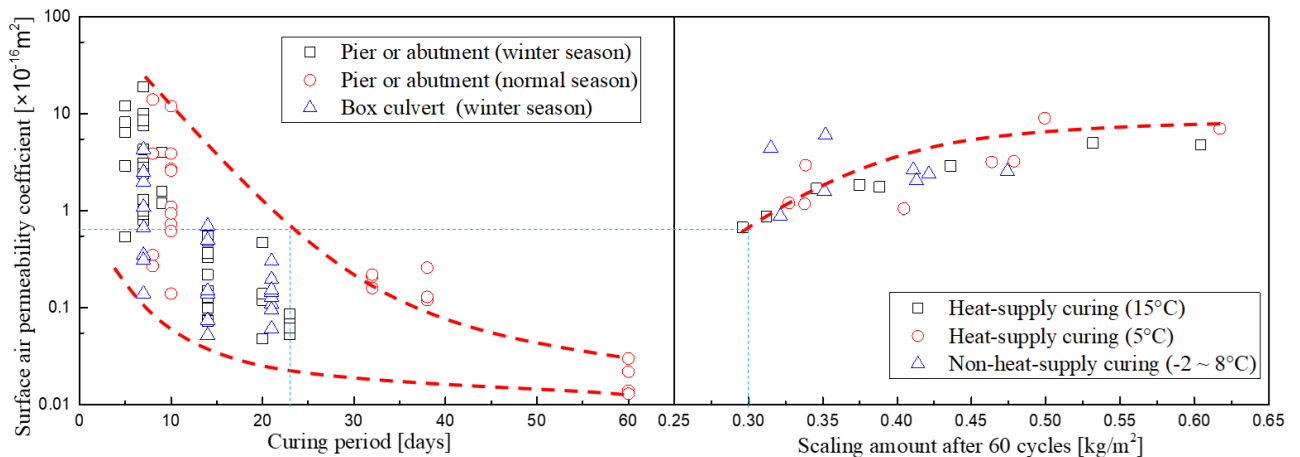


Figure 2.7. Relationship between curing period and the scaling amount after 60 cycles of freezing-thawing action.

- The additional curing after demolding or extending the initial curing period can effectively improve the surface quality of concrete, and the surface air permeability coefficient was decreased with the increase of the curing period. When the curing period was greater than about 14 days, there was less variation of the surface air permeability, and the variation trend and speed of the decrease of surface air permeability coefficient will reduce.
- The results of the visual rating of surface micro cracks show the relationship between the micro-cracks and the surface air permeability that the visual rating increases with the decrease of the surface air permeability coefficient. Thus, it is possible that the assessment of the surface quality of concrete through the visual rating of surface micro cracks.
- By using the permeability formwork, the surface air permeability was greatly reduced. In particular, using the permeability formwork was effective for the concrete that has a great amount of bleeding.
- It is helpful for the decision-makers in construction to consider an appropriate initial curing period based on the relationship between the surface air permeability coefficient with the scaling amount after 60 freezing-thawing cycles and the curing period.

As a result, the experimental results play a certain role in choosing the initial curing period to meet the durability requirements of concrete. The relationship between the curing period and anti-scaling performance needs to be further improved. Our investigations into this area are still ongoing to confirm our hypothesis.

## 2.6 Reference

Aba, M., Sakoi, Y., Kanehama, N., & Otomichi, K. J. P. o. t. J. C. I. (2016). Quality Attainment of Concrete on Box Culvert work and Substructure work of Bridge, and its Verification. *38*(1), 1611-1616.

Al-Khaiat, H., Haque, M. J. C., & Research, C. (1998). Effect of initial curing on early strength and physical properties of a lightweight concrete. *28*(6), 859-866.

- ASTM. (2012). Standard Test Method for Scaling Resistance of Concrete Surfaces Exposed to Deicing Chemicals. In *C672/C672M – 12*.
- Cady, P. D., Weyers, R. E. J. C., concrete, & aggregates. (1983). Chloride penetration and the deterioration of concrete bridge decks. *5*(2), 81-87.
- Caspeepele, R., Taerwe, L., & Frangopol, D. M. (2018). *Life Cycle Analysis and Assessment in Civil Engineering: Towards an Integrated Vision: Proceedings of the Sixth International Symposium on Life-Cycle Civil Engineering (IALCCE 2018), 28-31 October 2018, Ghent, Belgium* (Vol. 5): CRC Press.
- Elkedrouci, L., Diao, B., Pang, S., & Li, Y. (2018). *Combined Effect of Initial Curing Temperature and Crack Width on Chloride Penetration in Reinforced Concrete Beams*. Paper presented at the MATEC Web of Conferences.
- Güneyisi, E., Özturan, T., & Gesog˘lu, M. (2007). Effect of initial curing on chloride ingress and corrosion resistance characteristics of concretes made with plain and blended cements. *Building and Environment*, *42*(7), 2676-2685. doi:10.1016/j.buildenv.2006.07.008
- Kawabe, K., ABA, M., Sutoh, S., & Ohmori, Y. J. P. o. t. J. C. I. (2015). Quality Attainment of Concrete Structures by a Check Sheet to Grasp Construction Condition under Cold Weather Concreting. *37*(1), 1285-1290.
- Mangat, P., Limbachiya, M. J. C., & Research, C. (1999). Effect of initial curing on chloride diffusion in concrete repair materials. *29*(9), 1475-1485.
- Maruyama, K. (2010). *JSCE Standard Specifications for Concrete Structures 2007, Codes in Structural Engineering-Developments and Need for International Practice*. Paper presented at the Joint IABSE-fib Conference Dubrovnik 2010.
- Neves, R., da Fonseca, B. S., Branco, F., de Brito, J., Castela, A., & Montemor, M. F. (2015). Assessing concrete carbonation resistance through air permeability measurements. *Construction and Building Materials*, *82*, 304-309. doi:10.1016/j.conbuildmat.2015.02.075
- Patel, R., Parrott, L., Martin, J., Killoh, D. J. C., & research, C. (1985). Gradients of microstructure and diffusion properties in cement paste caused by drying. *15*(2), 343-356.
- Pigeon, M., Talbot, C., Marchand, J., Hornain, H. J. C., & Research, C. (1996). Surface microstructure and scaling resistance of concrete. *26*(10), 1555-1566.

- Şahin, R., Taşdemir, M. A., Gül, R., & Çelik, C. (2010). Determination of the optimum conditions for de-icing salt scaling resistance of concrete by visual examination and surface scaling. *Construction and Building Materials*, 24(3), 353-360. doi:10.1016/j.conbuildmat.2009.08.026
- Setzer, M. J., Fagerlund, G., Janssen, D. J. J. M., & structures. (1996). CDF test—test method for the freeze-thaw resistance of concrete-tests with sodium chloride solution (CDF). 29(9), 523-528.
- Tanaka, K., & Ikeda, H. J. I. R. (1987). Improvement of surface quality of concrete structures by unique formwork. 55.
- Torrent, R. J. J. M., & Structures. (1992). A two-chamber vacuum cell for measuring the coefficient of permeability to air of the concrete cover on site. 25(6), 358-365.
- Yu, L., François, R., Dang, V. H., L'Hostis, V., & Gagné, R. (2015). Development of chloride-induced corrosion in pre-cracked RC beams under sustained loading: Effect of load-induced cracks, concrete cover, and exposure conditions. *Cement and Concrete Research*, 67, 246-258. doi:10.1016/j.cemconres.2014.10.007
- Zhang, Z., & Qian, J. (2017). Effect of protogenetic anhydrite on the hydration of cement under different curing temperature. *Construction and Building Materials*, 142, 417-422. doi:10.1016/j.conbuildmat.2017.03.064

## CHAPTER 3 DURABILITY FOR RC SLAB OF BRIDGE

### 3.1 General

In this chapter, to obtain high-durability concrete suitable for cold climates, the deicing salt scaling resistance, alkali-silica reaction (ASR), restrained and free shrinkage, and the visual evaluation of RC bridge slab surface cracks were conducted in the laboratory and field. These results indicated that concrete with FB cement has a better deicing salt scaling resistance, however, it has little difference in terms of deicing salt scaling resistance regardless of cement types and W/B ratios, when the air content of fresh concrete reaches 6%. Concrete (especially for low W/B ratios) with BB cement has better resistance for ASR expansion, autogenous/drying shrinkage under restrained/free conditions, and cracking. In addition, the use of BB40-KEA has a better effect of early compensation for shrinkage and through the observation of the cracking of the RC slab 1 year later, it was found that the cracks appeared at the bottom of the RC slab and were almost mainly concentrated around the spacer blocks.

### 3.2 Introduction

The durability of RC bridge concrete exposed to harsh environments has always been the focus of attention. In the Tohoku region of Japan, due to the snowy climate in winter, most infrastructures such as roads and bridges have to use a large amount of deicing salt in order to ensure safe and smooth traffic (when the average temperature less than  $-3^{\circ}\text{C}$  in winter, the deicing salt agent was sprayed about 20 t/km). However, the excessive spreading of these agent lead to accelerate occurring deterioration (such as frozen deterioration of cover concrete, corrosion of reinforcement due to chloride ion, alkali silica reaction and so on) of concrete structures. Thus, deicing salt resistance and ASR of concrete are considered to be two important indicators for evaluating the durability of concrete.

In addition, early concrete cracking is also one of the main factors affecting its long-term durability. Controlling its autogenous shrinkage and drying shrinkage as much as possible is of great significance for reducing the risk of early concrete cracking.

Therefore, for “Revival Road” in Tohoku, considering the severity of the environments, a new initiative has been undertaken to secure highly durable bridge deck construction ensuring multiple countermeasures against deterioration (Y. Tanaka, Ishida, Iwaki, & Sato, 2017; Zerín, Hosoda, & Komatsu, 2018). In this work, investigation the effect of different cement types and W/B ratios on deicing salt scaling resistance, ASR, drying shrinkage, and restrained/free shrinkage in the laboratory. Furthermore, observe the early shrinkage of the actual RC bridge slab through the embedded strain gauge and the cracking after one year, it provides a reference for the continuous improvement of concrete durability.

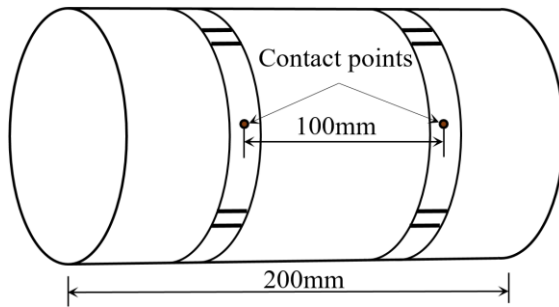
### **3.3 Materials and method**

The mix proportions of concrete are shown in Table 3.1. In these mix proportions of concrete, 3 types of cement (Ordinary Portland cement (N: density is  $3.16 \text{ g/cm}^3$ ), Fly ash cement (FB: density is  $2.96 \text{ g/cm}^3$ ), Blast furnace slag cement (BB: density is  $3.04 \text{ g/cm}^3$ )), four kinds of water-binder ratios (50%, 45%, 40%, 35%) and the lime type expansion agent (KEA) were used. The target of air content and slump of concrete were  $6 \pm 1.0\%$  and  $12 \pm 2.5 \text{ cm}$ , were adjusted by air-entraining agent (AEA) and water reducing agent (WRA), respectively. The maximum size of the coarse aggregate was 25 mm. The pit sand and crushed stone were employed as fine aggregates and the coarse aggregates, respectively.

Table 3.1. Mix proportions.

Mixture types	Cement types	W/B (%)	s/a (%)	Unit content: kg/m <sup>3</sup>						AEA (g/m <sup>3</sup> )
				W	C	S	G	EA	WRA	
N35	N	35	34.4	170	466	547	1187	20	7.78	29.2 (6A)
N40	N	40	35.3	170	405	627	1151	20	4.25	25.5 (6A)
N45	N	45	38.3	170	358	694	1119	20	3.78	22.7 (6A)
N50	N	50	43.3	170	320	740	1102	20	3.06	20.4 (6A)
FB35	FB	35	33.7	168	460	531	1187	20	7.20	28.8 (6A)
FB40	FB	40	37.7	168	405	614	1151	20	4.20	25.5 (6A)
FB45	FB	45	37.9	168	358	684	1119	20	3.73	22.7 (6A)
FB50	FB	50	42.9	168	316	730	1102	20	3.02	20.2 (6A)
BB35	BB	35	33.7	170	466	531	1187	20	7.29	29.2 (6A)
BB40	BB	40	37.7	170	405	614	1119	20	3.78	25.5 (6A)
BB45	BB	45	37.8	170	358	681	1151	20	4.25	22.7 (6A)
BB50	BB	50	42.9	170	320	730	1102	20	3.06	20.4 (6A)

※N, FB, BB are cement types and 50, 45, 40, 35 are water-binder ratios.



(a)

(b)



(c)

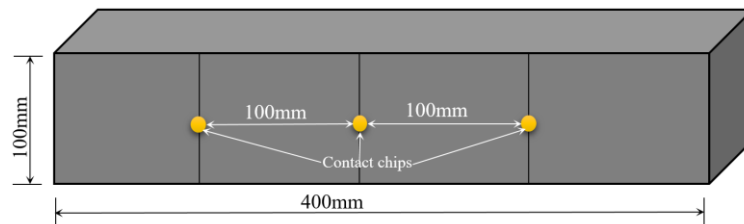
Figure 3.1. Using SWW method to test ASR expansion in concrete.

### 3.3.1 Deicing salt scaling resistance

Specimens with dimensions of  $100 \times 100 \times 100$  mm were cut from a prism specimen, each six samples were set as a batch for measuring the weight of scaled materials. The experimental process or procedure according to section 2.2.3.

### 3.3.2 Alkali-silica reaction

Three concrete cylinder specimens cast for each test series and the size of cylinder specimens is  $\Phi 100 \times 200$  mm. The expansion measurements were carried out in accordance with the SSW method and JCI AAR-3. After concrete mixing, using sodium hydroxide to adjust the total alkali content of concrete to  $5.5 \text{ kg/m}^3$ . The concrete specimens were demolded after being stored at wet room conditions for 24 h ( $\text{RH} > 95\%$ ). The contact points were set and the initial length was tested (see Figure 3.1(a) and (b)). Then, Wrap with blotting



(a)



(b)



(c)

Figure 3.2. Concrete drying shrinkage experiment.

paper moistened with 20% Na Cl solution and store in a sealed with film and place in a constant temperature chamber of 38°C (see Figure 3.1(c)).

Table 3.2. Curing methods of concrete.

Specimens types	Number of each type	Curing methods
100×100×1500mm	2	Moisture curing (RH>95%, Temperature: 20°C) for about 32 days, then placed in drying condition (RH: 60%, Temperature: 20°C) until the concrete cracks.
100×100×400mm	1	
JIS A 6202 B method	3	After demolding, the specimens were placed in the water (Temperature: 20°C) for 6 days, then placed in drying condition (RH: 60%, Temperature: 20°C) for about 1 year.



Figure 3.3. Uniaxial restrained and free shrinkage.

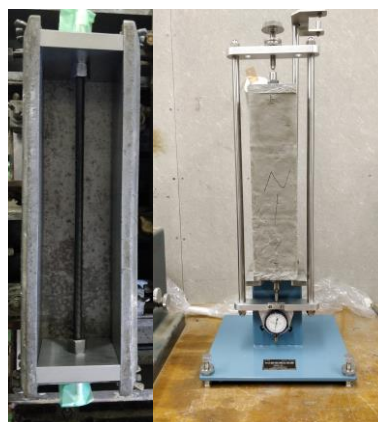


Figure 3.4. Restrained expansion and drying shrinkage.

### 3.3.3 Drying shrinkage and mass loss

Concrete specimens with dimensions of  $100 \times 100 \times 400$  mm were casting. Every three samples are a batch for measuring drying shrinkage and mass loss. After casting, concrete specimens were demolded at 24 h and then place in water for curing 6 days. Afterward, all the specimens were placed in a constant temperature and humidity chamber (Temperature:  $20^{\circ}\text{C}$ . RH: 60%). Setting up contact points and testing initial length and mass (see Figure 3.2).

### 3.3.4 Uniaxial restrained and free shrinkage

Concrete specimens with dimensions of  $100 \times 100 \times 1500$  mm were casting for uniaxial restrained shrinkage. Deformed bars (D32) were used for as restraint reinforcement according to JCI-SAS3-2. Concrete specimens with dimensions of  $100 \times 100 \times 400$  mm were casting for free shrinkage test (Figure 3.3). In addition, Concrete specimens were prepared in accordance with method B of JIS A 6202, which were used for testing restrained expansion and shrinkage of concrete (Figure 3.4). Curing methods of concrete specimens were shown in Table 3.2.

## 3.4 Laboratory study of concrete durability with different W/B ratios and cement types

### 3.4.1 Deicing salt scaling resistance

Figure 3.5 shows the effect of different W/B ratio on deicing salt scaling resistance of concrete. Although, it can be seen from Figure 3.5(a) and (b) that the weight of scaled materials increase with the decrease of W/B ratio, the different of weight of scaled materials at 60 cycles with the change of W/B ratio is not obvious. In contrast, for the BB cement, the weight of scaled materials increase with the increase of W/B ratio. Figure 3.6 shows the effect of different cement types on deicing salt scaling resistance of concrete. A common phenomenon can be observed that the weight of scaled materials of FB cement less than that of N and BB cement regardless of W/B ratio. This indicates that concrete with FB cement has a better deicing salt scaling resistance than that of N and BB. Nevertheless, when the air

content of fresh concrete reaches 6%, it has little difference in terms of deicing salt scaling resistance regardless of cement types and W/B ratios.

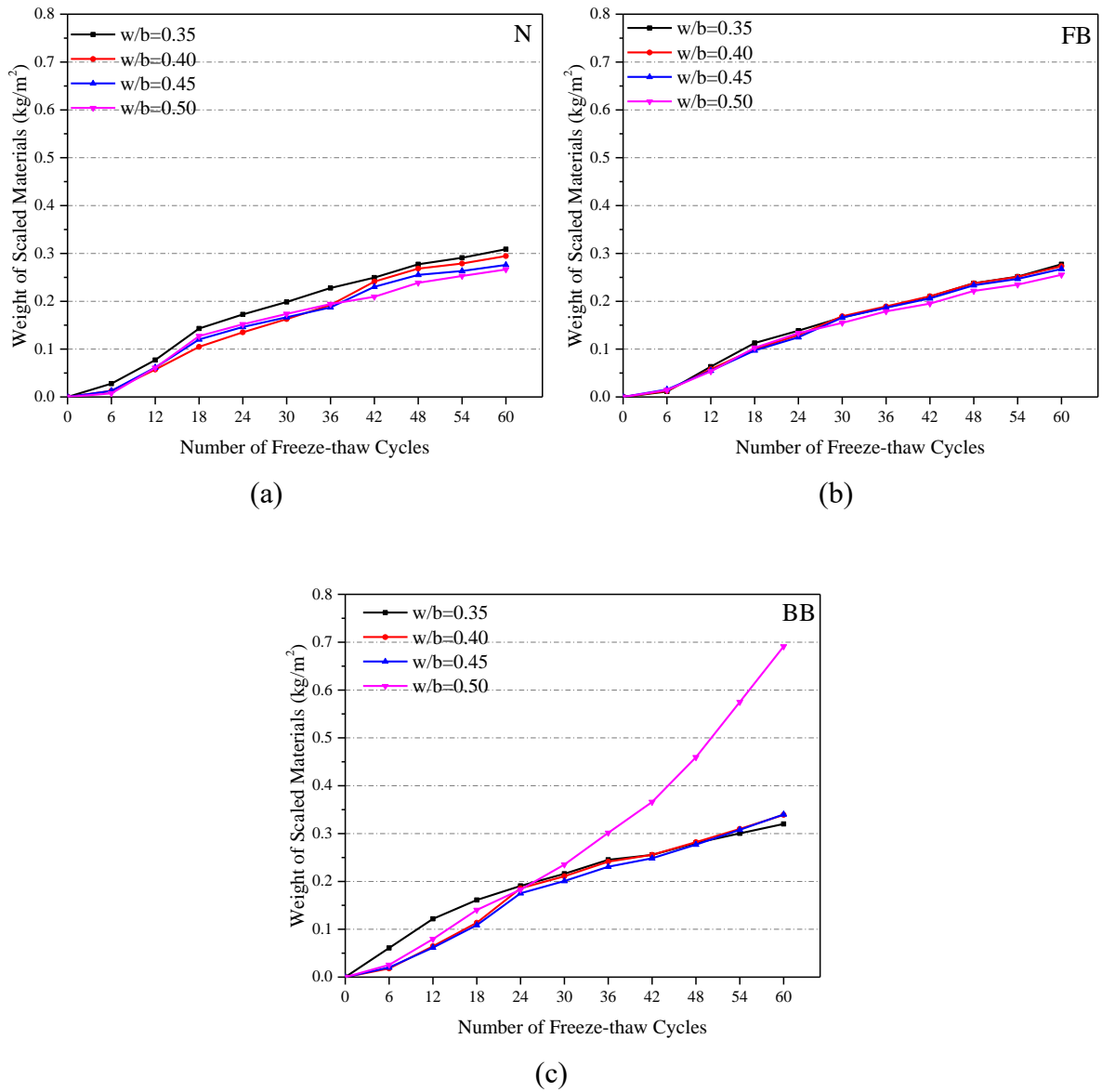


Figure 3.5. Cumulative scaled materials of concrete surface after 60 cycles of freeze-thaw cycles: (a) Ordinary Portland cement; (b) Fly ash cement; (c) Blast furnace slag cement.

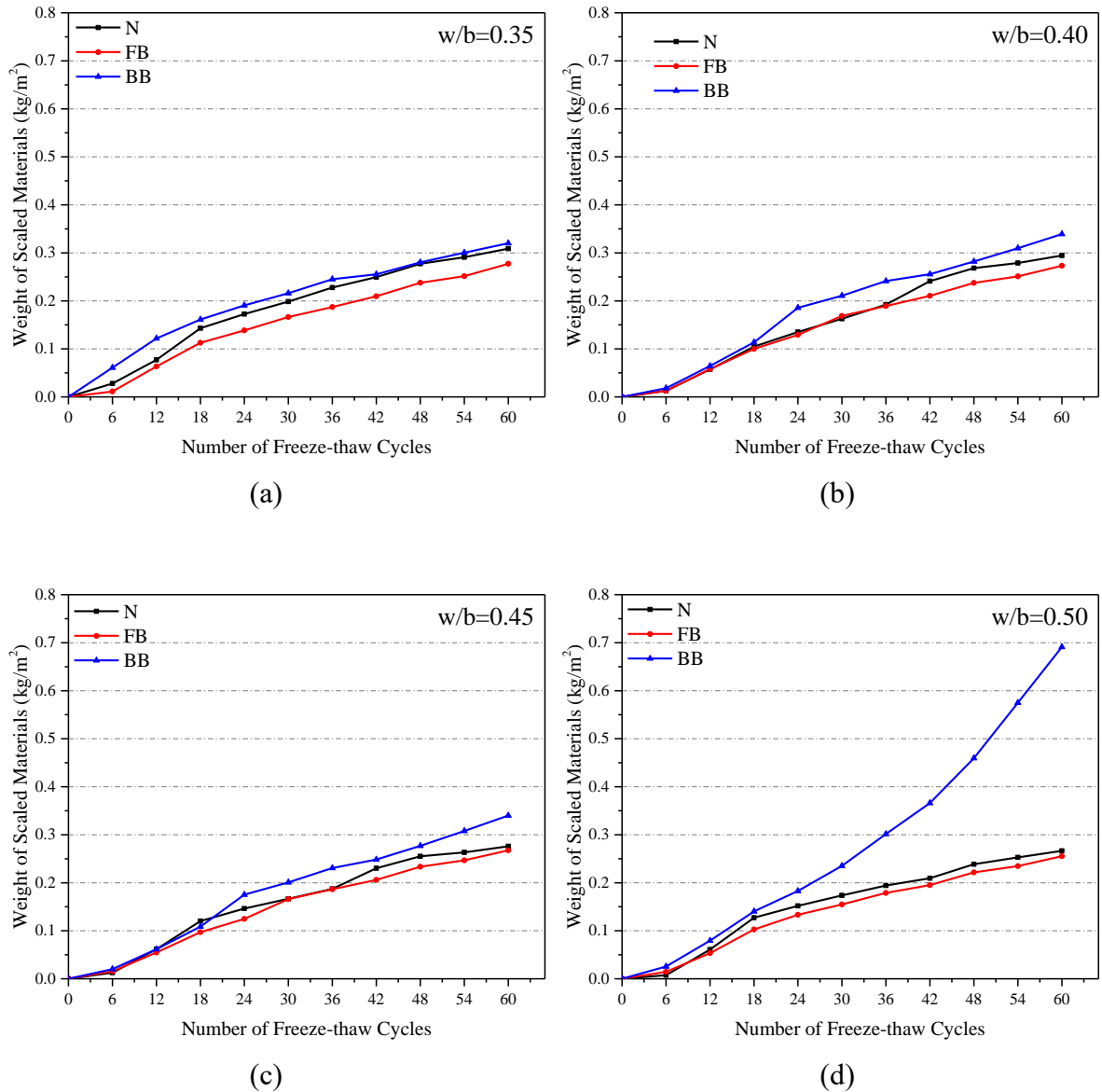


Figure 3.6. Cumulative scaled materials of concrete surface after 60 cycles of freeze-thaw cycles: (a) W/B=0.35; (b) W/B=0.40; (c) W/B=0.45; W/B=0.50.

### 3.4.2 Alkali-silica reaction

Figure 3.7 shows the results of ASR expansion of concrete with different cement types and W/B ratios. It can be noticed that concrete with FB and BB cements have a better ASR expansion resistance as compared to the concrete with N cement. For the concrete specimens with N cement, it can be noticed that when the age was around 70 days, the expansion of concrete specimens exceed 0.1% regardless of W/B ratios. For the concrete specimens with

FB cement, it can be found that a slight expansion of concrete specimens were caused due to the ASR at 182 days and ASR expansion increase with the increasing of W/B. In addition, as can be seen from Figure 3.7(c), for the concrete specimens with BB cement, it shows better ASR expansion resistance regardless of W/B ratios. This reason may be due to the replacement rate of slag in Blast furnace slag cement is 42.5%, while the replacement rate of fly ash in fly ash cement is 10 - 15%.

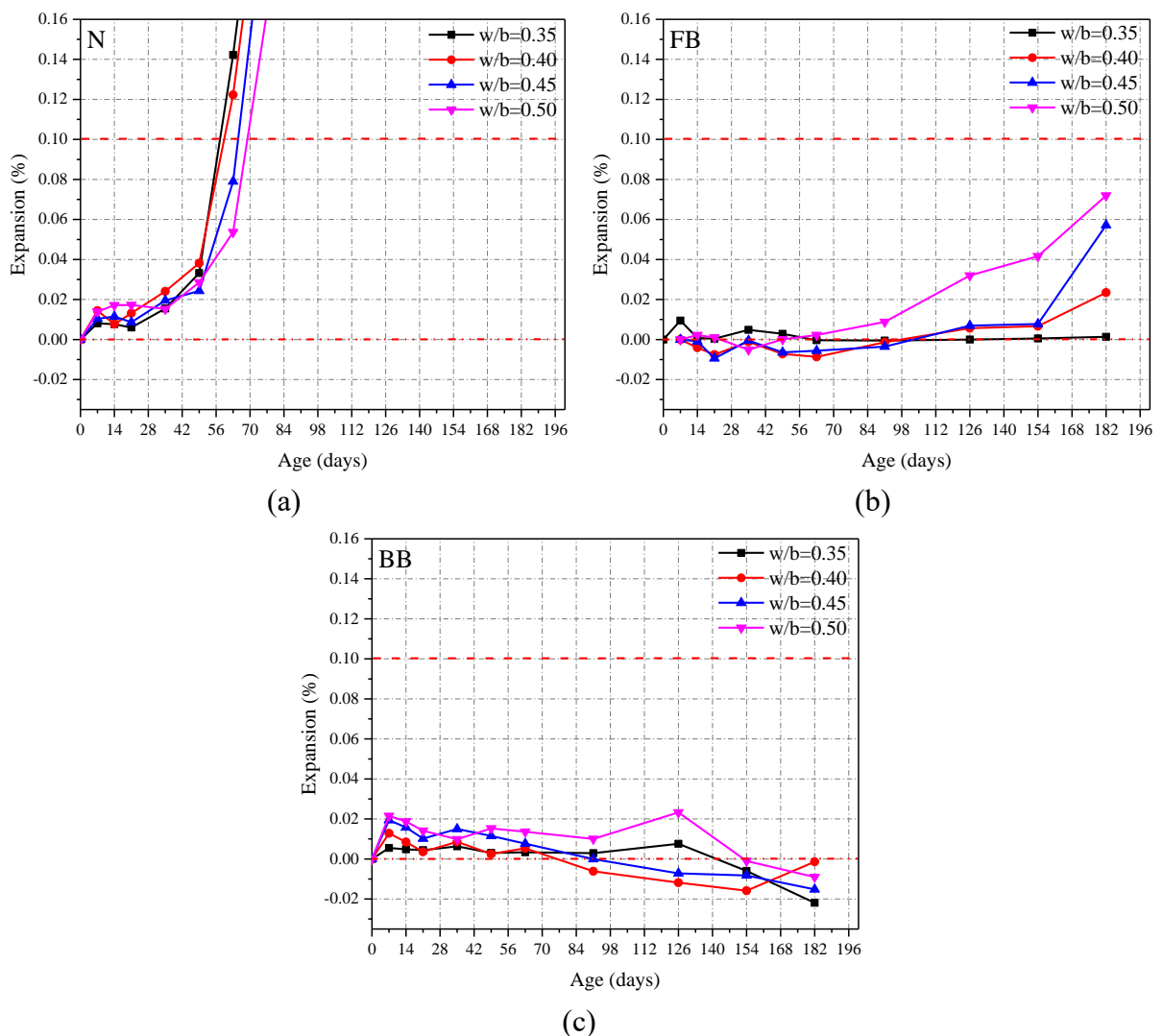


Figure 3.7. Expansion of concrete with (a) Ordinary Portland cement, (b) Fly ash cement, and (c) Blast furnace slag cement at different W/B ratios.

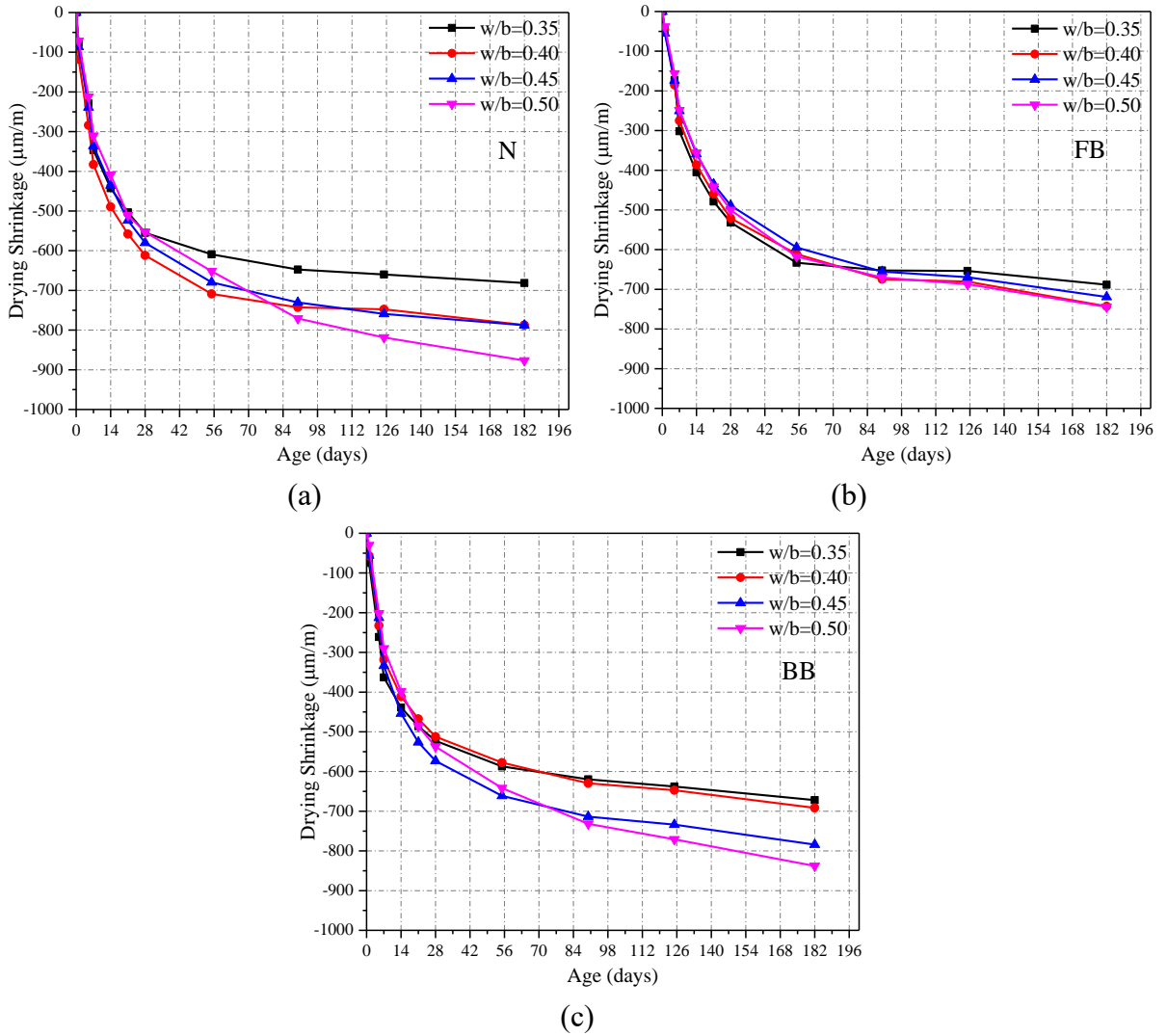


Figure 3.8. Influence of cement types and W/B ratios on drying shrinkage of concrete.

### 3.4.3 Drying shrinkage and mass loss

Figure 3.8 shows the results of drying shrinkage of the concrete specimens with different cement types and W/B ratios for 26 weeks. It can be noticed that concrete specimens with FB and BB cement present better drying shrinkage resistance as compared with concrete specimens with N cement. Also, it can be found that there is a tendency for drying shrinkage to increase with the increase of the W/B ratios regardless of cement types. For the concrete specimens with FB cement, W/B ratios have little influence on drying shrinkage. In contrast, for the concrete specimens with BB cement, there is a more obvious difference between high W/B ratio (0.45 and 0.50) and low W/B ratio (0.35 and 0.40). It shows a better

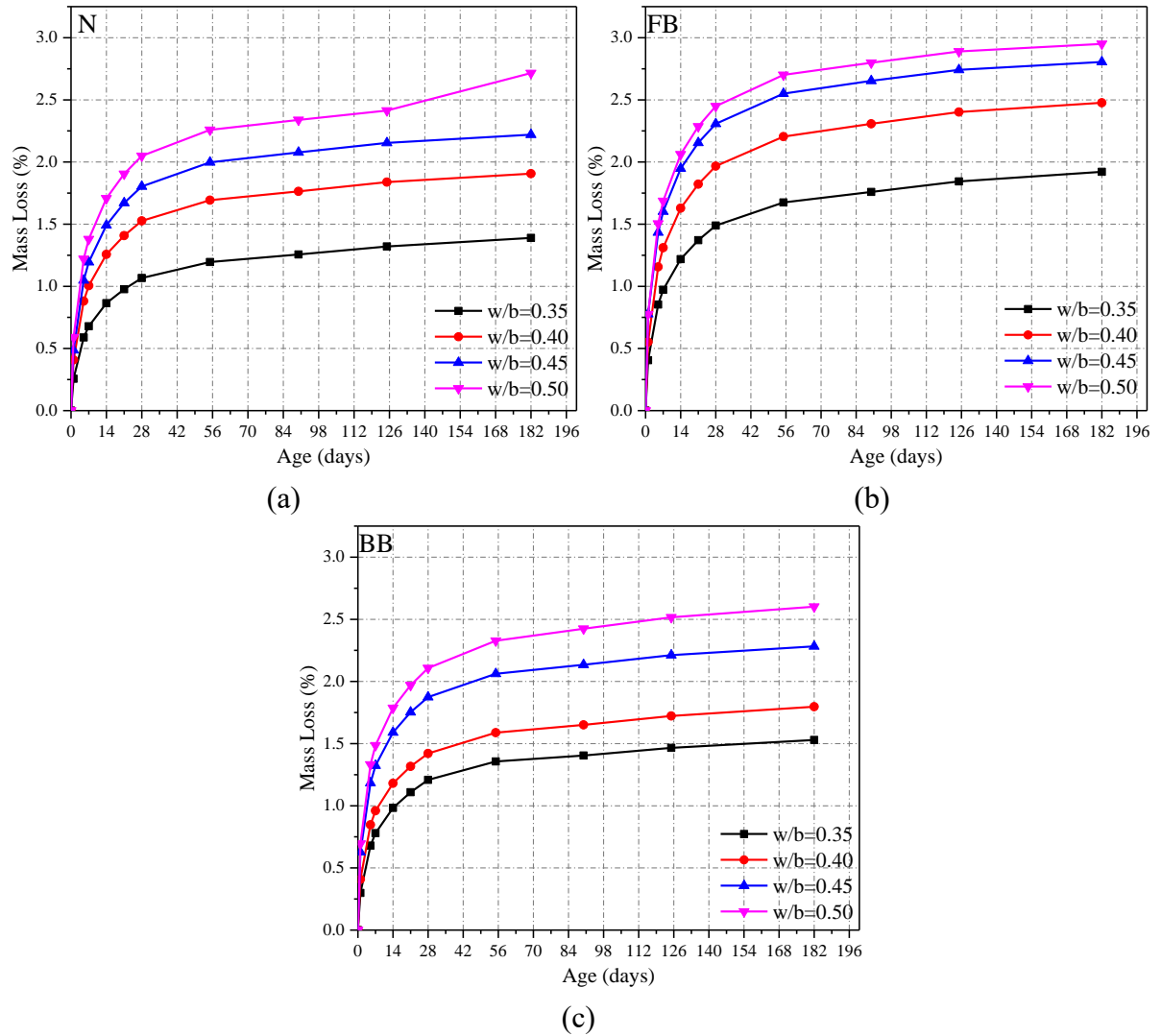


Figure 3.9. Influence of cement types and W/B ratios on mass loss of concrete.

drying shrinkage resistance for the concrete with low W/B ratios and this result has little different as compared with concrete with FB cement.

Figure 3.9 shows the results of mass loss of the concrete specimens with different cement types and W/B ratios for 26 weeks. It can be noticed that the mass loss increases with the increase of W/B ratios regardless of cement types. It also can be noticed that there is a more obvious difference between high W/B ratio (0.45 and 0.50) and low W/B ratio (0.35 and 0.40) for the concrete specimens with BB cement, which echoes to the results of concrete drying shrinkage.

Figure 3.10 shows the relationship between mass loss and drying shrinkage of concrete. It can be found that the initial slopes of the concrete with N cement is larger than that of the concrete with FB and BB cement and the initial slopes decrease with the increase of W/B ratios. This indicates that the drying shrinkage of concrete specimens with N cement increases faster than that of concrete specimens with FB and BB cement with the mass loss at initial age. When the mass loss exceeded around 0.5%, the slopes of the curves increase regardless of W/B ratios and cement types. Also, it can be observed that the slopes of the concrete with FB cement are lower than that of concrete with N and BB cement. It means that concrete specimens with FB cement have better resistance to drying shrinkage than that

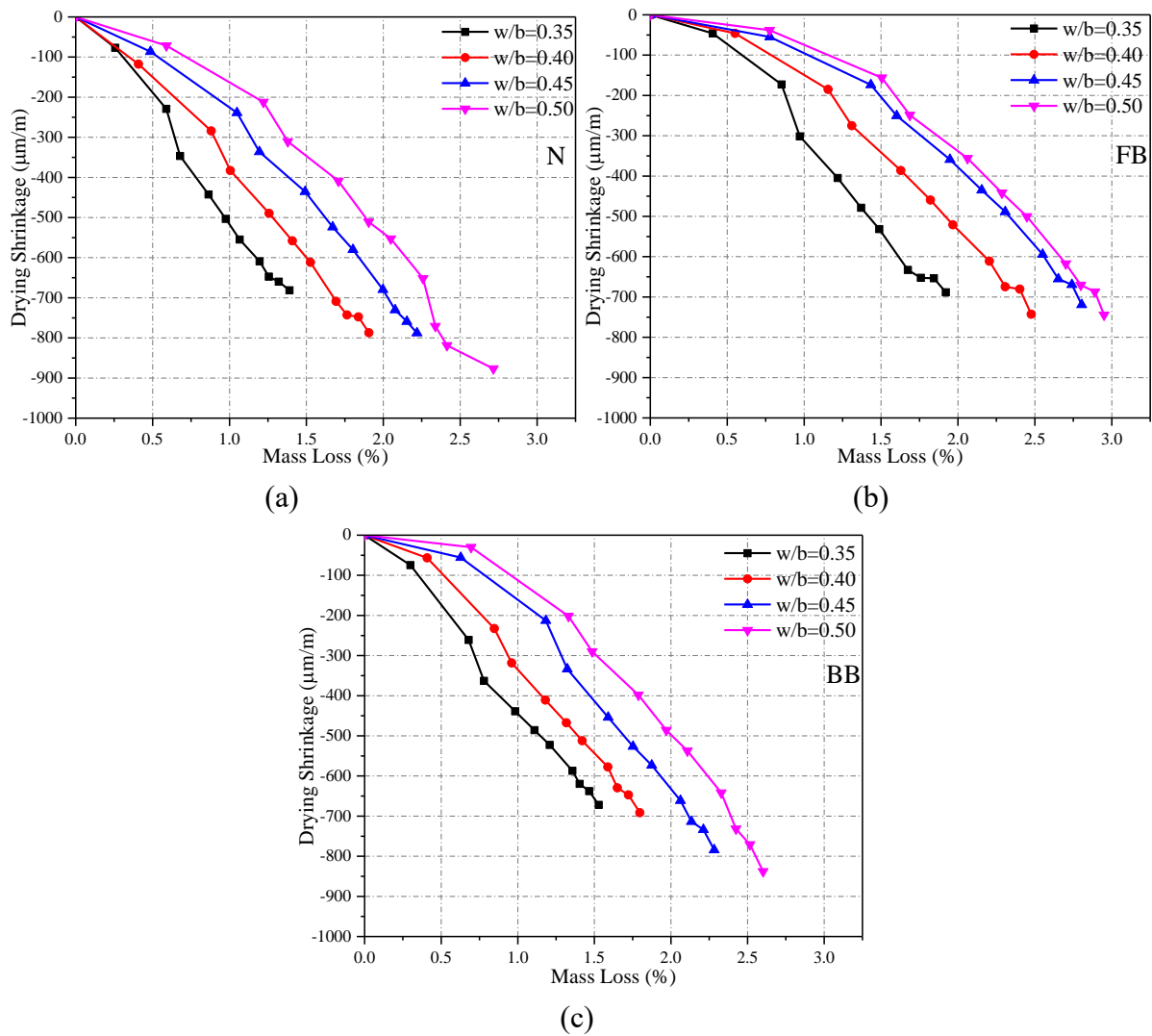


Figure 3.10. Relationship between mass loss and drying shrinkage.

of containing N and BB cement. However, it can also be seen that a lower W/B ratios have a higher resistance to drying shrinkage, especially for the concrete with BB cement.

### 3.4.4 Uniaxial restrained and free shrinkage

Figure 3.11 shows the uniaxial restrained shrinkage of concrete with different cement types and with/without KEA when the W/B is 0.40. It can be found that the addition of KEA effectively compensates the autogenous shrinkage and drying shrinkage of concrete. For FB-

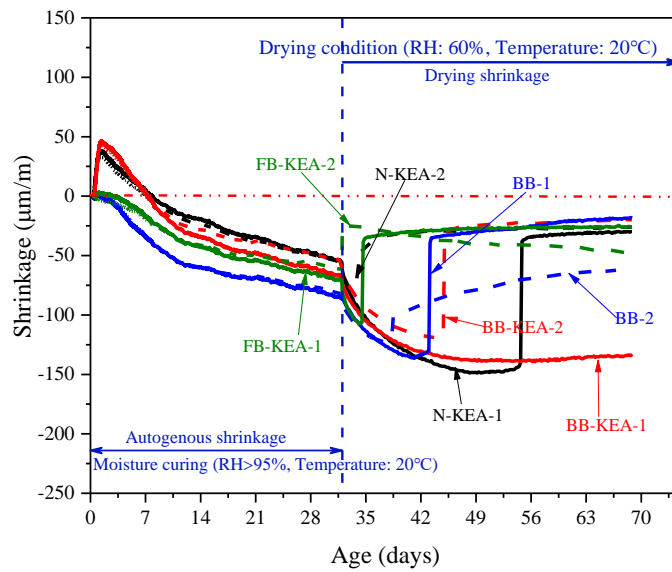


Figure 3.11. Uniaxial restrained shrinkage of concrete.

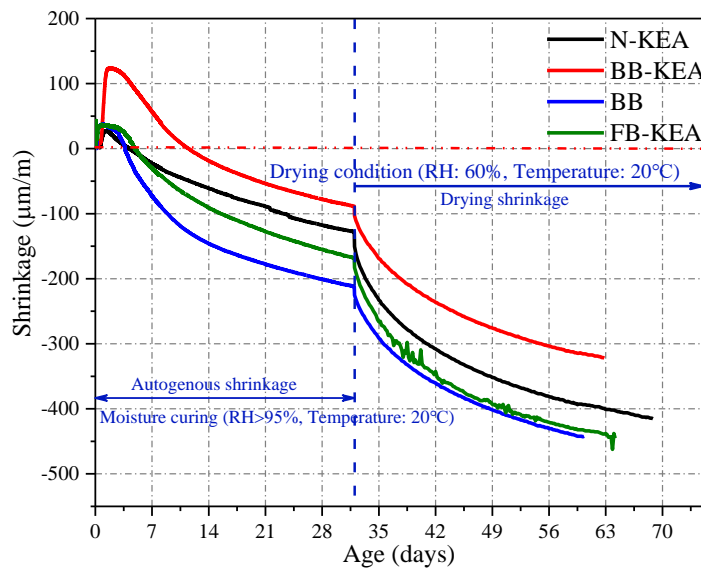


Figure 3.12. Uniaxial free shrinkage of concrete.

KEA, although KEA is added, no expansion is generated. Nevertheless, it can be seen that a good autogenous shrinkage resistance are presented on the concrete with FB cement. In addition, for the N - KEA, BB - KEA, and BB, it can be noticed that a higher risk of restrained shrinkage cracking were presented at the early age when concrete specimens were placed in drying condition (RH: 60%, Temperature: 20°C) as compared with BB - KEA. This result also can be observed in Figure 3.12. Figure 3.12 shows the free shrinkage of concrete with different cement types and with/without KEA when the W/B is 0.40. For the concrete with BB cement and KEA, it can be clearly seen that the addition of KEA effectively compensates for the autogenous shrinkage and drying shrinkage as compared with N - KEA, FB - KEA, and BB.

Figure 3.13 shows the restrained expansion and drying shrinkage of concrete with different cement types and with/without KEA when the W/B is 0.40. For N - KEA, BB - KEA, and BB, it can be noticed that some inflection points appear on the curve at day 188. This may indicates that the concrete may have cracked. On the contrary, the BB - KEA samples not only has better resistance to drying shrinkage, but also no cracks.

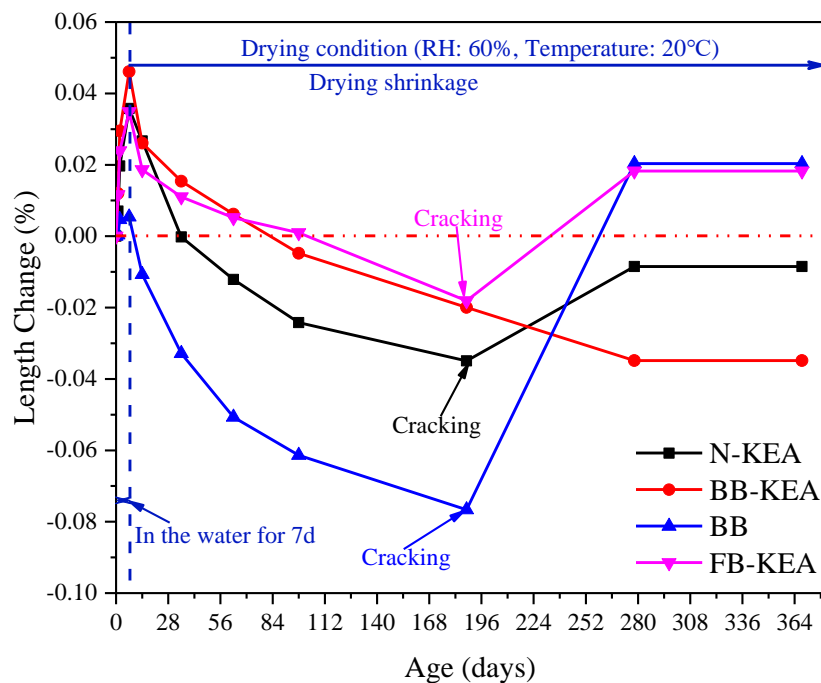


Figure 3.13. Restrained expansion and drying shrinkage of concrete.

To sum up, when the air content of fresh concrete reaches 6%, the cement types and W/B ratios have little effect on the deicing salt scaling resistance of concrete. For alkali-silica reaction of 26 weeks, concrete specimens with cement of N type generated larger expansion, concrete specimens with cement of FB type generated slight expansion, and concrete specimens with cement of BB type has almost no expansion. Concerning drying shrinkage, it shows a better drying shrinkage resistance for the concrete with FB cement, and BB cement with low W/B ratios. In addition, for the uniaxial restrained and free shrinkage, it can be found that BB - KEA (W/B=0.40) shows good resistance to cracking, autogenous shrinkage, and drying shrinkage. Thus, BB - KEA (W/B=0.40) was selected for practical improvement based on the above test results, and its durability will be verified again in the next section.

### **3.5 Field study of concrete durability**

#### **3.5.1 Effect of construction execution process on deicing salt resistance of concrete**

Figure 3.14 shows the effect of different execution processes on deicing salt scaling resistance of mock and actual slabs. For the mock slab (see Figure 3.14(a)), it can be noticed that compared with the concrete after vibration, the concrete after being pumped has higher deicing salt scaling resistance. This may be related to the escape of bubbles caused by vibration. To reduce the escape of air bubbles and ensure sufficient concrete vibration. Thus, 8sec vibration time was used in the actual bridge slab. For the actual slab (see Figure 3.14(b)), it can be seen that similar phenomena is also presented in the actual bridge slab, that is, the reduction in deicing salt scaling resistance after vibration of the concrete. However, the concrete sampled on-site showed poor deicing salt resistance compared with the concrete prepared in the laboratory. One of the reasons that may be related to the concrete was placed in the mold again during the execution process and vibrated causing the secondary escape of bubbles. In addition, another reason may be the inability to meet the curing conditions of constant temperature and humidity on site.

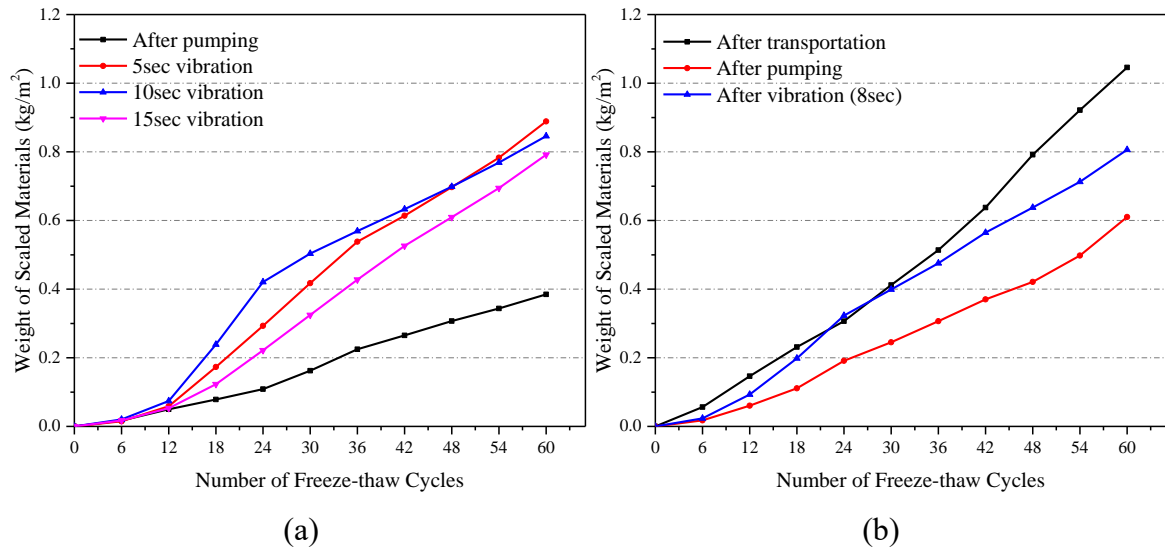


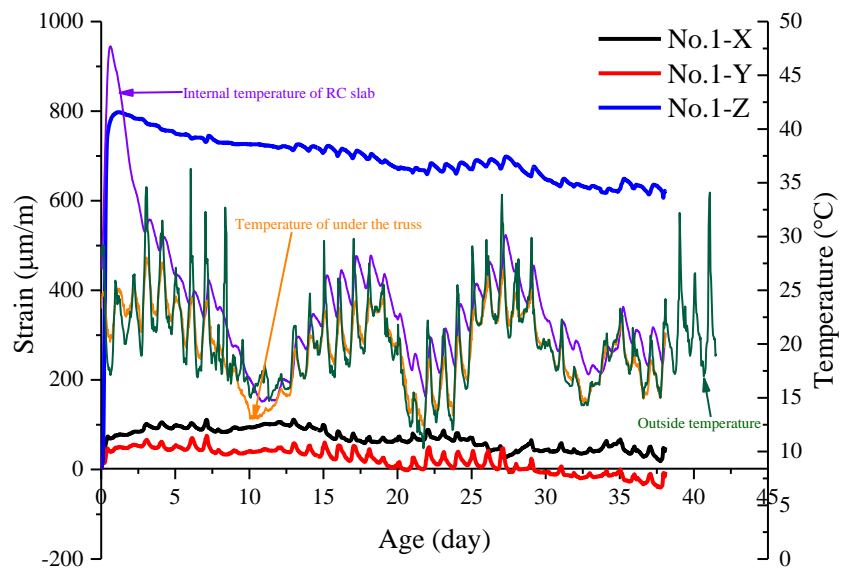
Figure 3.14. Cumulative scaled materials of concrete surface after 60 cycles of freeze-thaw cycles: (a) mock slab; (b) actual slab.

### 3.5.2 Restrained shrinkage of actual RC slab on construction site

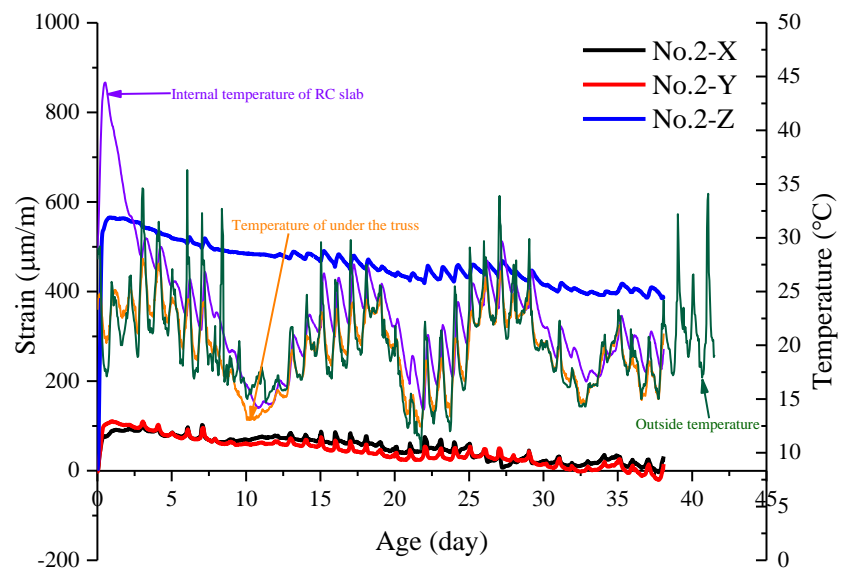
In order to verify the effect of BB - KEA (W/B=0.40) in mitigating shrinkage and reducing the risk of concrete cracking in practical applications. Setting of embedded strain gauges for each measuring point and shrinkage and temperature history of two measuring points on the bridge deck were shown in Figure 3.15. It can be seen that the vertical axis (Z - axis) of the RC slab presented the largest expansion strain at the initial stage due to the negligible structural restraints. It may be caused by the combination of thermal and chemical expansion of mass concrete. It can be noticed that the internal temperature of the RC slab almost reached 50°C in the initial stage. Furthermore, it also can be found that the RC slab did not show significant shrinkage during the initial 38 days, regardless of horizontal (X - axis and Y - axis) and vertical (Z - axis) axis. Therefore, the RC bridge slab has a better effect of early compensation for shrinkage.



(a) Embedded strain gauge measuring point setting



(b) Point No. 1



(c) Point No. 2

Figure 3.15. Restrained shrinkage and temperature history of actual RC slab.

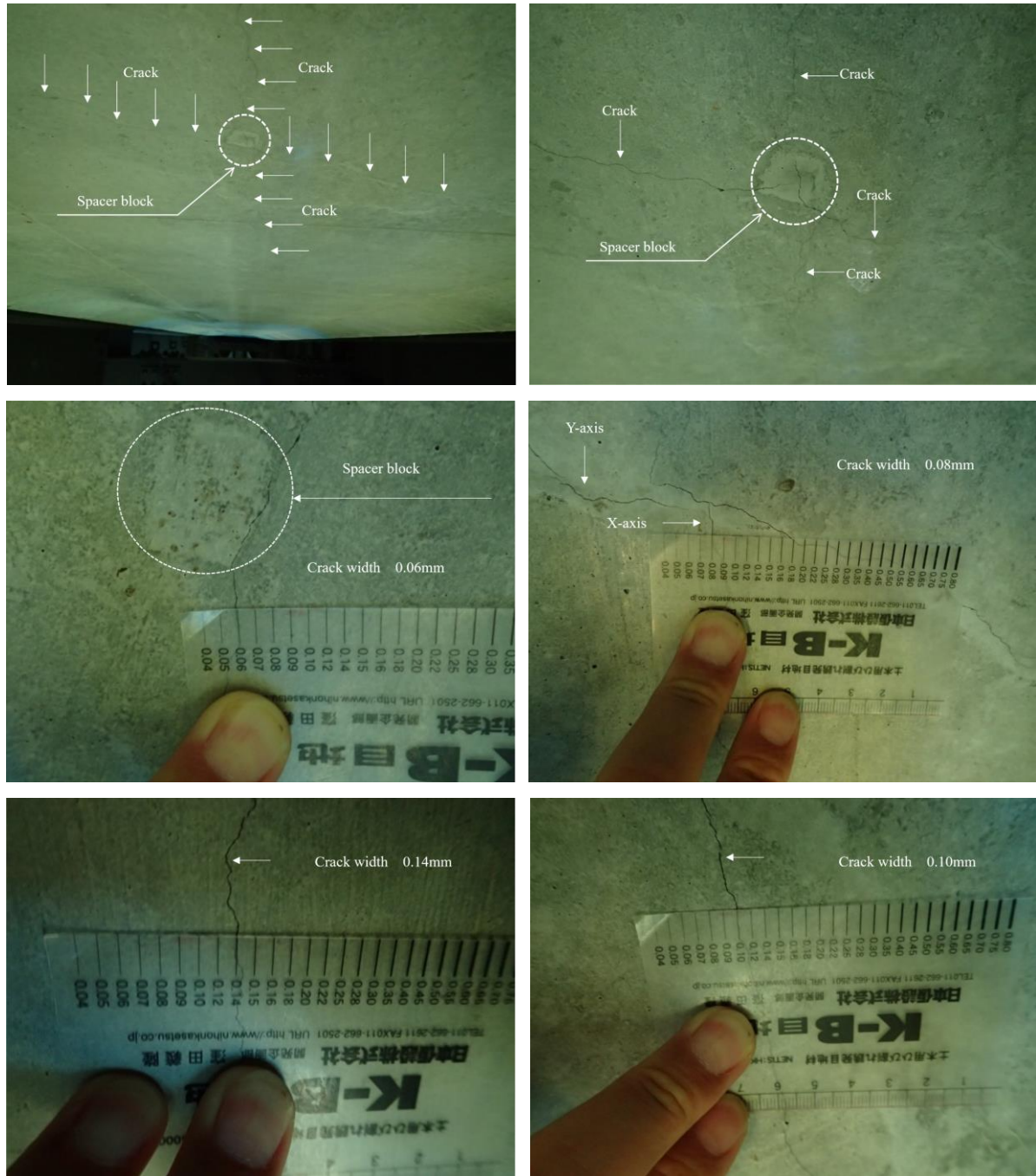


Figure 3.16. Cracks appear at the bottom surface of the RC slab (2019.08.06).

Figure 3.16 shows the distribution of cracks on the bottom surface of the RC bridge slab after 1 year. It can be noticed that the cracks on the bottom surface of the RC bridge slab were almost all around the spacer block. It may be mainly related to the inconsistency

between the hardened spacer blocks and the shrinkage of the fresh concrete. Also, it can be observed that the maximum crack width was 0.14 mm.

### 3.6 Summary

In this chapter, the deicing salt scaling resistance, ASR, drying shrinkage and mass loss and uniaxial restrained and free shrinkage with various cement types and W/B ratios were conducted. Moreover, in order to ensure the final quality of the RC bridge slab and continuous improvement, the deicing salt scaling resistance of each execution process on mock RC slab, restrained shrinkage and cracking of actual RC slab were conducted. The following summary may be drawn:

- Concrete with FB cement has a better deicing salt scaling resistance than that of N and BB. Nevertheless, when the air content of fresh concrete reaches 6%, it has little influence in terms of deicing salt scaling resistance regardless of cement types and W/B ratios. In addition, for the concrete specimens with BB cement, it shows better ASR expansion resistance regardless of W/B ratios.
- Drying shrinkage and mass loss increase with the increase of W/B ratios. Moreover, concrete specimens with FB cement have better resistance to drying shrinkage than that of containing N and BB cement. However, it can also be seen that a lower W/B ratios have a higher resistance to drying shrinkage, especially for the concrete with BB cement.
- Concerning uniaxial restrained and free shrinkage, it can be found that BB - KEA (W/B=0.40) shows good resistance to cracking, autogenous shrinkage, and drying shrinkage.
- The reduction in deicing salt scaling resistance after vibration of the concrete. However, in terms of vibration time, there is little difference in the effect of concrete on the deicing salt scaling resistance. This may be related to the secondary random escape of bubbles caused by the secondary vibration when the concrete sample is loaded into the mold on site.

- Concerning the restrained shrinkage of actual RC slab on construction site, the use of BB40 - KEA has a better effect of early compensation for shrinkage. In addition, through the observation of the cracking of the RC slab 1 year later, it was found that the cracks appeared at the bottom of the RC slab and were almost mainly concentrated around the spacer blocks (the maximum crack width was 0.14 mm).

### 3.7 Reference

- Tanaka, Y., Ishida, T., Iwaki, I., & Sato, K. (2017). MULTIPLE PROTECTION DESIGN FOR DURABLE CONCRETE BRIDGE DECK IN COLD REGIONS. *Journal of JSCE*, 5(1), 68-77. doi:10.2208/journalofjsce.5.1\_68
- Zerin, A. I., Hosoda, A., & Komatsu, S. J. J. o. S. E., A. (2018). Numerical simulation of early age expansion and autogenous shrinkage behavior of blast furnace slag concrete with expansive additive. *64*, 666-674.

## CHAPTER 4 AIR VOID SYSTEM FOR RC SLAB OF BRIDGE

### 4.1 General

To attain frost resistance of concrete structures, the air void system in hardened concrete play an important role. As a target of RC slab in this chapter, the air void system of RC bridge slabs of Mount Aobuna No. 1 Bridge and Shinyanagibuchi Bridge were studied.

Concerning the RC slab of Mount Aobuna No. 1 Bridge, the effect of concrete with the different mix proportions and the execution process on air void characteristics were investigated. The results showed that the air void frequency increase with water-binder ratio decrease, especially the diameter 0-200 $\mu$ m. Confirming the air void in the range of 0-200 $\mu$ m was one of the significant factors for featuring the distribution of air void and the spacing factor.

For the RC slab of Shinyanagibuchi Bridge, the deicing salt scaling resistance and the air void characteristics of mock and actual RC bridge slabs under each execution stage were investigated. The results showed that the dosage of the expansive agent (EA) has little influence on deicing salt scaling resistance of concrete. PP fiber can improve the anti-scaling performance of concrete surfaces, however, the curing methods of fiber concrete would be one of the significant factors to determine the surface scaling resistance. It can be confirmed that the void frequency is one of the significant factors for evaluating the spacing factor of concrete. Moreover, the NDT test in-situ shows that the actual RC slab has fine compactness. All in all, the considerable results in this study can be provided by tasking the mock RC slab for practical improvement of the actual RC slab. In addition, the rise of target air content, using PPF, and the adequate wet curing period would be contributed to make durable concrete for scaling resistance of concrete.

## 4.2 Introduction

The deteriorations of concrete due to the severe environment and climate are the major problems affecting the long-term durability of the concrete structure. Many researches have been conducted to improve the durability of concrete nearly a century, such as deicing salt scaling resistance, corrosion of reinforcement due to freezing-thawing action, chloride ion penetration, alkali-silica reaction and so on (Kim et al., 2016; Shields, Garboczi, Weiss, & Farnam, 2018). However, it would need the key to attain the durability of concrete which is practically treated with the deterioration resistance focusing on actual concrete structures.

Recently years, the air-entraining (AE) agent is commonly utilized to improve freeze-thaw resistance of concrete. Air voids entrained by AE agent can reduce the hydrostatic pressure generated by ice formation in cement paste during freeze-thaw cycles (Michel Pigeon, 2014). Therefore, air voids in concrete play an important role in protecting structure from frost damage. However, the distribution characteristics and the spacing factor of air void are two important factors to ensure durable concrete structures. Promentilla et al. (Promentilla & Sugiyama, 2010) found that the number of air void increase in the range from 20 $\mu$ m to 200 $\mu$ m for mortars with AE agent. Referring to the suggestions of Pigeon and Powers (Michel Pigeon & Malhotra, 1995; Powers, 1945), smaller spacing factor of air void is one of the factors to improve the frost resistance of concrete. Yuan et al. (Yuan, Wu, & Zhang, 2018) found that the mass loss of concrete due to freezing and thawing decreases with the average air void diameter and the spacing factor decreases. Almost studies have tended to conduct targeting on the relationship between the air voids and frost resistance of concrete in laboratory. Research on the distribution characteristics and spacing factor of air void of concrete with the multiple mix proportions and the construction conditions on site were also relatively few.

In addition, the management of infrastructures has been focused on as the maintenance cost of existing structures rises rapidly with an increase in the number of deteriorated RC structures in the long-term usage. For example, over 40% of bridges in the Tohoku region of

Japan have been reached a usage period of more than 50 years by 2025, which means a large number of bridges would have potential risks on its performance (Ministry of Land, 2017). Lifetime improvement of these concrete structures is the most important issue to reduce the maintenance costs in the future. Moreover, since about 30 years ago, on the road in the cold region of Japan, the deicing salt has been spread for traveling safety of the car. The heavy spreading of deicing salt was induced frost damage of the cover concrete as surface scaling, which leads to a decrease in the surface quality of concrete and accelerates the multiple deteriorations of structures. Especially, the RC slab of the bridge has been greatly affected, and it will be strongly required more high durability.

On the other hand, in Tohoku region, it has been promoted the construction project of infrastructures after the great east Japan earthquake and tsunami disaster in 2011. Lifetime improvement of these concrete structures is most important problem to reduce the future maintenance costs. For this reason, the Tohoku Regional development bureau has published the manual for counterplan to frost damage of concrete structures under spreading deicing salt (Bureau, 2017). This manual was proposed increase of the target air content at loading of freshly mixed concrete on site. That is to cover decreasing of air content while the execution process of construction and to attain air content in hardened concrete. In case of concrete structures under most severe environment on frost damage risk, the W/B less than 45% and the target air content of 6% were requested. Therefore, the investigation of properties of air void system in construction stage would be significant.

In this chapter, for the RC slab of Mount Aobuna No. 1 Bridge, the influences of mixture proportions, the vibration time and the pumping process of concrete on the distribution characteristics of air void were studied in laboratory and construction site of RC slab. Moreover, the relationship between spacing factor and air void frequency in different diameter ranges was discussed.

For the RC slab of Shinyanagibuchi Bridge, polypropylene fiber (PPF) was utilized, to prevent the hazards for the third party as the flaking of concrete. The scaling resistance test

with different dosage of expansive agent (EA) were investigated in laboratory, and the de-icing salt scaling resistance and the air void characteristics of mock and actual RC bridge slabs under each construction stages were investigated (such as non-fiber concrete after transporting, fiber concrete before pumping, fiber concrete after pumping and fiber concrete after vibrating (Time: 5 sec, 10 sec, 15 sec). Simultaneously, the surface air permeability and the surface water absorption of the actual slab were measured with a non-destructive test (NDT) method to evaluate the surface quality of the RC slab. These showed that the frost resistance as deicing salt scaling was improved after adding PPF. It may be covered the reducing of deicing salt resistance of concrete even though decreasing the quality of air void character while the pumping and vibrating compaction in construction processes. In addition, the influence of curing methods on deicing salt scaling resistance of concrete was also evaluated.

### 4.3 RC slab of Mount Aobuna No. 1 Bridge

#### 4.3.1 Materials and mix proportion

The mix proportions of concrete are shown in Table 4.1. In these mixture proportions of concrete, 3 types of cements (Ordinary Portland cement (N: density is 3.16 g/cm<sup>3</sup>), Fly ash cement (FB: density is 2.96 g/cm<sup>3</sup>), Blast furnace slag cement (BB: density is 3.04 g/cm<sup>3</sup>)), four kinds of water-binder ratios (50%, 45%, 40%, 35%) were used. The target of air content and slump of concrete were 6±1.0% and 12±2.5 cm, were adjusted by air-entraining (AE) agent and superplasticizer, respectively. The maximum size of coarse aggregate

Table 4.1. Mix proportions of concrete.

Mixture type	Cement type	W/B (%)	s/a (%)	Unit content: kg/m <sup>3</sup>					
				W	C	S	G	EA	AE agent
N50	N	50	43.3	170	320	740	1102	20	3.06
N35	N	35	34.4	170	466	547	1187	20	7.78
FB50	FB	50	42.9	168	316	730	1102	20	3.02
FB35	FB	35	33.7	168	460	531	1187	20	7.20
BB50	BB	50	42.9	170	320	730	1102	20	3.06
BB40	BB	40	37.7	170	405	614	1151	20	4.25
BB35	BB	35	33.7	170	466	531	1187	20	7.29

※N, FB, BB are cement types and 50, 45, 40, 35 are water-binder ratios.

was 25 mm. The fine aggregates and the coarse aggregates used in the test were pit sand and crushed stone, respectively. Expansive additive was also used in order to reduce cracks.

### 4.3.2 Method

#### (1) Specimens

Two types of concrete specimens were used in this study (Figure 4.1). One was prism specimen (Size:  $100 \times 100 \times 400$  mm) that was casted in laboratory and in actual construction site of RC slab of bridge. Another is cylindrical core (Size:  $\phi 150 \times 200$  mm) sampled from RC mock slab specimen (Size:  $5 \times 10.5 \times 0.2$  m, see Figure 4.2). The influence of concrete vibration (5 sec, 10 sec, and 15 sec) on air void was surveyed with RC mock slab specimen, the influence of pumping of concrete was also surveyed with sampling specimens

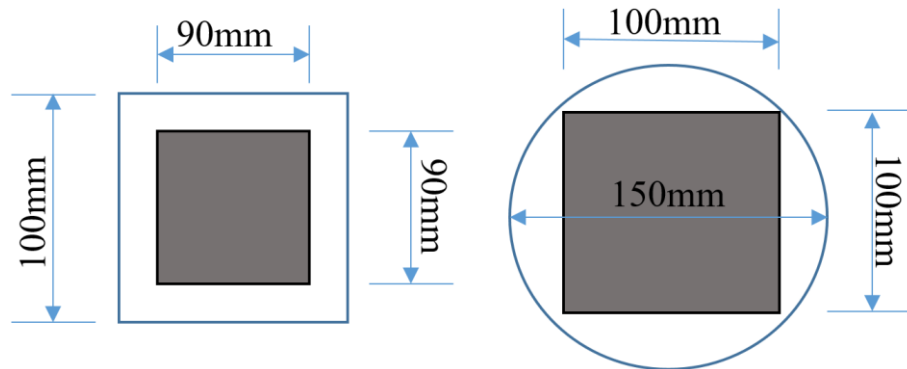


Figure 4.1. Size of samples for observation of air void.

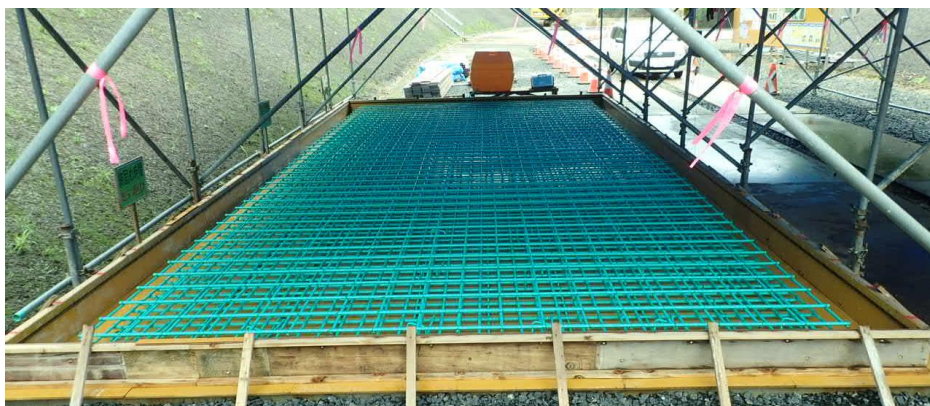


Figure 4.2. RC mock slab specimen.

Table 4.2. Parameters of air void in laboratory.

Parameters	N50	N35	FB50	FB35	BB50	BB40	BB35
Paste content [%]	27.79	32.43	28.07	32.92	28.16	30.96	32.96
Total length of traverse [mm]	2700	2700	2700	2700	2700	2700	2700
Total number of air voids	1296	1450	1134	1470	1146	852	1446
Air content of fresh concrete [%]	6.6	6.3	6.4	7.1	7.0	6.2	7.0
Air content of hardened concrete [%]	7.3	6.6	4.7	7.0	6.4	5.8	7.8
Air content in diameter less than 500 $\mu\text{m}$ [%]	5.1	3.8	4.0	5.3	4.5	3.8	6.1
Air content in diameter less than 200 $\mu\text{m}$ [%]	2.1	2.4	2.1	2.5	1.9	1.4	2.7
Spacing factor [ $\mu\text{m}$ ]	138	111	132	130	147	188	143

Table 4.3. Parameters of air void on site.

Parameters	Mock slab				Actual construction site		
	AP	Vib 5sec	Vib 10sec	Vib 15sec	BP	AP	After Vib
Paste content [%]	31	31	31	31	30.96	30.96	30.96
Total length of traverse [mm]	2700	3300	3300	3300	2700	2700	2700
Total number of air voids	1439	1604	1242	1295	1402	1492	1536
Air content of fresh concrete [%]	6.4	5.8	4.3	5.4	6.0	—	—
Air content of hardened concrete [%]	6.6	6.7	6.3	6.9	5.1	5.1	6.4
Air content in diameter less than 500 $\mu\text{m}$ [%]	5.3	5.1	4.4	4.7	3.8	4.1	4.8
Air content in diameter less than 200 $\mu\text{m}$ [%]	2.9	2.5	1.7	1.8	2.5	2.6	2.9
Spacing factor [ $\mu\text{m}$ ]	128	139	174	172	109	106	114

Notes: “After pumping” is abbreviated as AP; “Vibration” is abbreviated as Vib; “Before pumping” is abbreviated as BP.

on actual construction site. The RC mock slab specimen was produced in Towada area of Aomori prefecture (2018.7), and after the RC slab of bridge was also constructed in that same place (2018.7). The mix proportion on site was adopted the concrete of BB40. Wet curing for one month is adopted in all specimens and actual construction.

## (2) Testing the air void of concrete

The method of testing the air void of concrete was according to ASTM standard C457 that is procedure A (Linear Traverse Method)(ASTM, 1998). The total number of air void, the air content of hardened concrete, the spacing factor, the total length of traverse and the paste content are shown in Table 4.2 and Table 4.3, and the formula for calculating the spacing factor ( $\bar{L}$ ) is presented in Eq. (1).

The air void of concrete was observed with different length of traverse. Therefore, using the air void frequency instead of number of air void to feature the distribution characteristics

of air void in hardened concrete. The air void frequency can reflect as the number of air void on the unit traverse length (m), the air void frequency increase with the number of air void increase. The formula for calculating the void frequency (n) is presented in Eq. (2).

$$\bar{L} = \frac{3}{\alpha} \left[ 1.4 \left( 1 + \frac{P}{A} \right)^{\frac{1}{3}} - 1 \right] \quad (1)$$

Where,

$\bar{L}$ : Spacing factor ( $\mu\text{m}$ );

$\alpha$ : Specific surface ( $\mu\text{m}^2 / \mu\text{m}^3$ );

P/A: Paste-air ratio.

$$\text{Void Frequency (n)} = \frac{N}{T_t} \quad (2)$$

Where,

N: Total number of air voids;

T<sub>t</sub>: Total length of traverse (m).

### 4.3.3 Results and discussions

#### *Distribution characteristics of air void*

Air void parameters of specimens made in laboratory are presented in Table 4.2. Air content of fresh concrete is in the target air content range, but in case of the concrete of FB50, the air content of hardened concrete have great decrease, it may be due to the lower retention of air void in fresh concrete. There is no clear correlation between the air content in fresh and the number of air void in hardened concrete. Comparing the air content of hardened concrete in three different diameter ranges, it is confirmed that in the case of air content of diameter less than 200  $\mu\text{m}$ , the air content increase with water-binder ratio decrease except the concrete of BB40. The part of air content of hardened concrete increased than that of fresh concrete. It may be including the sampling error due to limited measurement of the fresh concrete.

The distribution of air void frequency with six mix proportions are shown in Figure 4.3. It is noticed that a large number of air void frequency was presented in the range of diameter 51 - 300  $\mu\text{m}$  than other diameter. Especially in the fine air voids, the air void frequency of  $W/B = 35\%$  are greater than that of  $W/B=50\%$ , regardless of different cement type. This reason is believe to be due to the retention of air void in fresh concrete, it would depend on increasing viscosity of concrete as unit powder content ( $W/B$ ), and on the dosage of AE agent. Simultaneously, while the air void frequency gradually decrease with the range of diameter from 50  $\mu\text{m}$  to 500  $\mu\text{m}$  increase. However, the range of the diameter 0 – 50  $\mu\text{m}$  and greater than 500 $\mu\text{m}$  were different from the previous trend. When the ranges of diameter is 0 – 50  $\mu\text{m}$  and greater than 500  $\mu\text{m}$ , these have fewer air void frequency. In case of the range of diameter greater than 500  $\mu\text{m}$ , the concretes with fly ash (FB) have fewer air void frequency than other two cement types (N, BB). It would be because of unit content of powder material and fine aggregates.

From Figure 4.3, it is confirmed that the air void distribution in hardened concrete would be composed from three part with formation like an arch shape. The range of diameter 0 – 200  $\mu\text{m}$  is fine part that may be air entraining by AE agent. The range of diameter greater

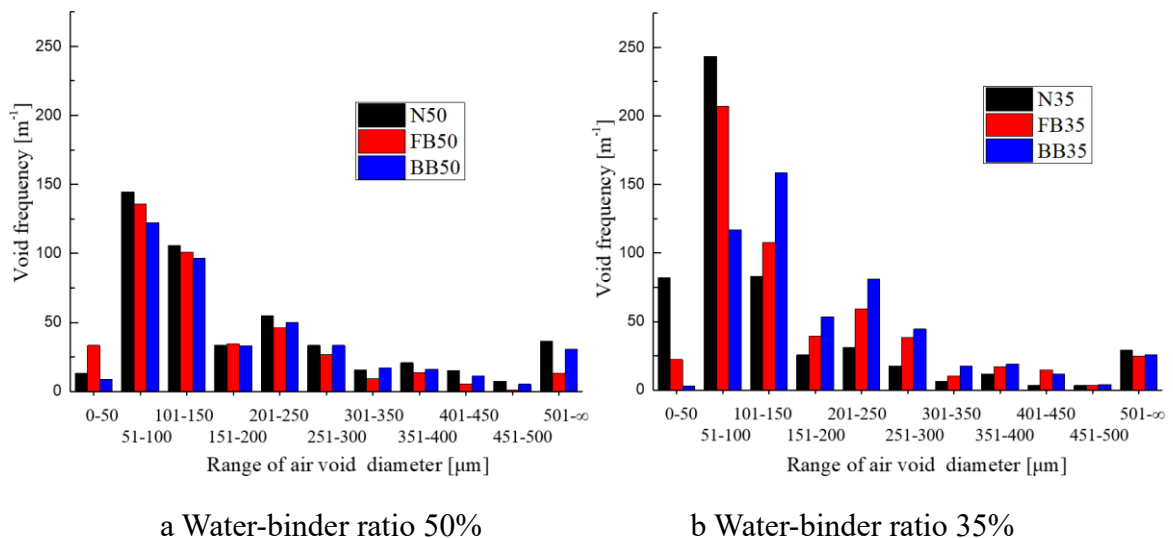
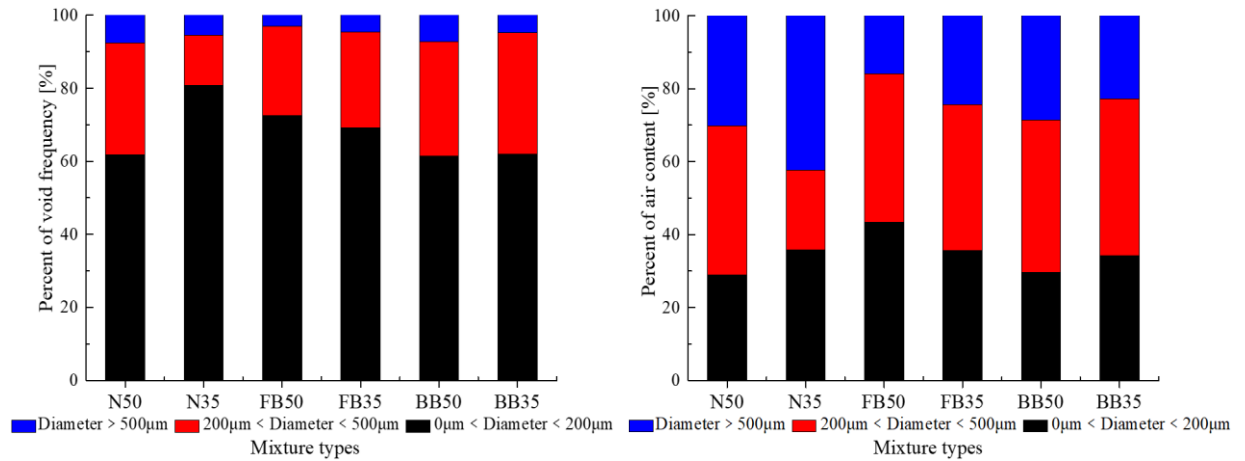


Figure 4.3. Distribution characteristics of air void.



a Distribution of percent of void frequency      b Distribution of percent of air content

Figure 4.4. Measurement of laboratory.

than 500 µm is large part that may be forming by entrapped air during mixing of concrete. The range of diameter 201 - 500 µm is middle part that may be combining the entrained air and the entrapped air. Then, the air void characteristics of concrete could be considered from the viewpoint of these three part given within a distribution.

#### *Air void frequency and air content of concrete made in laboratory and construction site*

##### (1) Measurement on laboratory specimen

The relationships in diameter range with the percent of air void frequency and the percent of air content are shown in Figure 4.4. From these figures, the percent of air void frequency and the percent of air content are divided into three parts by diameter range that include 0 - 200 µm, 201 - 500 µm and greater than 500 µm. It can be noticed that in case of the range of diameter 201 - 500 µm and greater than 500 µm, the percent of air content was greater, but the percent of air void frequency was less. On the other side, in case of the range of diameter 0 - 200 µm which is entrained by AE agent, is contrary to the above results, and the percent of air void frequency was greater than that of air content. Moreover, the percent of air void frequency in the diameter 0 - 200 µm is greater than 50%, compare to the range of other diameter. In case of N35, the percent of frequency of fine air voids is most large. This reason would depend on dosage of AE agent. From these results, the value of fine air

void frequency than that of air content will be promising as important key to evaluate the effect of air entrainment.

(2) Measurement on RC mock slab specimen

Parameters of air void on RC mock slab specimen with different vibrating time of concrete, are presented in Table 4.3. Air content of fresh concrete is in the target air content range. The air content of hardened concrete tends to decrease with the increase of vibration time in RC mock slab.

The concrete of BB40 was used on RC mock slab specimen. Influence of vibration time on distribution of air void frequency in hardened concrete are shown in Figure 4.5. It can be noticed while the fine diameter 0 - 200  $\mu\text{m}$ , the air void frequency tends to decrease with vibration time increase. While the diameter greater than 300  $\mu\text{m}$ , the air void frequency increase with vibration time increase, especially in the diameter greater than 450  $\mu\text{m}$ . The reason of this result that the many fine air voids may develop into larger voids with vibration time increase.

Figure 4.6 shows the characteristics distribution of percent of air void in certain range. For these two figures, in case of the diameter 0 - 200  $\mu\text{m}$ , the percent of air content and the percent of air void frequency decrease with vibration time increase. It is consistent with the above conclusion. While the vibration of 15 sec, the percent of air void frequency decrease in about 20%.

(3) Measurement on specimen made in actual construction stage

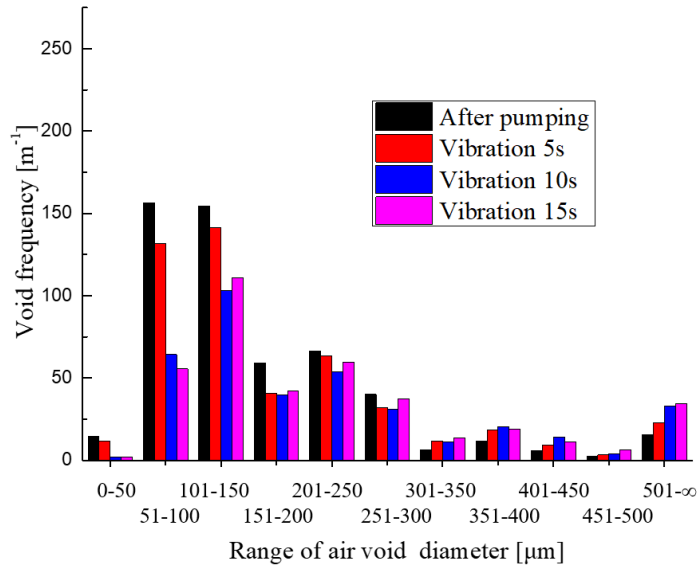
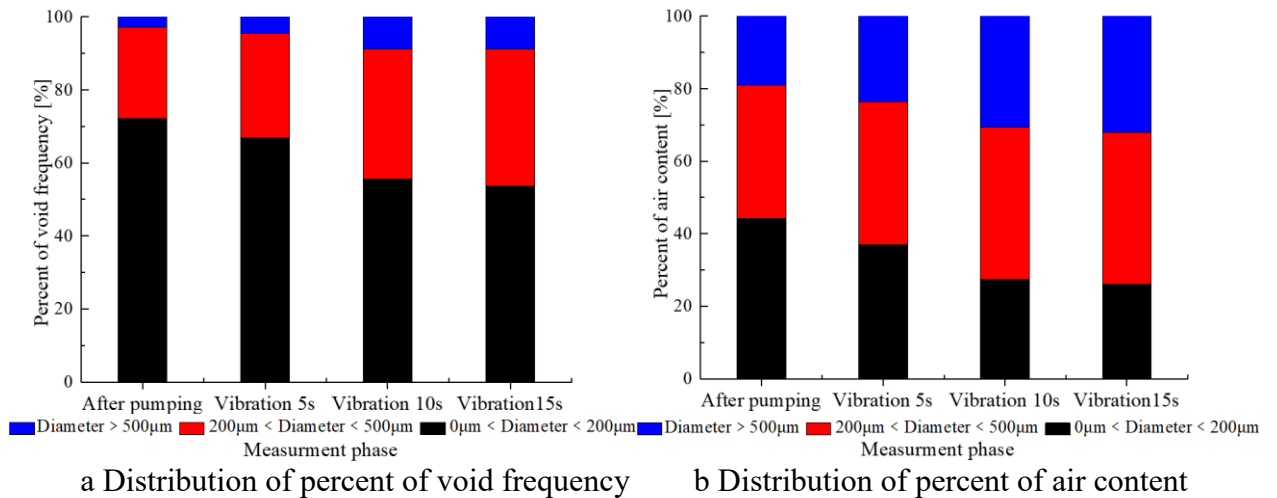


Figure 4.5. Distribution characteristics (mock slab).



a Distribution of percent of void frequency

b Distribution of percent of air content

Figure 4.6. Measurement of mock slab.

Parameters of air void on specimen made in construction stage, are also presented in Table 4.3. Air content of fresh concrete is in the target air content range. Significant decrease of the air content in hardened concrete was confirmed with the pumping process in actual construction.

The vibration time of 8sec was used on compacting concrete in the actual construction. Influence of before pumping, after pumping and after compacting on distribution of the air void in hardened concrete were shown in Figure 4.7 and Figure 4.8. It can be indicated when the range is in diameter 0 - 200 μm, changing of the percent of air void frequency and the

percent of air content with the process of pumping concrete is few (see Fig.8 a and b). Because, the pumping height is relatively short, and the vibration time is not excessive.

*Relationships in spacing factor with air content and air void frequency*

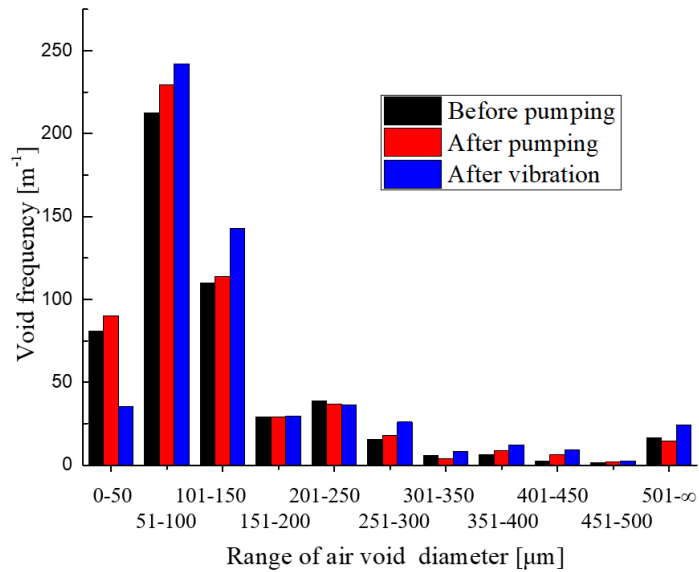
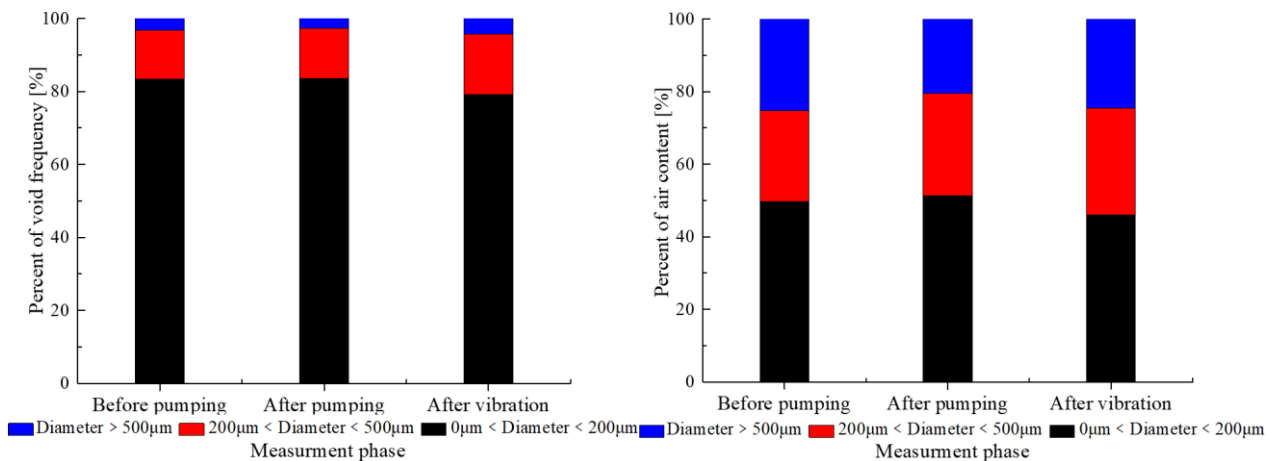


Figure 4.7. Distribution characteristics (actual construction).



a Distribution of percent of void frequency      b Distribution of percent of air content

Figure 4.8. Measurement of actual construction.

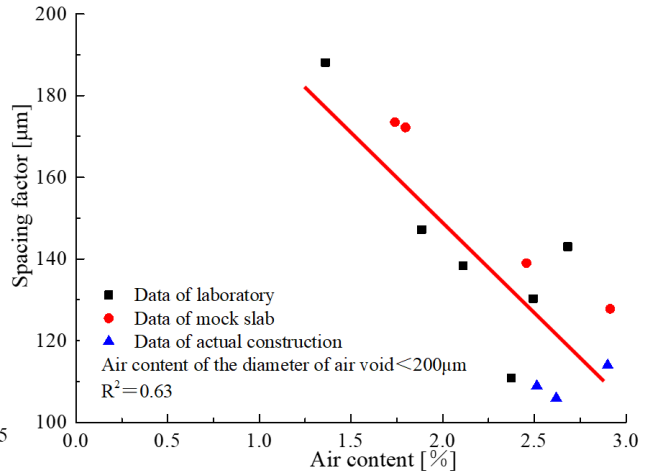
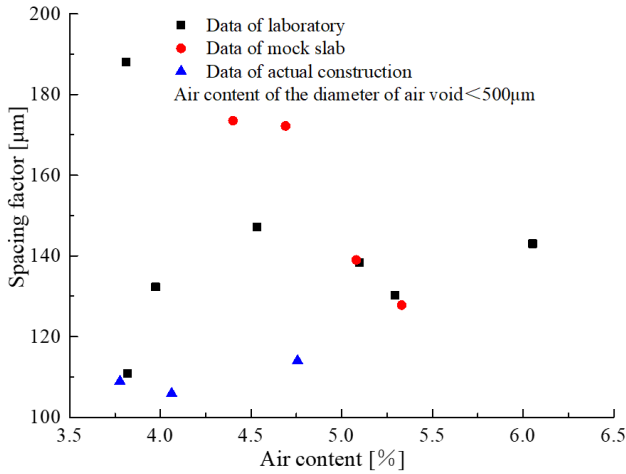


Figure 4.9. Air content of the diameter 0 - 500  $\mu\text{m}$ . Figure 4.10. Air content of the diameter 0 - 200  $\mu\text{m}$ .

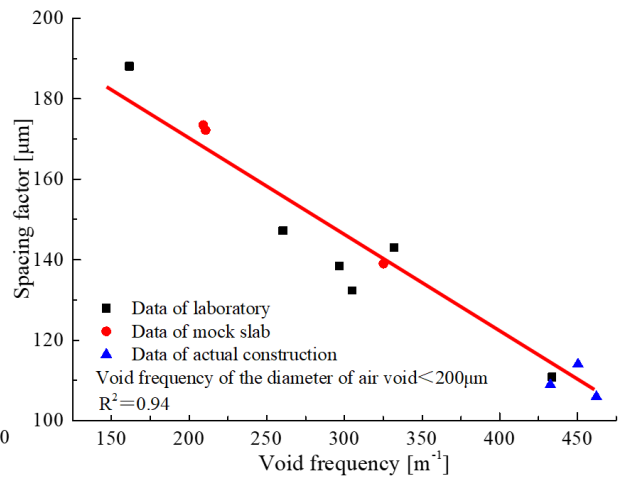
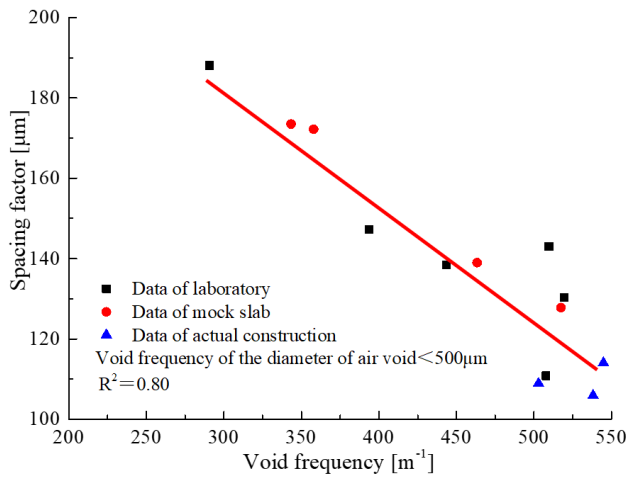


Figure 4.11. Void frequency of the diameter 0 - 500  $\mu\text{m}$ . Figure 4.12. Void frequency of the diameter 0 - 200  $\mu\text{m}$ .

Relationships in the spacing factor with the air content and the air void frequency are shown in Figures 4.9 - 4.12. The data of laboratory, the data of RC mock slab specimen and the data of actual construction are contained in these 4 figures. From Figure 4.9, it can be noticed that between the spacing factor and the air content in the range of diameter 0 - 500  $\mu\text{m}$  is not correlation. Figures 4.10 - 4.12 are shown that the spacing factor decrease with the air void frequency and air content increase. The spacing factor fits better with the air void

frequency than with the air content in linear condition. Especially, while the range of diameter 0 - 200  $\mu\text{m}$ , the correlation coefficient of the regression curve was 0.94. This result is illustrated that the spacing factor can be reflected indirectly through the number of air void, regardless of different mix proportions and execution on RC slab. Simultaneously, this result is consistent with the results of the section (*Air void frequency and air content of concrete made in laboratory and construction site*) that the air void frequency greater than 50% in the range of diameter 0 - 200  $\mu\text{m}$ . Therefore, the diameter less than 200  $\mu\text{m}$  is one of the significant factors to evaluate the distribution of air void and the spacing factor. The specific surface ( $\alpha$ ) in spacing factor Eq. (1) is greatly influenced by the number of air void, and the spacing factor may be characterized by the void frequency regardless of mix proportions and execution on site. Air void characteristics in cement matrix would be featured depending its random property.

#### 4.4 RC slab of Shinyanagibuchi Bridge

##### 4.4.1 Materials and method

The blast furnace slag cement (BB) (Density is 3.04  $\text{g}/\text{cm}^3$ ), river sand, crushed stone, polypropylene fiber (PPF, short fiber. Density is 0.91  $\text{g}/\text{cm}^3$ ) (See Figure 4.13.) and expansive agent (EA) were employed. The mix proportions were shown in Table 4.4.

##### *Surface scaling resistance test*

Concrete specimens with dimensions of 100  $\times$  100  $\times$  400 mm were obtained from the filed site, and these specimens were cut into cubic specimens (100  $\times$  100  $\times$  100 mm). The testing surface of samples was the side that is in contact with the steel formwork. After curing, the surface of the samples was sealed by epoxy resin except for the testing surface and opposite surface. Prior to the freezing-thawing test, the test surface was placed in a 3% brine solution for 7 days to obtain capillary saturation. Then, the samples were exposed to freezing-thawing condition for 12 h each cycle (Temperature: 20  $\Leftrightarrow$  -20 $^{\circ}\text{C}$ , two cycles a day) (ASTM, 2012; Setzer et al., 1996).

Table 4.4. Mix proportions of concrete.

Cement type	W/B (%)	s/a (%)	Unit content: kg/m <sup>3</sup>							Target slump (cm)	Target air content (%)
			W	Binder		S	G	AEA	Fiber		
				C	EA						
BB	43	40	170	395.0	0	671	1013	3.16	0.455	15	6.0
	43	40	170	375.0	20	671	1013	3.16	0.455	15	6.0
	43	40	170	372.5	22.5	671	1013	3.16	0.455	15	6.0
	43	40	170	370.0	25	671	1013	3.16	0.455	15	6.0



Figure 4.13. Polypropylene fiber.

Experimental research in the laboratory: The scaling resistance test of different dosage of the expansive agent (EA) were investigated. The dosage of EA were 0 kg/m<sup>3</sup>, 20 kg/m<sup>3</sup>, 22.5 kg/m<sup>3</sup> and 25 kg/m<sup>3</sup>, respectively.

Mock RC bridge slab: After transportation (non-fiber concrete), before pumping (fiber concrete), after pumping (fiber concrete) and after vibrating (Time: 5sec, 10sec, 15sec) were measured (See Figure 4.14(a)).

Actual RC bridge slab: The specimens were obtained after vibrating (Time: 8sec) in the actual slab. The effect of methods of wet curing (WC) and dry curing (DC) on surface scaling was investigated (See Figure 4.14 (b)).

#### ***Air void distribution***

The method of testing the air void of concrete was according to ASTM standard that is procedure A (Linear Traverse Method) (ASTM, 1998). The formula for calculating the spacing factor ( $\bar{L}$ ) and the void frequency (n) same as Section 4.3.



(a)

(b)

Figure 4.14. RC bridge slab: (a) Mock RC slab and (b) Actual RC slab.



(a)

(b)

Figure 4.15. Non-destructive testing on site (NDT): (a) Surface water absorption test (SWAT) and (b) Torrent method.

### ***Surface water absorption and air permeability***

To evaluate the durability of RC structures in terms of water resistance, a simple, quick and completely non-destructive surface water absorption test (SWAT) and surface air permeability test (Torrent method) (see Figure 4.15).

## **4.4.2 Results and discussions**

### ***Surface scaling resistance test***

Figure 4.16 shows the results of the scaling resistance test of different dosages of the expansive agent (EA). It can be noticed that the mass loss of concrete decreases with the

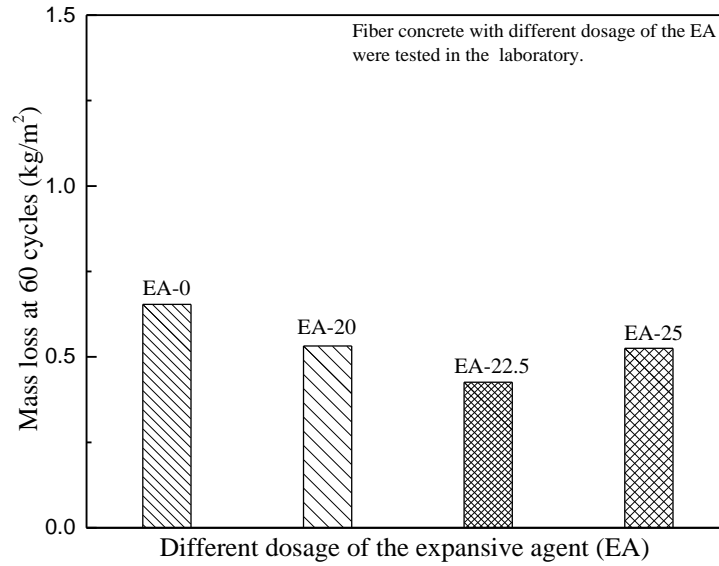


Figure 4.16. Scaling resistance of different dosages of the EA.

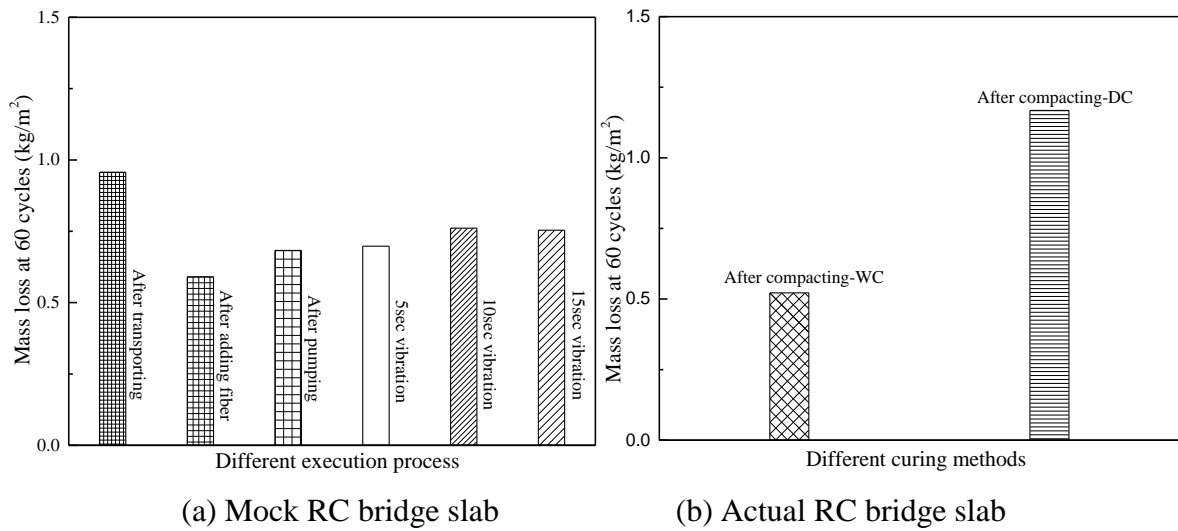
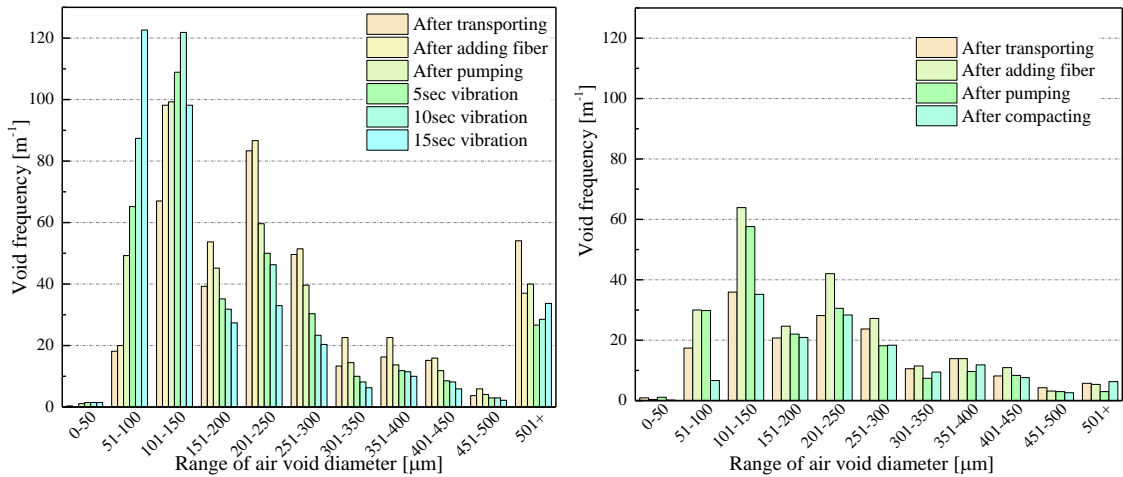


Figure 4.17. Scaling resistance of the RC slab (Concrete specimens obtained from execution process).

increase of the dosage of EA. However, in case the dosage of EA is 25 kg/m<sup>3</sup>, the mass loss of concrete increases a little. Therefore, the dosage of EA has little influence on scaling resistance in this study.

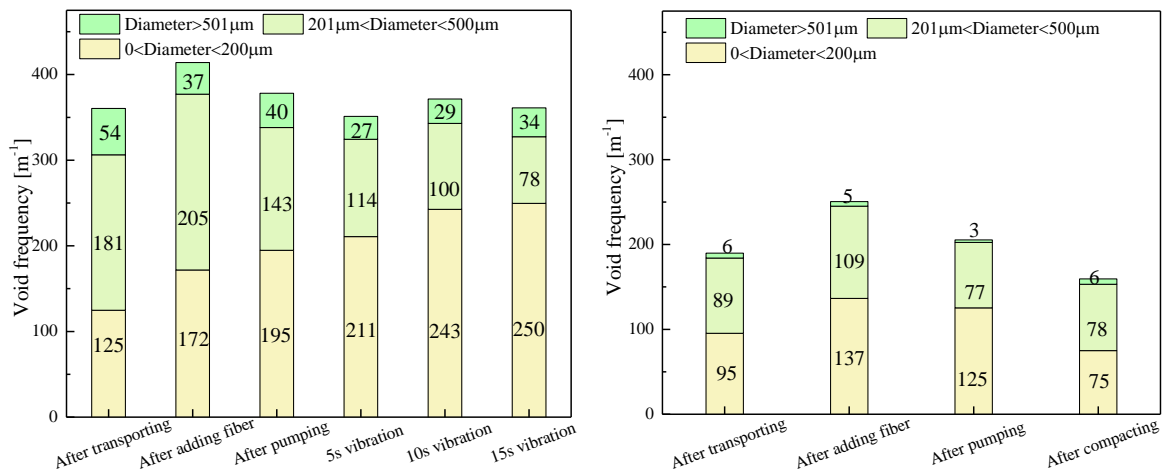
Figure 4.17 shows the results of the concrete surface scaling resistance test on mock RC slab as well as the actual RC slab. From Figure 4.17(a), it can be noticed that the mass loss of concrete decreases with the fiber added. However, it also can be found that the mass loss of concrete a few increases after pumping. At the same time, the mass loss of concrete increases with the increase of the vibration time. Furthermore, the additional of PP fiber may



(a) Mock RC bridge slab

(b) Actual RC bridge slab

Figure 4.18. Distribution characteristics of air void (Concrete specimens obtained from execution process).



(a) Mock RC bridge slab

(b) Actual RC bridge slab

Figure 4.19. Distribution of void frequency. (Concrete specimens obtained from execution process.)

also improve the bond performance of the cement matrix and form fiber-matrix reticulate interfaces to enhance the performance of scaling resistance (Berkowski & Kosior-Kazberuk, 2015; Quanbing & Beirong, 2005). Figure 4.17(b) shows the mass loss with different curing methods. It seems to be indicated that wet curing (WC) has better frost damage scaling resistance than dry curing (DC). To sum up, PP fiber can improve the anti-scaling performance of concrete surface, however, the curing methods of fiber concrete would be one of the significant factors to determine the surface scaling resistance of the concrete under severe environment.

#### *Air void distribution*

Figure 4.18 shows the distribution characteristics of the air void. From these results, it can be noticed that the air void frequency mainly distributed in the range of 51 - 300  $\mu\text{m}$  diameter. Moreover, three peaks appear in three diameter ranges with a formation like an arch shape regardless of the mock slab and actual slab. The three parts have a diameter range of 0 - 200  $\mu\text{m}$ , 201 - 500  $\mu\text{m}$ , and greater than 500  $\mu\text{m}$ , respectively. The range of diameter 0-200 $\mu\text{m}$  is the fine void part that may be air-entraining by the AEA. The range of diameter greater than 500 $\mu\text{m}$  is the large part that may be forming by entrapped air during the mixing of concrete. The range of diameter 201 - 500  $\mu\text{m}$  is middle part that maybe combining the entrained air and the entrapped air. Therefore, three ranges of the void frequency divided were shown in Figure 4.19. From these figures, the air void frequency is mainly divided into three parts by diameter range that includes 0 - 200  $\mu\text{m}$ , 201 - 500  $\mu\text{m}$  and greater than 500  $\mu\text{m}$ . From this result, it can be noticed that the air void frequency increases as PP fiber added, and then the air void frequency decreases as the execution progress regardless of the mock slab, and actual. In addition, from the result of the mock slab, it also can be observed that the vibration time seems that have little influence on the air void frequency.

Figure 4.19 (a) shows the distribution of the void frequency on the mock RC slab. In the case of the range of diameter is 0 - 200  $\mu\text{m}$ , it can be observed that the void frequency increases as the execution progress. Moreover, it can be found that the range of diameter 201

Table 4.5. Parameters of air void on mock slab.

Parameters	After trans- porting	After adding fiber	After pumping	5sec vibration	10sec vibration	15sec vibration
Void frequency [m <sup>-1</sup> ]	361	414	378	351	372	361
Air content of hardened con- crete [%]	7.9	7.7	7.1	6.2	6.0	6.0
Spacing factor [μm]	196	176	173	168	158	153

Table 4.6. Parameters of air void on actual slab.

Parameters	After trans- porting	After adding fiber	After pump- ing	After com- pacting
Void frequency [m <sup>-1</sup> ]	190	251	205	159
Air content of hardened concrete [%]	2.7	3.4	2.6	2.4
Spacing factor [μm]	274	218	234	286

- 500 μm, the void frequency increases with adding PP fiber. Subsequently, the void frequency decreases as the execution process as well as clearly notice that the air void that escapes during the pumping and vibration process seem to mainly appear in the diameter range 201 - 500 μm.

Figure 4.19 (b) shows the distribution of the void frequency on the actual RC slab. It can be found that the void frequency increases with adding PP fiber. Subsequently, the void frequency decreases as the execution process regardless of 0 - 200 μm or 201 - 500 μm.

Air void distribution characteristics in hardened concrete is an extremely complex issue. Even though the same execution process, materials and chemical admixtures both on mock slab and actual slab, it is difficult to ensure stability void distribution characteristics in actual RC slab.

One of the reasons for the improvement of concrete scaling resistance after adding fiber may be probably due to the “air entrainment” properties of the microfibers led to the increase of void frequency as well as a decrease of the spacing factor (Michel Pigeon & Malhotra,

1995), it can be observed from Tables 4.5 and 4.6. And then, the reason for the scaling amount increases may due to pumping and vibration, the air void escaping from fresh concrete caused the decrease of void frequency, which can be noticed in Figure 4.19.

Relationships in the spacing factor with the air void frequency are shown in Figures 4.20 and 4.21. The data of the RC mock slab and the data of the actual RC slab are contained in these two figures. A previous study (Meng, Minoru, Yuki, & TSUKINAGA, 2019) has shown that there is no good linear correlation between the spacing factor and the air content. Form these figures, it can be found that the spacing factor decrease with the air void frequency increase. The void frequency of two range of diameter is shown in Figures 4.20 and 4.21. It can be observed that the spacing factor fits better with the air void frequency in a linear condition, regardless of the mock slab, the actual slab and curing methods. Simultaneously, the correlation coefficients of the regression curve are 0.88 and 0.88, respectively.

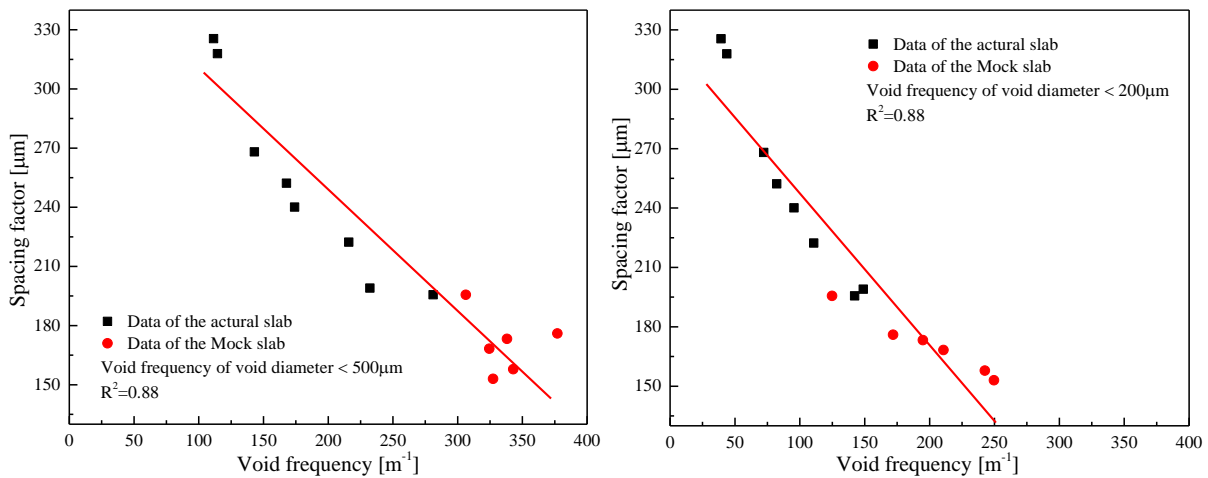


Figure 4.20. Void frequency of the diameter 0-500μm. Figure 4.21. Void frequency of the diameter 0-200μm.

Table 4.7. The results of the NDT test in-situ.

Testing points of RC slab (execution lots)	1	2	3
Surface water content [%]	4.07	4.50	4.17
Air permeability coefficient [ $\times 10^{-16}m^2$ ]	0.042	0.130	0.046
Air penetration depth [mm]	14	26	15
Cumulative water absorption at 600 sec [ml/m <sup>2</sup> ]	0	154	0

Especially, in the case of the range of diameter 0 - 200  $\mu\text{m}$ , it can be found that the black and red points have a better distribution on both sides of the line than the range of diameter 0 - 500  $\mu\text{m}$ . These results are illustrated that the spacing factor can be reflected indirectly through the number of air void, regardless of different execution processes and curing methods on the RC slab. In addition, the void frequency of fine diameter is one of the significant factors to evaluate the air void distribution as the spacing factor in hardened concrete. Accordingly, air void characteristics in the cement matrix would be featured depending on its random property.

#### *Surface water absorption and air permeability*

Table 4.7 shows the results of the NDT test in-situ. NDT tests were conducted on the actual RC slab for verifying the compactness of the RC slab. The surface water content of three areas on the RC slab was detected less than 5%. From these results, it can be clearly noticed that the air permeability coefficient and the cumulative water absorption of 600 sec were significantly low, which suggested that the actual RC slab has fine compactness. However, it also can be noticed that the unevenness of concrete quality on the same RC bridge slab due to the micro-cracks of the concrete surface. Therefore, the issue of how to ensure the concrete quality should be further discussed from the viewpoint of the long term durability of structures.

#### **4.5 Summary**

- By comparing the distribution characteristics of air void of hardened concrete with different mix proportions, it is confirmed that a large number of air void was presented in the diameter of 50 - 300  $\mu\text{m}$ . Especially for the fine air voids, the air void frequency of W/B 35% are greater than that of W/B 50%, regardless of different cement type. It would depend on retention of air void due to increasing viscosity of concrete as unit powder content (W/B), and on the dosage of AE agent.
- In case of the range of diameter 0 - 200  $\mu\text{m}$  which is entrained by AE agent, the percent of air void frequency was greater than 50%, compare to the range of other diameter, with different mixture proportion and execution on slab. From these results, the value of fine air

void frequency than that of air content will be promising as important key to evaluate the effect of air entrainment.

- Excessive vibration is lowered the quality of air void as the range of diameter 0 - 200  $\mu\text{m}$ . However, influence of pumping process is relatively small.
- The spacing factor fits better with the air void frequency than with the air content in linear condition. Especially, while the range of diameter 0 - 200  $\mu\text{m}$ , the correlation coefficient of the regression curve is 0.94. This result is illustrated that the spacing factor can be reflected indirectly through the number of air void, regardless of different mix proportions and execution on RC slab. In addition, the diameter less than 200  $\mu\text{m}$  is one of the significant factors to evaluate the distribution of air void and the spacing factor.
- Using PP fiber and wet-curing can improve the deicing salt scaling resistance of concrete surfaces. In addition, the curing methods of fiber concrete would be one of the significant factors to determine the surface scaling resistance of the concrete under the severe environment. The dosage of EA has little influence on deicing salt scaling resistance of concrete.
- Air void distribution characteristics in hardened concrete is an extremely complex issue. Even though the same execution process, materials and chemical admixtures both on mock slab and actual slab, it is difficult to ensure a stability void distribution characteristics. Furthermore, the spacing factor fits better with the air void frequency in a linear condition regardless of the mock slab and actual slab. Void frequency is one of the significant factors for evaluating the spacing factor of concrete.
- The results of the NDT test in-situ show that the actual RC slab has fine compactness. However, it also can be noticed that the unevenness of concrete quality on the same RC bridge slab due to the micro-cracks of the concrete surface. Therefore, the issue of how to meet the requirement of concrete quality needs further consideration through the usage of the environmental condition after initial curing of concrete structures.
- To sum up, the considerable results in this study can be provided by tasking the mock RC slab for the practical improvement of the actual RC slab, for instance, slump, the air content of fresh concrete, vibration time and admixture dosage. However, it is probably not enough to make a clear judgment on the stability of air void distribution of the actual RC

slab by the mock RC slab, which the attribute of many important variables impact on the air void quality of concrete, such as pumping condition, temperature changes, handling and transporting. Although, the rise of target air content, the using PPF and the adequate wet curing period would be contributed to make durable concrete for deicing salt scaling resistance of concrete.

#### 4.6 Reference

- ASTM. (1998). Standard Test Method for Microscopical Determination of Parameters of the Air-Void System in Hardened Concrete. In *C457 – 98*.
- ASTM. (2012). Standard Test Method for Scaling Resistance of Concrete Surfaces Exposed to Deicing Chemicals. In *C672/C672M – 12*.
- Berkowski, P., & Kosior-Kazberuk, M. (2015). Effect of Fiber on the Concrete Resistance to Surface Scaling Due to Cyclic Freezing and Thawing. *Procedia Engineering*, *111*, 121-127. doi:10.1016/j.proeng.2015.07.065
- Bureau, T. R. D. (2017). The manual for counterplan to frost damage of concrete structures under spreading deicing salt (in Japanese).
- Kim, J., McCarter, W. J., Suryanto, B., Nanukuttan, S., Basheer, P. A. M., & Chrisp, T. M. (2016). Chloride ingress into marine exposed concrete: A comparison of empirical- and physically- based models. *Cement and Concrete Composites*, *72*, 133-145. doi:10.1016/j.cemconcomp.2016.06.002
- Meng, Z., Minoru, A., Yuki, S., & TSUKINAGA, Y. J. P. o. t. J. C. I. (2019). Air Void Characteristics of Concrete with Different Mix Proportions and Execution on RC Slab. *41*(1), 653-658.
- Ministry of Land, I. T. a. T. R. B. (2017, 10 October 2017). Road annual report. Retrieved from [http://www.mlit.go.jp/road/sisaku/yobohozen/yobohozen\\_maint\\_h28.html](http://www.mlit.go.jp/road/sisaku/yobohozen/yobohozen_maint_h28.html)
- Pigeon, M. (2014). *Durability of concrete in cold climates*: CRC Press.
- Pigeon, M., & Malhotra, V. M. J. J. o. m. i. c. e. (1995). Frost resistance of roller-compacted high-volume fly ash concrete. *7*(4), 208-211.
- Powers, T. C. (1945). *A working hypothesis for further studies of frost resistance of concrete*.

Paper presented at the Journal Proceedings.

- Promentilla, M. A. B., & Sugiyama, T. J. J. o. A. C. T. (2010). X-ray microtomography of mortars exposed to freezing-thawing action. *8(2)*, 97-111.
- Quanbing, Y., & Beirong, Z. (2005). Effect of steel fiber on the deicer-scaling resistance of concrete. *Cement and Concrete Research*, *35(12)*, 2360-2363. doi:10.1016/j.cemconres.2005.04.003
- Setzer, M. J., Fagerlund, G., Janssen, D. J. J. M., & structures. (1996). CDF test—test method for the freeze-thaw resistance of concrete-tests with sodium chloride solution (CDF). *29(9)*, 523-528.
- Shields, Y., Garboczi, E., Weiss, J., & Farnam, Y. (2018). Freeze-thaw crack determination in cementitious materials using 3D X-ray computed tomography and acoustic emission. *Cement and Concrete Composites*, *89*, 120-129. doi:10.1016/j.cemconcomp.2018.03.004
- Yuan, J., Wu, Y., & Zhang, J. (2018). Characterization of air voids and frost resistance of concrete based on industrial computerized tomographical technology. *Construction and Building Materials*, *168*, 975-983. doi:10.1016/j.conbuildmat.2018.01.117

**CHAPTER 5 SHRINKAGE FOR RC SLAB OF BRIDGE USING  
SUPERABSORBENT POLYMERS (SAP) INTERNAL CURING**

**5.1 General**

In this work, the effects of the individual or hybrid addition of superabsorbent polymers (SAP) with varying dosages (0.1%, 0.2%, 0.3%, and 0.6%) and the lime-type expansive agent (KEA) on the length and mass change, compressive strength, and pore structures (MIP) of mortars were investigated. The results showed that the incorporation of SAP can effectively mitigate its autogenous shrinkage and the length change value of the mortar with SAP smaller than reference (Ref) until 49 d, regardless of the presence of KEA. The hybrid addition of SAP and KEA increases the initial expansion of the specimens as compared with individual addition of SAP, which is a beneficial effect on compensating for the shrinkage of the mortar under drying conditions. Moreover, the addition of SAP seems to delay cement hydration and increase the volume of macropores (greater than 100 nm), thereby reducing the compressive strength of the mortars. The introduction of KEA slightly promoted the formation of micropores, resulting in a slight increase in compressive strength compared with the samples without KEA. Furthermore, in our view, it promotes pore refinement, so as to reduce moisture evaporation.

**5.2 Introduction**

Shrinkage cracks in concrete and mortar occur due to evaporation of moisture in the porous, differential settlement, and temperature gradient (Cohen, Olek, Dolch, & Research, 1990; Collins, Sanjayan, & Research, 2000; Weyers, Conway Jr, Cady, & Research, 1982; Wittmann & research, 1976). It is a common phenomenon considered to be a potential factor causing the deterioration of concrete structure durability. Cracks appearing on the surface of

concrete structures may allow water, chloride ions, and gas to penetrate, causing corrosion of steel bar, accelerated frost damage, and can cause severe impairment in long-term service and safety of the concrete structure (Cabrera & composites, 1996; Otieno, Beushausen, & Alexander, 2016). The general way to mitigate early-age shrinkage cracking is to employ an expansive agent (EA) and improve initial curing regimes (M. Zhang, Sakoi, Aba, & Tsukinaga, 2019). Among the expansive agents, the two most common and important ones are calcium sulphoaluminate-based and lime type agents(CaO-based), which react with water to produce restrained expansion in reinforced concrete structures and ultimately reduce the risk of shrinkage cracking, especially for CaO-based expansive agents which can increase the volume by approximately 90% after forming portlandite via reacting with water (Chatterji & Research, 1995). Therefore, the presence of water is critical, regardless of the type of expansion agent; at the same time, it also shows the importance of curing regimes.

Conventional curing regimes, such as moisture curing, sheet curing, and permeability formwork curing, are difficult to bring about obvious effects on concrete curing through external moisture penetration due to a relatively low surface porosity of cement-based materials with a low water-cement ratio. Accordingly, internal curing (IC) is considered to be a potential way for the mitigation of autogenous shrinkage and the maintenance of internal relative humidity (IRH) by releasing water/solution of internal curing materials to prevent internal self-desiccation of concrete(308, 2001; Lura, 2003). Lightweight aggregate (LWA) and superabsorbent polymers (SAP) are currently thought to be the two most effective internal curing regimes on the mitigation of autogenous shrinkage; they were originally proposed by Philleo and Jensen (Jensen, Hansen, & research, 2001, 2002; Philleo, 1991), respectively. The effectiveness of eliminating its autogenous shrinkage was then confirmed by other scholars (Bentz & Jensen, 2004; Cusson & Hoogeveen, 2008; Liu, Farzadnia, Shi, & Ma, 2019b; Oh & Choi, 2018; Wang et al., 2017; Zhutovsky, Kovler, Bentur, & Structures, 2002). Besides, compared with LWA, the presence of SAP in the form of powder materials is used in concrete via adding additives, which is promising for practical engineering applications (Mechtcherine & Reinhardt, 2012).

SAPs are some types of cross-linked polyelectrolytes that can absorb tens to hundreds times more than their own weight as contact with water or aqueous solutions (Mechtcherine et al., 2013; Mechtcherine & Reinhardt, 2012; D. Snoeck, Van den Heede, Van Mullem, & De Belie, 2018). Internal curing by SAP as a “micro-reservoir” may absorb and release liquids inside the concrete, providing a continuous water resource supply for cement hydration, and creating the possibility of long-term curing of concrete (Liu et al., 2017). However, it is interesting that the advantages of SAP internal curing are not limited to the inhibition of autogenous shrinkage at the early age of concrete (Almeida & Klemm, 2018; Kong, Zhang, & Lu, 2014; Liu, Farzadnia, Shi, & Ma, 2019a; Liu et al., 2019b; Lyu et al., 2019; Ma, Liu, Wu, & Shi, 2017; Oh & Choi, 2018; D. Snoeck, Dewanckele, Cnudde, & De Belie, 2016; D. Snoeck, Jensen, & De Belie, 2015; D. Snoeck, Pel, & De Belie, 2018; Soliman & Nehdi, 2010). Moreover, it can be found from a variety of studies that SAPs were used in concrete and mortar to improve resistance to carbonization (Gupta, 2018; Ma et al., 2017), frost damage resistance (Laustsen, Hasholt, & Jensen, 2013; Mechtcherine et al., 2019; Mechtcherine et al., 2016; Yang, He, Shao, & Li, 2018), and internal relative humidity (IRH) (Shen, Wang, Chen, Wang, & Jiang, 2015; Song, Choi, & Choi, 2016; Wehbe & Ghahremaninezhad, 2017), change of rheology (Mechtcherine & Reinhardt, 2012; Schroefl, Mechtcherine, Vontobel, Hovind, & Lehmann, 2015; Schröfl, Snoeck, & Mechtcherine, 2017), as well as to promote self-sealing (Lee, Wong, & Buenfeld, 2016; Didier Snoeck, Van Tittelboom, Steuperaert, Dubruel, & De Belie, 2012) and self-healing (Gruyaert et al., 2016; D. Snoeck, Steuperaert, Van Tittelboom, Dubruel, & De Belie, 2012; D. Snoeck, Van den Heede, et al., 2018; Didier Snoeck et al., 2012). In the view of practical application, however, among many advantages, it is seems to be particularly important to control the cracking of the early-age massive concrete through internal curing.

In general, utilizing expansive agents is one of the most effective ways to compensate for shrinkage behavior and reduce the crack risk, with internal curing materials being another. Theoretically, the expansive agent reacts to generate sufficient expansion and needs the aid of abundant water, some of which can be obtained from the internally cured material. Indeed, several studies (B. Chen, Ding, Cai, Bai, & Zhang, 2016; W. Chen et al., 2013; Li, Liu, Tian, Wang, & Xu, 2017; Wang et al., 2017) have suggested that the combination of LWA and an expansion agent can effectively improve shrinkage behavior. Wang et al. (Wang et al., 2017) showed that the combination of LWA and expansive agents can effectively decrease the cracking sensitivity of concrete at an early age. Li et al. (Li et al., 2017) showed that the combined use of SLWA and EA exhibits high efficacy in mitigating shrinkage deformation and can limit the reduction of mechanical properties caused by a single EA. However, there is limited information on the combined effect of SAP and EA on shrinkage behavior. Yu et al. (P. Yu, Mo, & Deng, 2019) investigated the synergetic effect of MgO-based expansive agent (MEA) and SAP on the long-term drying shrinkage, autogenous shrinkage, internal humidity and mechanical strength of concrete, and experimental results showed that the hybrid system of 0.4% SAP and 6% MEA could not only eliminate autogenous shrinkage but also control the deformation of expansion to a minimum. Hence, it is speculated that the coexistence of lime-type expansion agent and SAP may have a beneficial effect on the shrinkage behavior of mortar. Nonetheless, it is still not clear on the combined effect of lime-type expansive agent and SAP on the mortar.



Figure 5.1. Micro-cracks appear on RC bridge slab.

Furthermore, in the Tohoku region of Japan, infrastructure construction projects have been promoted after the great east Japan earthquake and tsunami disaster in 2011. Lifetime improvement of these concrete structures is the most important issue to reduce future maintenance costs. Blast furnace slag cement (BB), composed of 42% ground granulated blast furnace slag, is employed heavily on the field. Although various safeguards are applied throughout the construction execution process such as expansion agent (EA) added to compensate for shrinkage, optimization of vibration time, control of slump, setting time, and curing conditions (wet cured for 7 days, sheet cured for 21 days). However, the cracking of the RC slab surface has not been sufficiently improved (see Figure 5.1).

Therefore, in order to ensure that the cracking of the RC bridge slab due to the shrinkage behavior was reduced. The effects of the addition of SAP and lime-type expansive agent (KEA) on the length change, mass change, compressive strength, and pore structures of the mortars were mainly studied. The purposes of this study are to (1) study the effects of various dosages of SAP and with or without KEA on the length change, mass change, and compressive strength of mortars, (2) investigate the influence of various dosages of SAP with or without KEA on the pore size distribution and characteristics of mortars with different ages, (3) evaluate the effect of pore structure on the drying shrinkage behavior and compressive strength of mortar.

### **5.3 Materials and curing conditions**

#### **5.3.1 Materials**

In the study, the blast furnace slag cement (BB) and the lime-type expansion agent (KEA) were employed. Their chemical compositions and physical properties are shown in Tables 5.1 and 5.2. Pit sand was used as a fine aggregate with apparent density, fineness modulus, and water absorption of 2.57 g/cm<sup>3</sup>, 2.52, and 2.96%, respectively, the crushed stone as coarse aggregate was used with the maximum size of 25 mm. Commercial SAP powder based on a cross-linked potassium salt poly acrylate (particle size  $476.6 \pm 52.9 \mu\text{m}$

Table 5.1. Chemical compositions of blast furnace slag cement (BB) and expansion agent (KEA) (wt %).

Material	CaO	SiO <sub>2</sub>	Al <sub>2</sub> O <sub>3</sub>	Fe <sub>2</sub> O <sub>3</sub>	MgO	SO <sub>3</sub>	K <sub>2</sub> O	Na <sub>2</sub> O	Cl <sup>-</sup>	Ig. loss
BB	55.23	25.58	8.57	1.93	3.69	2.16	0.36	0.21	0.16	1.65
KEA	76.20	4.80	1.40	1.00	0.70	15.80	-	-	-	0.10

Table 5.2. Physical properties of blast furnace slag cement (BB) and expansion agent (KEA).

Material	Specific surface area (cm <sup>2</sup> /g)	Density (g/cm <sup>3</sup> )	Setting time (min)		Compressive strength (MPa)		
			Initial	Final	3 d	7 d	28 d
BB	3720	3.04	188	267	21.6	36.7	62.2
KEA	3520	3.16	150	230	28.9	44.0	62.0

(n=100), see Figure 5.2(a)) was used as an internal curing material. The SAP is bulk-polymerized and consists of irregular particle shapes (Mechtcherine & Reinhardt, 2012). The sorption capacity of the SAP powder tested with the tea-bag method (Mechtcherine & Reinhardt, 2012; Mechtcherine et al., 2018; D. Snoeck, Van den Heede, et al., 2018) at 1, 5, 10, 30, 60 min, 3 and 24 h was presented in Figure 5.2(b). The SAP powder sorption capacity of using the tap water (TW), the extracted solution of BB cement (W/C=5), and the extracted solution mixed with the expansion agent and BB cement (BB + KEA, W/B=5, BB / KEA=20) were 123.2 g/g, 36.9 g/g, and 34.5 g/g, respectively. It was also noticed that there was an approximately 72% decrease of SAP sorption capacity induced by cement filtrate solution compared with tap water (TW). In addition, in order to facilitate the application of SAP in winter concreting in the future, the adsorption capacity of SAP under the condition of 0°C - 10°C was tested. It can be found that temperature (0°C - 10°C) has little effect on the adsorption capacity of SAP. However, the temperature (0°C - 10°C) has little influence on the sorption capacity of the SAP.

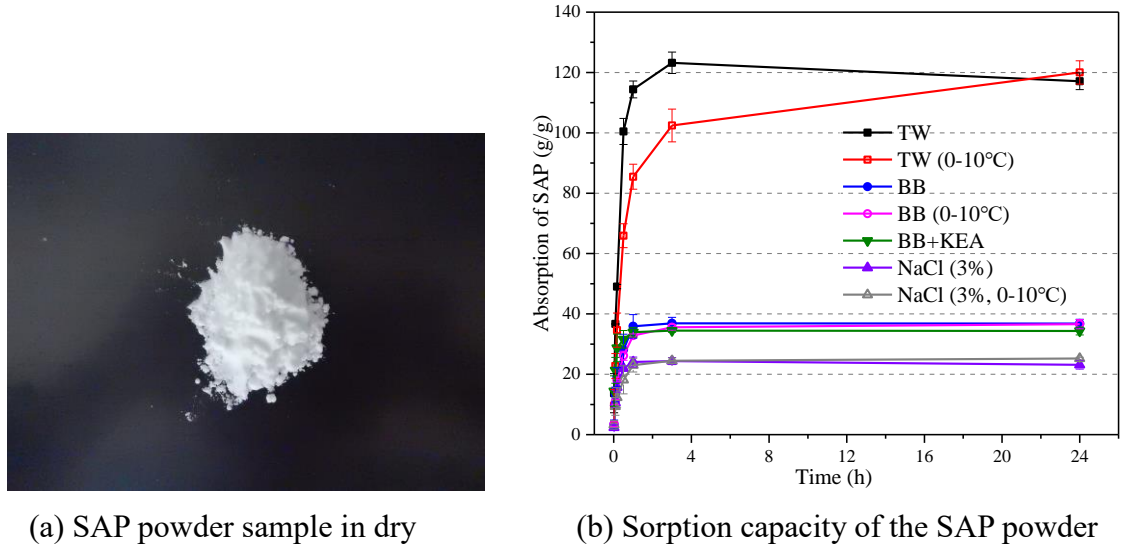


Figure 5.2. SAP sample and sorption capacity of the SAP powder.

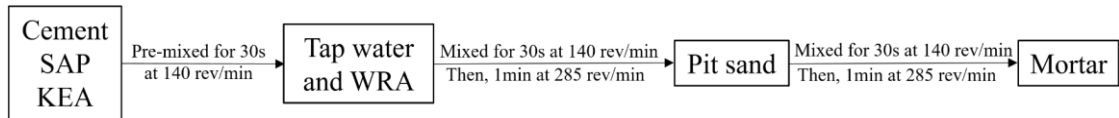


Figure 5.3. Mixing procedure of mortar incorporated SAP.

Table 5.3. Mix proportions and slump flow after 15 jolts of mortar. Unit: kg/m<sup>3</sup>.

Mixture types	W/B <sub>tot</sub>	W/B <sub>eff</sub>	Additional water	W	C	S	KEA	WRA	SAP	Flow after 15 jolts (mm)
Ref	0.40	0.40	-	170	425	614	-	4.25	-	180.5
S0.1	0.44	0.40	14.9	170	425	614	-	4.25	0.43	179.5
S0.2	0.47	0.40	29.8	170	425	614	-	4.25	0.85	177.0
S0.3	0.50	0.40	44.6	170	425	614	-	4.25	1.28	180.5
S0.6	0.61	0.40	89.3	170	425	614	-	4.25	2.55	181.5
Ref-KEA	0.40	0.40	-	170	405	614	20	4.25	-	180.5
KEA+S0.1	0.44	0.40	14.875	170	405	614	20	4.25	0.43	181.0
KEA+S0.2	0.47	0.40	29.75	170	405	614	20	4.25	0.85	183.5
KEA+S0.3	0.50	0.40	44.625	170	405	614	20	4.25	1.28	185.5
KEA+S0.6	0.61	0.40	89.25	170	405	614	20	4.25	2.55	185.0

Notes: WRA is water reducing agent. W/B<sub>tot</sub> is the ratio of total water content, including the water absorbed by the SAP, to the total binder. For the W/B<sub>eff</sub> (effective W/B), the amount of water absorbed by SAP is excluded.

### 5.3.2 Curing conditions

All specimens were prepared in a laboratory to ensure that the curing conditions were consistent with the field. Immediately after casting, specimens were sealed with plastic film for 24 h, and then they were demolded. After demolding, they were cured in water for 6 d, then they were cured sealed with plastic film for 21 d in a constant temperature and humidity chamber (20°C and RH 60 ± 5%). After 28 d of curing, all plastic film was removed, and the surfaces of specimens were exposed to a drying environment (20°C and RH 60 ± 5%).

## 5.4 Internal curing mortar with SAP

### 5.4.1 Mixture proportions and mixing procedure

Mortars with varying SAP dosages (0.1%, 0.2%, 0.3%, and 0.6% (wt) of cementitious materials), as well as addition of KEA, were investigated. Adjustment with additional water to ensure that the mortar with and without SAP had a similar slump flow. All mixtures are shown in Table 5.3. Those named “Ref - KEA” (with KEA) and “Ref” (without KEA) were used as the reference mix proportions. Specimens with the individual addition of SAP were marked as S0.1, S0.2, S0.3, S0.6, with the number following the letter “S” in the specimen

$$\varepsilon_{lcn} = (l_1 - l_n) / l_1 \times 1000 \quad (5-1)$$

$$m_l = (m_n - m_l) / m_l \times 100 \quad (5-2)$$

Where,  $\varepsilon_{lcn}$  is length change at the  $n^{\text{th}}$  day, unit:  $\mu\text{m}/\text{m}$ ;  $l_1$  is the length on the first day, unit: mm;  $l_n$  is the length on an  $n^{\text{th}}$  day, mm;  $m_l$  is the mass loss, unit: %;  $m_l$  is the mass on the first day, unit: g;  $m_n$  is the mass on an  $n^{\text{th}}$  day, unit: g.

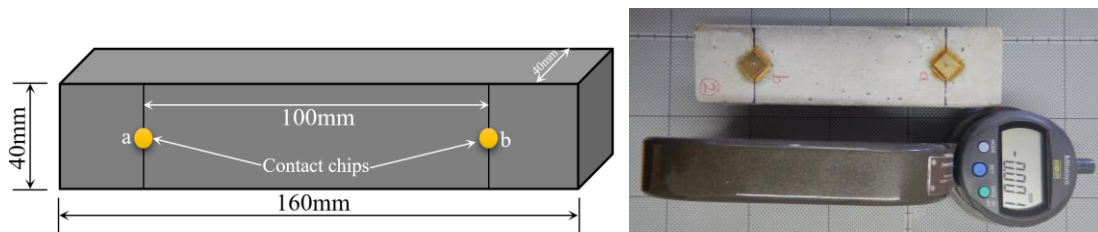


Figure 5.4. Specimen and hand-held strain comparator.

name indicating the percentage of SAP by weight of binder. Specimens with the hybrid addition of SAP and KEA were marked as KEA + S0.1, KEA + S0.2, KEA + S0.3, KEA + S0.6. An automatic mortar mixer was used for mixing all samples and the mixing procedure as follows Figure 5.3 (Ma et al., 2017; Mechtcherine & Reinhardt, 2012). The cementitious material and SAP were equally placed and pre-mixed for 30 s at 140 rev/min in a bowl in order to ensure SAP powder homogeneous dispersion.

### **5.4.2 Testing methods**

#### ***Length and mass change***

The prismatic mortar specimens with a dimension of 40 mm × 40 mm × 160 mm were cast for measuring the length change and mass loss. A hand-held strain comparator with an accuracy of 0.001 mm was employed to measure the length at 1, 3, 5, and 7 days, and then every 7 days until 91 days according to the JIS A 1129-2 contact-type strain gauge method (see Figure 5.4). Meanwhile, an electronic balance with an accuracy of 0.01 g was used to record the mass of specimens. After demolding and sticking the contact chips, the initial length and mass were recorded. Two lateral surfaces perpendicular to the specimen casting surface were measured and the mean results obtained from every three tested specimens were reported.

The length and mass change at n days was calculated as follows Eq. (5-1) and (5-2).

#### ***Compressive strength***

The compressive strength testing was carried out on mortar specimens with a size of 50 mm in diameter, 100 mm in height according to Japanese Industrial Standard (JIS A 1108). The compressive strength was determined from an average of each batch (three samples) at 7 d, 28 d, and 91 d, respectively.

#### ***Pore size distribution and characteristics***

The pore characteristics of mortar were determined by Mercury Intrusion Porosimetry (MIP) at 7 d, 28 d, and 91 d, respectively. The mortar specimens were cut into approximately 5-mm-block samples and placed into an acetone bath for preventing the cement hydration

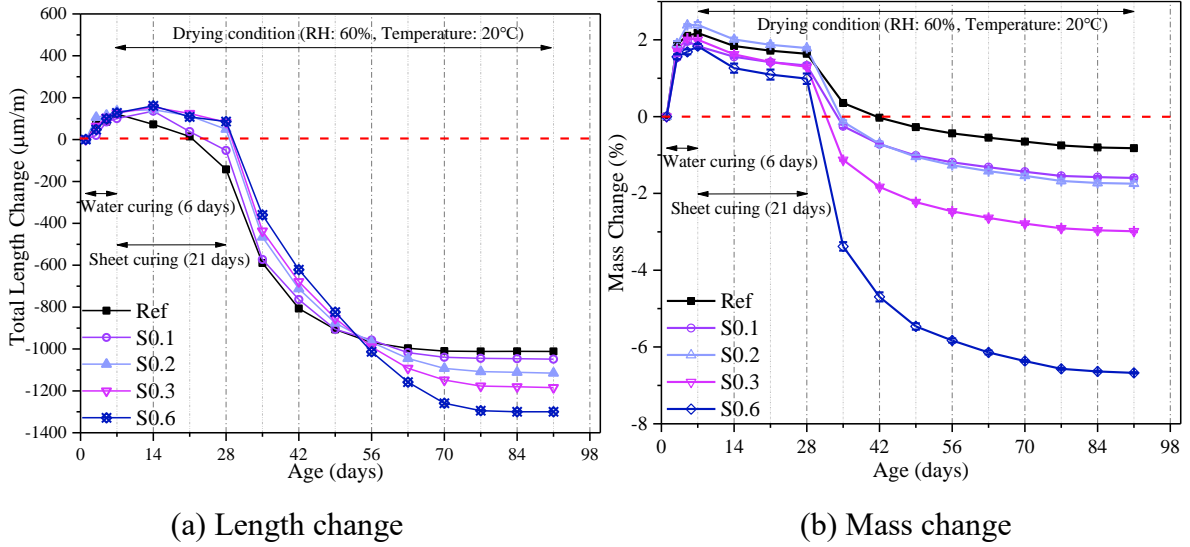


Figure 5.5. Effect of the individual addition of SAP on length and mass.

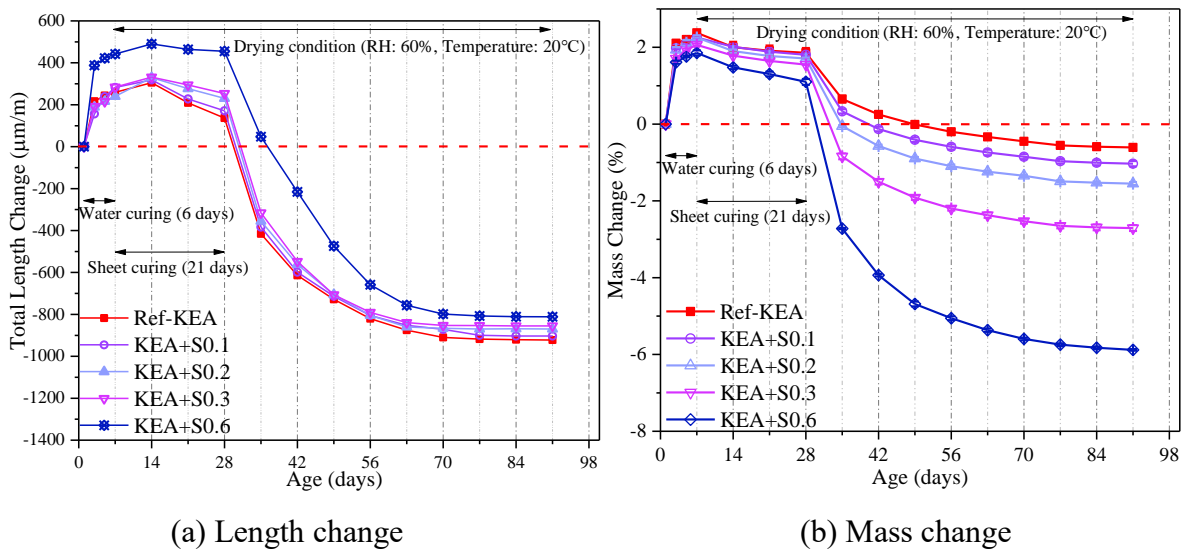


Figure 5.6. Effect of the hybrid addition of SAP and KEA on length and mass.

reaction. The resulting samples were stored in an oven to ensure that the free water in the pores is completely evaporated, prior to MIP testing.

### 5.4.3 Effect of individual and hybrid addition of SAP and KEA on the length and mass change

Figures 5.5 and 5.6 show the influence of individual and hybrid addition of SAP and KEA on the length and mass change of mortar specimens for a duration of 91 days. The initial time was set at 24 h after casting. Overall, the length and mass change curves showed the decrease after the initial increase, and a tendency to slowly become stable as the age prolonged. These tendencies may be mainly related to variations in curing methods that were assumed under laboratory conditions. As can be seen in Figures 5.5 and 5.6, after 6 days of water curing, compared with the control specimens (Ref), the addition of KEA and SAP caused mortar specimens expansive behavior to be extended for about one week regardless of individual and hybrid addition. Furthermore, it can be found that the decline rate of the length change between 14 to 28 days of mortar adding SAP was slower than that without SAP and the slope of the curve gradually decreased with the increase of SAP content. This main reason is thought to be due to the mitigation of autogenous shrinkage. Therefore, it can be noticed that the addition of SAP reduced the autogenous shrinkage of mortar, whereas the addition of KEA enhanced this effect. Figure 5.5(a) presents the influence of the addition of only SAP on the total length change. As shown in Figure 5.5(a), the addition of SAP was not only effective in the reduction of the autogenous shrinkage but also the length change value of the mortar with SAP is smaller than Ref until 49 d. Moreover, for the mortar with SAP, the shrinkage continues for a long time, and the length change value of SAP mortar exceeds that of Ref. Noticeably, the inclusion of SAP decreased the shrinkage magnitude by 5-30% before 49 d as compared to the Ref. The reason may be due to the continuous release of water from the SAP bubble to compensate for the loss of moisture in the dry environment, and it causes the expansion of the matrix volume in the early stage, and it leads to compensation for the matrix volume contraction caused by the moisture loss under the drying environment (Soliman & Nehdi, 2010; P. Yu et al., 2019). As the drying prolonged after 49 d, however, the amount of water released by SAP can no longer meet the evaporative water loss rate and was insufficient to maintain the internal RH of the mortar, resulting in its ability

to inhibit the shrinkage of mortar was weakened. Hence, there is an adverse effect of SAP on shrinkage under drying conditions at later-age stages (Liu et al., 2019b; Ma et al., 2017; Soliman & Nehdi, 2010). At the 91st day, as can also be seen from the figure, the addition of 0.1%, 0.2%, 0.3%, and 0.6% SAP increased the total shrinkage by 3.6%, 10.2%, 17.1%, and 28.4%, respectively, as compared to Ref. On the contrary, the addition of KEA (Ref-KEA) carried out a beneficial effect leading to the total shrinkage reduced by around 8.9% as compared with Ref, which can be noticed from Figures 5.5(a) and 5.6(a).

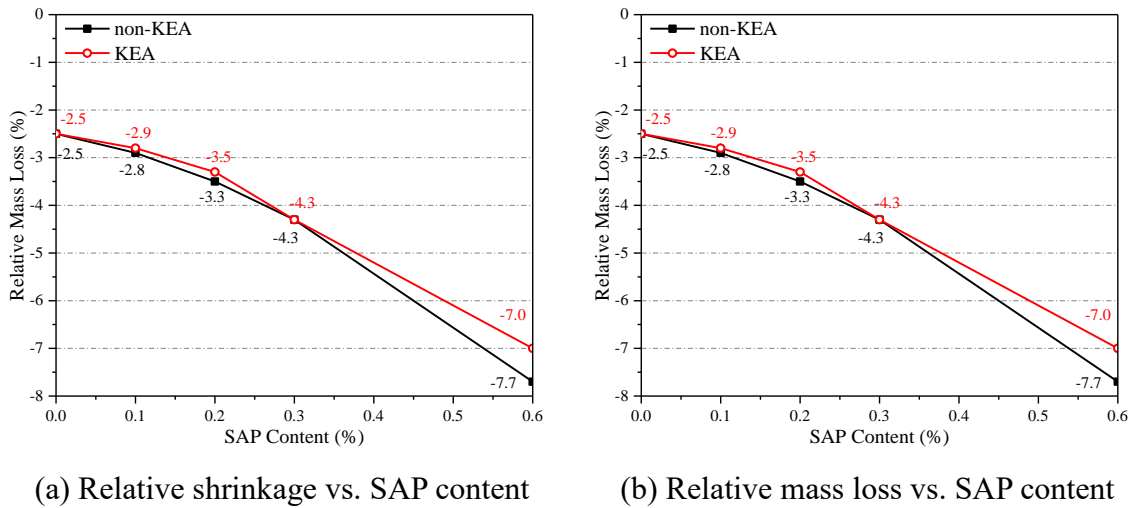
Figure 5.6 shows the effect of the hybrid addition of SAP and KEA on the total length and mass change. Generally, the trend of length and mass change was similar to that of the individual addition of SAP. As can be seen from Figure 5.6(a), owing to the hybrid addition of SAP and KEA, the initial expansion strain peaks increased by 162.3%, 170.9%, 172.8%, and 302.9%, respectively, as compared to Ref (see in Figure 5.5(a)), whereas, compared with Ref-KEA, the initial expansion strain increased by 4.6%, 8.1%, 8.8%, and 60.7%, respectively. Moreover, it can also be found that the addition of KEA can mitigate the adverse influence of SAP on the drying shrinkage in the later period as well as compared with Ref, the addition of 0.1%, 0.2%, 0.3%, and 0.6% SAP decreased the total shrinkage at 91st day by 10.8%, 14.1%, 15.5%, and 19.8%, respectively (thanks to the hybrid addition of SAP and KEA, the initial expansion of the mortar was increased). In addition, the comparison of Figure 5.5(b) and Figure 5.6(b) can be found that the introduction of the KEA reduced the mass loss at 91 d by around 26.1% (Ref - KEA), 35.6% (KEA + S0.1), 11.3% (KEA + S0.2), 9.3% (KEA + S0.3), and 11.9% (KEA + S0.6), respectively. After 28 days, the mortar specimens were completely exposed to the dry environment (RH: 60%, Temperature: 20°C). It can be assumed that after 28 days the samples were almost completely in a drying shrinkage state. Thus, the relative shrinkage at this time can be defined as the total drying shrinkage. The influence of SAP content and with/without KEA on the relative shrinkage and relative mass loss magnitude (see Eq. (5-3) and Eq. (5-4) for its definition) between the 28 and 91 days were presented in Figure 5.7. It was worth noting from the results that the relative shrinkage

and the relative mass loss increased with the increase of SAP contents under drying conditions regardless of individual/hybrid addition of SAP and KEA. For the hybrid addition of SAP and KEA, when the SAP contents were greater than or equal to 0.2%, its relative shrinkage was smaller compared to the individual addition of SAP. Hence, it can be concluded that the addition of SAP seems to be negative for relative shrinkage, whereas, the addition of KEA seems to improve the adverse effects especially when the SAP content is greater than or equal to 0.2%, the combined effect of SAP and KEA is more prominent.

$$\text{Relative shrinkage} = L_{91} - L_{28} \tag{5-3}$$

$$\text{Relative mass loss} = M_{91} - M_{28} \tag{5-4}$$

Where  $L_{91}$  represents the change in length on the 91st day ( $\mu\text{m} / \text{m}$ ),  $L_{28}$  is the change in length on the 28th day ( $\mu\text{m} / \text{m}$ ),  $M_{91}$  represents the change in mass on the 91st day (%),  $M_{28}$  is the change in mass on the 28th day (%).



(a) Relative shrinkage vs. SAP content (b) Relative mass loss vs. SAP content  
 Figure 5.7. Relative shrinkage and relative mass loss under drying condition. (After 28 days.)

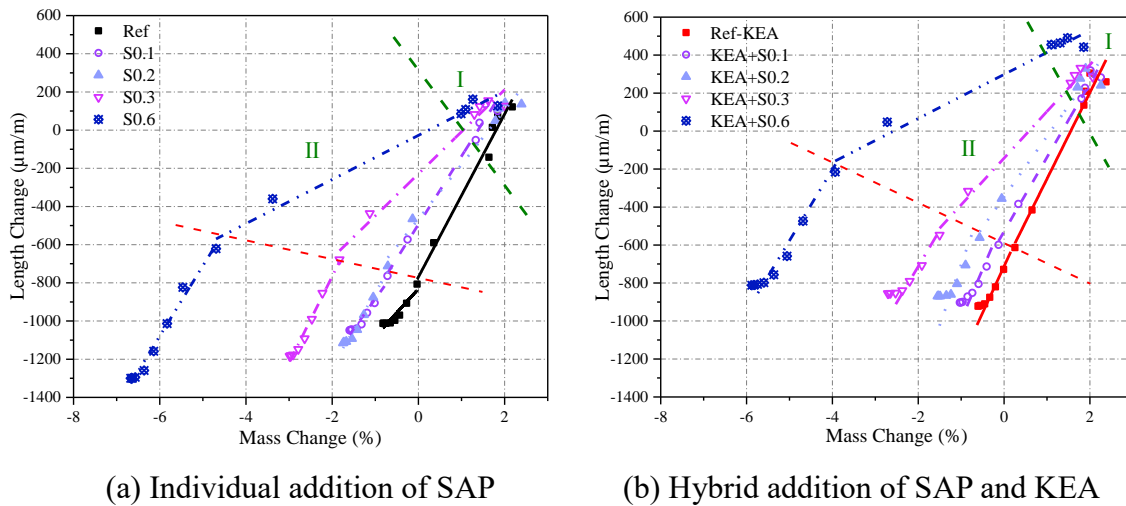
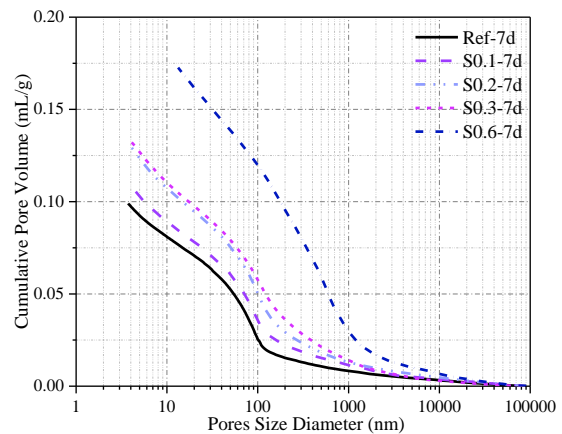
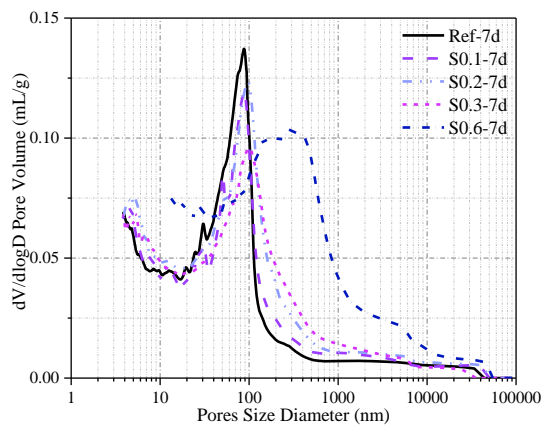
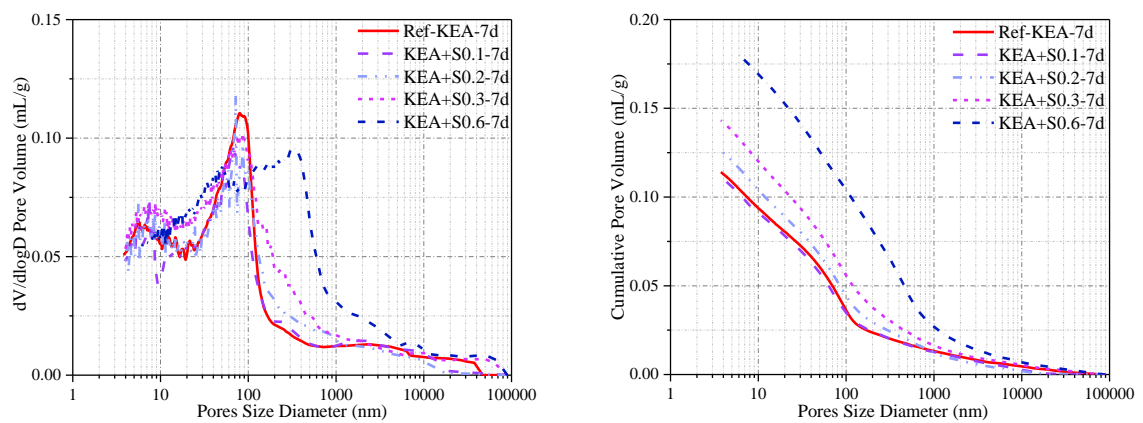
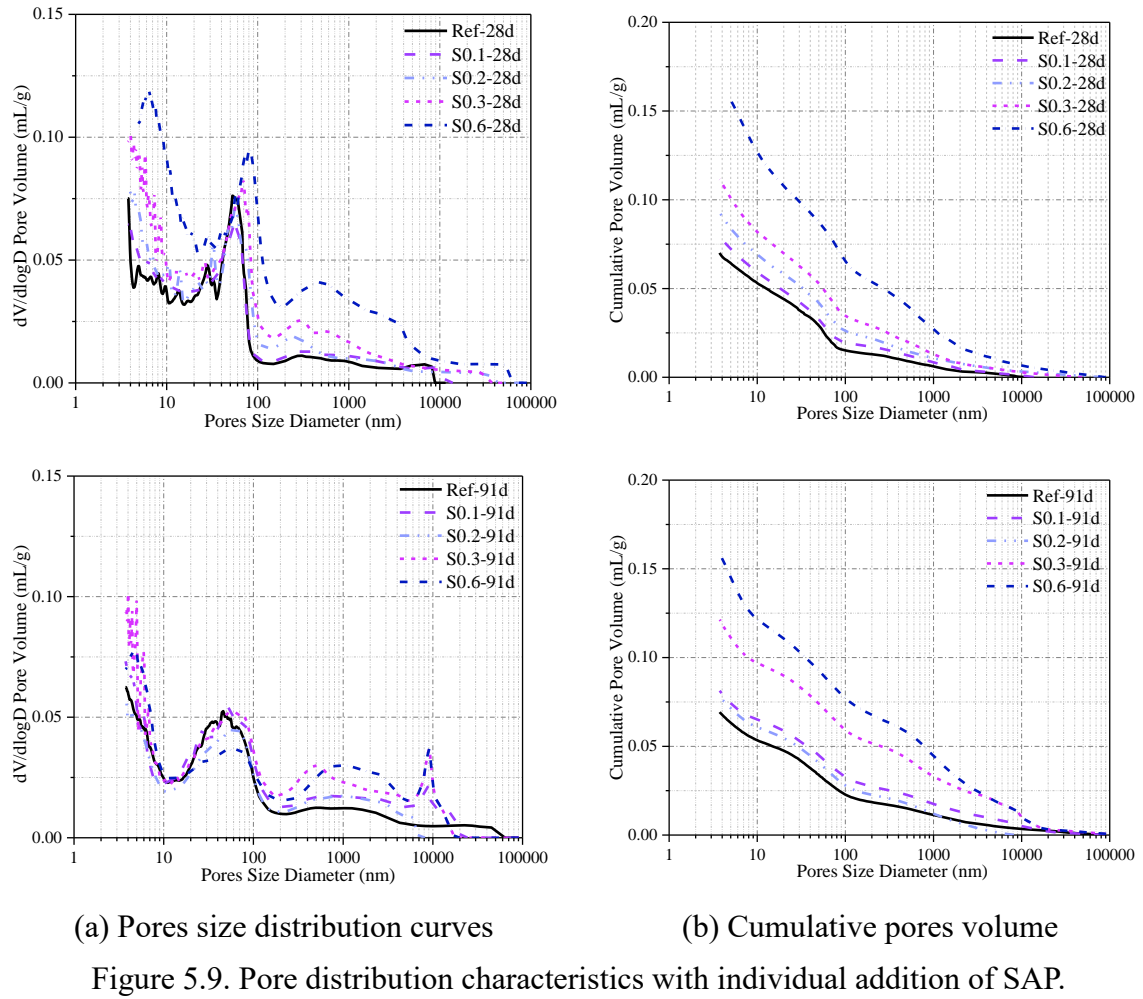


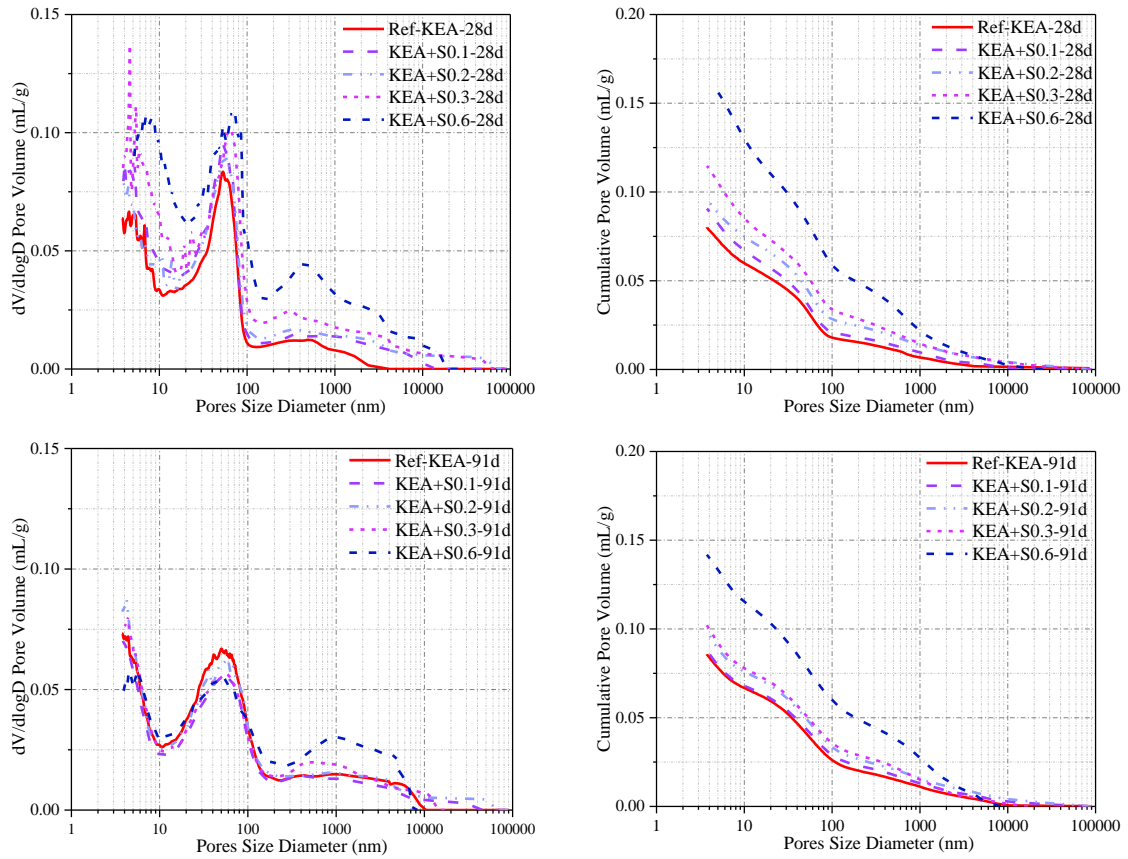
Figure 5.8. Relationship between length and mass change under the drying condition (from day 7 to 91).

Figure 5.8 shows the correlation between the length and mass change under drying conditions (From day 7 to 91). As can be seen from the figures, Figures 5.8(a) and (b) have similar trends regardless of the individual/hybrid addition of SAP and KEA as well as have a good linear correlation between length and mass change under the drying condition. However, the addition of SAP and KEA caused a change in the slope of the length and mass correlation curves, which can be noticed that the slope decreased with the increase of SAP content as compared with Ref. Besides, it also can be noticed that the slope of the case of KEA addition became slightly larger than that of non-KEA. The reason may be attributed to the addition of KEA promotion of pore refinement, due to its reaction with water to produce the more voluminous calcium hydroxide (Corinaldesi & Nardinocchi, 2016). In addition, this correlation can be divided into two phases according to curing methods. In the first phase from day 7 to 28 (annotated I phase as sheet-curing under drying environment), mortar specimens had slight mass loss and shrinkage. In the second phase from day 28 to 91 (annotated II phase as air-curing under drying environment), it can be found that initially (above the red dotted line), mortar specimens had a large mass loss but small length change, and then (below the red dotted line) small mass loss but large length, while this phenomenon becomes

more obvious as the SAP content increases regardless of the presence of KEA. The phenomenon above the red dotted line is mainly related to the SAP content (about 42 days before), and the slopes of the curves below the red dotted line are almost similar, indicating that it seems to have nothing to do with the SAP content (about 42 days later). In summary, the results showed that the addition of SAP slowed down the shrinkage of the mortar under the drying environment, whereas the addition of KEA accelerated the shrinkage slightly may relate to the pore refinement. In general, drying shrinkage mainly caused by moisture evaporation and migration which is related to the formation of surface tension of the liquid and radius of menisci curvature according to the Kelvin and Laplace equations (Kovler & Zhutovsky, 2006), meanwhile, it also is related to the micropores volume (Monteiro, 2006). Consequently, the pores distribution characteristics are significant for shrinkage analysis under a drying environment (W. Zhang, Hama, & Na, 2015). The results of pores size distribution characteristics and the relationship between drying shrinkage and pores volume were discussed in Sections 3.2 and 3.4.







(a) Pore size distribution curves

(b) Cumulative pore volumes

Figure 5.10. Pore distribution characteristics with hybrid addition of SAP and KEA.

#### 5.4.4 Pores distribution characteristics

Mortar samples with the same curing and drying conditions were measured by the MIP technique, the results were shown in Figures 5.9 and 5.10. Overall, mortar samples with SAP have a higher volume of pores than the Ref, and the volume of pores increased with the increase of SAP content, meanwhile, they have similar pore size distribution regardless of presence of SAP and KEA. Furthermore, it can be noticed that mortar samples with SAP show a similar multimodal characteristic, and the shift of the peak point (10 nm-100 nm) to the right increased with the increase of SAP content. Figure 5.9 shows the size of the pores distributions and cumulative pore volume of the individual addition of SAP at 7 days, 28 days, and 91 days. As can be seen from Figure 5.9(a), the peak values gradually decreased,

and slight shifts to the left as the age increased, especially for the sample with 0.6% SAP. In addition, it can be observed that the diameter of pores in the range of 100 nm - 100,000 nm, the volume of the pores size distributions with SAP was more than the Ref, and the change of peak points in the range of 10 nm - 100 nm: when the age was between day 7 and day 28, the peak value of Ref was significantly reduced compared to the samples with SAP. In contrast, when the age was between day 28 and day 91, compared with Ref, the peak value of the SAP samples significantly decreased. Therefore, the addition of SAP seems to delay the hydration of cement.

Figure 5.10 shows the pores distribution and cumulative pore volume of the hybrid addition of SAP and KEA at 7 days, 28 days, and 91 days. Although the incorporation of KEA seems to have similar trends compared to the samples without KEA, the addition of KEA resulting in the curve shifting to the left more significantly. It may indicate that the addition of KEA promoted pore refinement (Corinaldesi & Nardinocchi, 2016), a similar conclusion can also be echoed in Figure 5.8 In addition, peak points in the range of 10 nm-100 nm: when the age was between day 7 and day 28, the peak value of Ref - KEA was significantly reduced compared to the samples with SAP. In contrast, when the age was between day 28 and day 91, compared with Ref - KEA, the peak value of the SAP samples significantly decreased. This phenomenon is consistent with the results of pore distribution characteristics with individual addition of SAP. Thus, it may mainly be related to the introduction of SAP and not to the addition of KEA. Besides, comparing Figures 5.9 and 5.10, it can be seen that when the age is 28 days to 91 days, the pore volume, in the range of 0 - 100 nm, of the samples with SAP reduced greater than Ref and Ref-KEA, respectively. It seems to mean that the SAP played a significant role in storing water inside the mortar matrix and promoting further hydration (Lyu et al., 2019; Ma et al., 2017; Oh & Choi, 2018; Wehbe & Ghahremaninezhad, 2017).

### 5.4.5 Compressive strength

Compressive strength was determined with the mortar samples under the same curing and drying conditions. Figure 5.11 shows the effect of the individual or hybrid inclusion of SAP and KEA on compressive strength of mortar specimens at 7 d, 28 d, and 91 d, respectively. It can be seen that the addition of SAP had a negative influence on the compressive strength of the mortar at all ages, especially for an early age, and the compressive strength of mortar specimens decreased with the increase of SAP content. Similar results were also attained by some scholars (Gupta, 2018; Kong et al., 2014; Song et al., 2016). In this work, the addition of KEA to mortar specimens had little effect on its compressive strength, however, some studies have shown that the use of KEA causes a slight increase of compressive strength (Gagné, 2016). It also seemed that the introduction of SAP had a significant influence on compressive strength, especially for the mortar with 0.6% SAP content, the compressive strength reduced more than 50%. The adverse influence of SAP on the compressive strength of mortar specimens was also reported by Refs. (Kong et al., 2014; Song et al., 2016) and was mainly attributed to SAP, which expands after absorbing water, became a hydrogel, and formed voids in the cementitious materials after water release. Indeed, the distinction in compressive strength of mortar samples with and without SAP decreased over time, indicates that the initial difference in porosity is at least partially compensated by further hydration and reduced porosity due to mixing the SAP (Hasholt, Jensen, Kovler, & Zhutovsky, 2012; Jensen et al., 2002), as manifested as the pore volume from day 28 to 91 caused large reduction due to the addition of SAP (see in Figures 5.9 and 5.10).

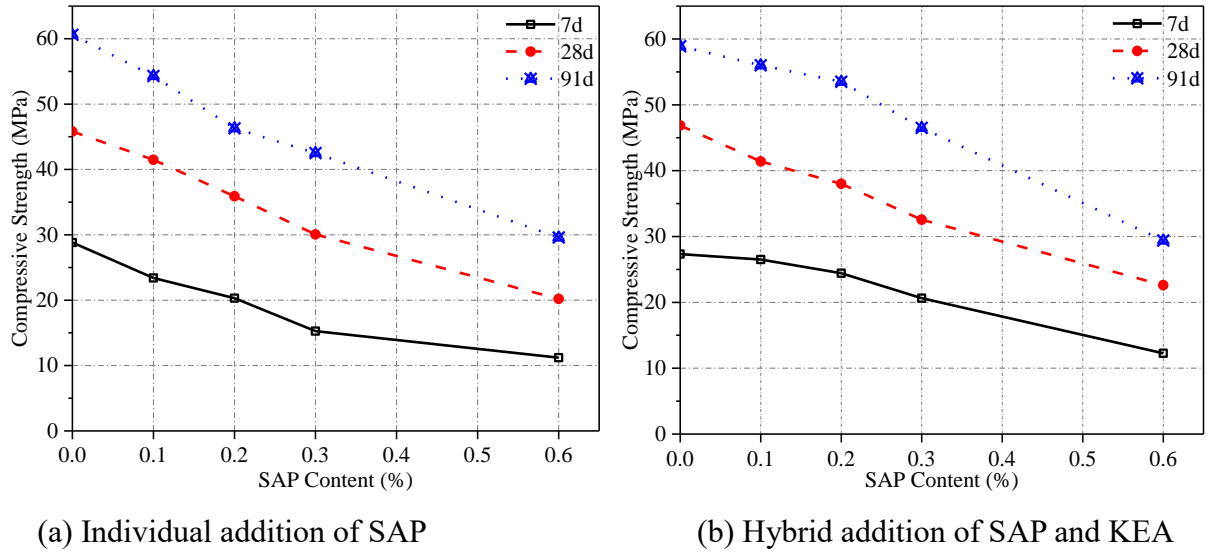


Figure 5.11. Compressive strength with different SAP dosages and with/without KEA.

#### 5.4.6 Effect of pore structure on the drying shrinkage, mass loss and the compressive strength

After 21 days of sheet curing, the surfaces of the mortar specimens were completely exposed to the drying conditions. Thus, it is considered that the mortar specimens were completely drying shrinkage from 28 to 91 days and assume the relative shrinkage (from 28 to 91 days) as dry shrinkage. In general, for the drying shrinkage, pores with a size of less than 50 nm have a significant effect (Monteiro, 2006), whereas, in this work, the most probable pore diameters of mortars were mostly in the 0 - 100 nm diameter range and closer to 100 nm; these results can be observed in Figures 5.9 and 5.10. Therefore, the pores volume (pore diameter < 100 nm) at 28 d was a considerable indicator for evaluating dry shrinkage of mortars in this study. The relationship among the SAP content, the drying shrinkage, the mass loss, and the pore volume (pore diameter < 100 nm) were presented in Figure 5.12. As can be seen in Figure 5.12(a), the pore volume (pore diameter < 100 nm) increased with the increase of SAP content. At the same time, the pore volume (pore diameter < 100 nm) of mortar with KEA was slightly higher compared with the non-KEA. A similar result can also be seen in Figure 5.12(d), especially for the samples of S0.6 and KEA - S0.6, although the total pore volume of S0.6 was larger than that of KEA - S0.6, its pore volume (diameter < 100 nm) is

smaller than KEA - S0.6. Thus, it was verified again that KEA promotes the pore refinement (Corinaldesi & Nardinocchi, 2016). Figures 5.12(b) and (c) show the correlation between the drying shrinkage/the mass loss and pore volume (pore diameter < 100 nm). It can be found that the drying shrinkage/the mass loss increased with increasing pore volume. Furthermore, it verified that the high correlation between the drying shrinkage/the mass loss and pore volume less than 100 nm diameter. A similar result was also obtained by Chol (Chol, Lee, Lee, & Nam, 2019). From the results in Figures 5.12(c) and (d), they also proved the reason that the mass loss of the sample with KEA was less than that without the KEA, which were shown in Figure 5.5(b) and Figure 5.6(b). To sum up, the addition of SAP and KEA resulted in an increase in pore volume with pore diameter in the range of 0 - 100 nm at 28 d, especially for samples with KEA, and this result ultimately increased the drying shrinkage. However, for samples with KEA, the moisture evaporation reduced due to that KEA promoted the pore refinement.

A macropore, according to the general classification by the IUPAC (Aligizaki, 2005; W. Zhang et al., 2015), means a pore diameter greater than 50 nm in diameter which is mainly related to the strength. In addition, the fractal dimension and the capillary pore volume are related to the compressive strength as the positive power function and negative power function respectively according to the conclusion by Lin (Jin, Zhang, & Han, 2017). Thus, in this study, the compressive strength vs. the pore volume (pore diameter > 50 nm) was plotted in Figure 5.13. As can be seen from the regression results that the relation between the compressive strength and the pore volume (pore diameter > 50 nm) follows a power function with a relatively high correlation regardless of SAP content and with/without KEA, especially for the compressive strength vs. the pore volume at 7 d and 28 d, their regression coefficient were 0.91 and 0.92, respectively. Accordingly, a pore volume greater than 50 nm can characterize the compressive strength regardless of presence of SAP and KEA.

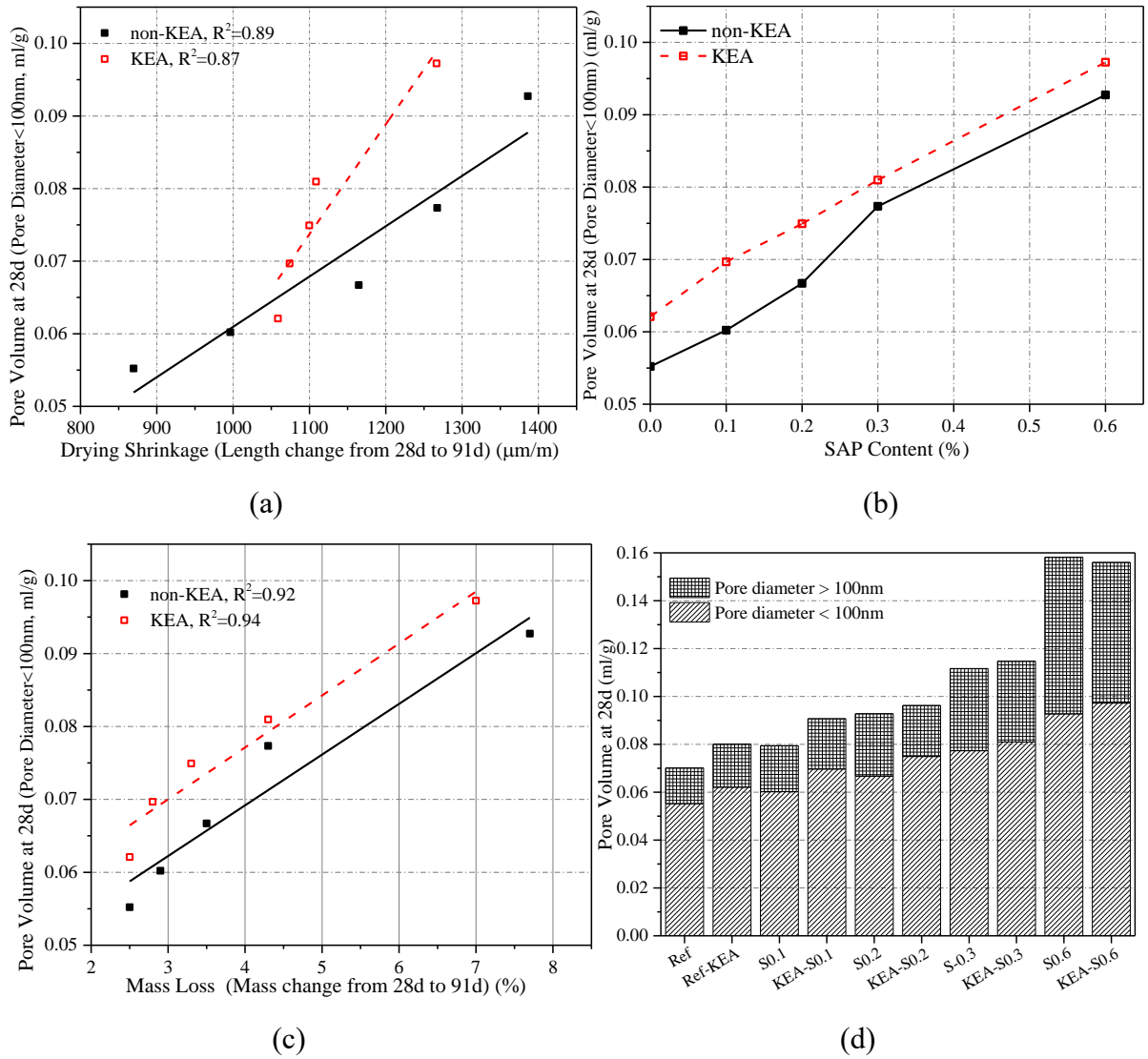


Figure 5.12. The relationship among the SAP content, the drying shrinkage, the mass loss, and the pore volume < 100 nm diameter. (a) Relationship between SAP content and pore volume < 100 nm diameter. (b) Correlation between the drying shrinkage and pore volume < 100 nm diameter. (c) Correlation between the mass loss and pore volume < 100 nm diameter. (d) Pore volume distribution with 100 nm as boundary at 28 d.

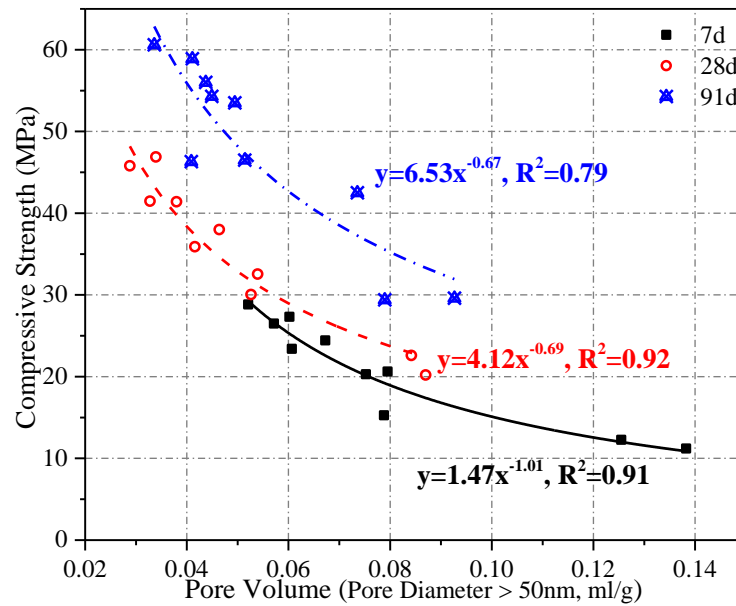


Figure 5.13. The relationship between the compressive strength and the pore volume > 50 nm diameter.

## 5.5 Internal curing concrete with SAP

### 5.5.1 Mixture proportions

Concrete specimens with varying SAP dosages (0.3% and 0.6% (wt) of cementitious materials) and addition of KEA with 20 kg/m<sup>3</sup> and 30 kg/m<sup>3</sup>, were investigated. Two incorporation methods of SAP are considered, namely adding dry SAP powder (such as KEA20 + S0.3) to concrete or adding pre-soaked SAP (such as P-KEA20 + S0.3). Adjustment with additional water to ensure that the concrete with and without SAP had a similar slump. All mixtures are shown in Table 5.4. The slump and air content of fresh concrete were show in this table.

Table 5.4. Mix proportions, slump and air content of concrete.

Mixture type	$W_{\text{eff}}/B$	$W_{\text{tot}}/B$	SAP	AW	Unit content: kg/m <sup>3</sup>						g/m <sup>3</sup>	mm	%
					W	C	S	G	KEA	WRA			
Ref	0.4	0.4	-	-	170	425	614	1151	-	4.3	-	138	4.3
KEA20+A5%	0.4	0.4	-	-	170	405	614	1151	20	4.3	23.4 (5.5A)	143	6.2
KEA30+A5%	0.4	0.4	-	-	170	395	614	1151	30	4.3	23.4 (5.5A)	123	6.0
KEA20+S0.3	0.4	0.42	1.3	10.6	170	405	614	1151	20	8.5	-	140	5.2
KEA20+S0.6	0.4	0.61	2.6	89.3	170	405	614	1151	20	4.3	-	141	1.5
KEA30+S0.3	0.4	0.42	1.3	10.6	170	395	614	1151	30	8.5	-	142	5.3
KEA30+S0.6	0.4	0.61	2.6	89.3	170	395	614	1151	30	4.3	-	142	2.5
P-KEA20+S0.3	0.4	0.42	1.3	10.6	170	405	614	1151	20	8.5	-	111	4.0
P-KEA20+S0.6	0.4	0.61	2.6	89.3	170	405	614	1151	20	4.3	-	149	2.8
P-KEA30+S0.3	0.4	0.42	1.3	10.6	170	395	614	1151	30	8.5	-	126	5.3
P-KEA30+S0.6	0.4	0.61	2.6	89.3	170	395	614	1151	30	4.3	-	137	2.8

Notes: AW is additional water, WRA is water reducing agent, AE is air Air-entraining agent, SL is slump, and AC is air content.  $W/B_{\text{tot}}$  is the ratio of total water content, including the water absorbed by the SAP, to the total binder. For the  $W/B_{\text{eff}}$  (effective W/B), the amount of water absorbed by SAP is excluded.

### 5.5.2 Testing methods

#### *Length and mass change*

The prismatic concrete specimens with a dimension of 100 mm × 100 mm × 400 mm were cast for measuring the length change and mass loss. A hand-held strain comparator with an accuracy of 0.001 mm was employed to measure the length change according to the JIS A 1129-2 contact-type strain gauge method (see Figure 5.14). Meanwhile, an electronic balance with an accuracy of 0.01 g was used to record the mass of specimens. After demolding and sticking the contact chips, the initial length and mass were recorded. Two lateral surfaces perpendicular to the specimen casting surface were measured and the mean results obtained from every three tested specimens were reported.

The length and mass change at n days were calculated as follows Eq. (5-1) and (5-2).

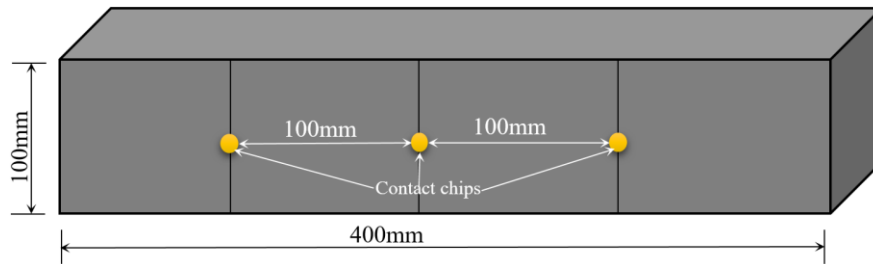


Figure 5.14. Concrete specimens for measuring changes in length and mass.

### ***Pore size distribution and characteristics***

The pore characteristics of mortar were determined by Mercury Intrusion Porosimetry (MIP) at 7 days, 28 days, and 91 days, respectively. The mortar specimens were cut into approximately 5-mm-block samples and placed into an acetone bath for preventing the cement hydration reaction. The resulting samples were stored in an oven to ensure that the free water in the pores is completely evaporated, prior to MIP testing.

### ***Compressive strength***

The compressive strength testing was carried out on mortar specimens with a size of  $\Phi 100 \text{ mm} \times 200 \text{ mm}$  according to Japanese Industrial Standard (JIS A 1108). The compressive strength was determined from an average of each batch (three samples) at 7 days, 28 days, and 91 days, respectively.

### **5.5.3 Influence of incorporation methods of SAP on internal curing effect**

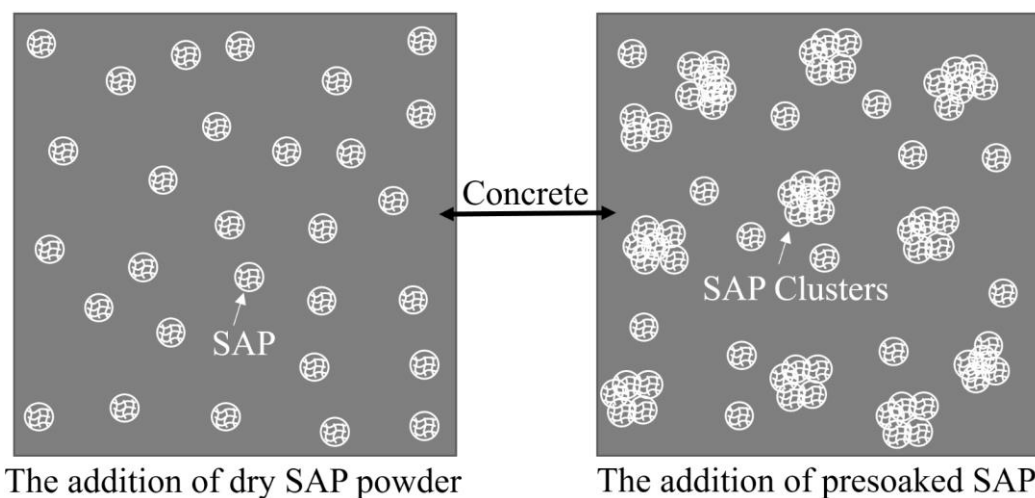


Figure 5.15. Distribution characteristics of SAP in hardened concrete.

Figure 5.15 shows the distribution characteristics of SAP in hardened concrete. It can be noticed that the two incorporation methods show different distribution characteristics in concrete. These distribution characteristics can also be observed in Figure 5.16. It is indicated that the dry SAP powder is more evenly distributed and less likely to generate larger clusters in the concrete during the mixing process than the presoaked SAP.

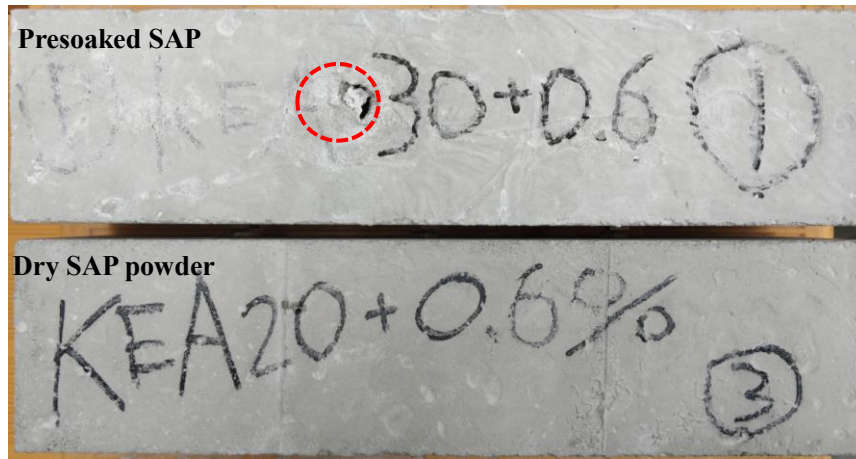


Figure 5.16. The phenomenon on the surface of hardened concrete.

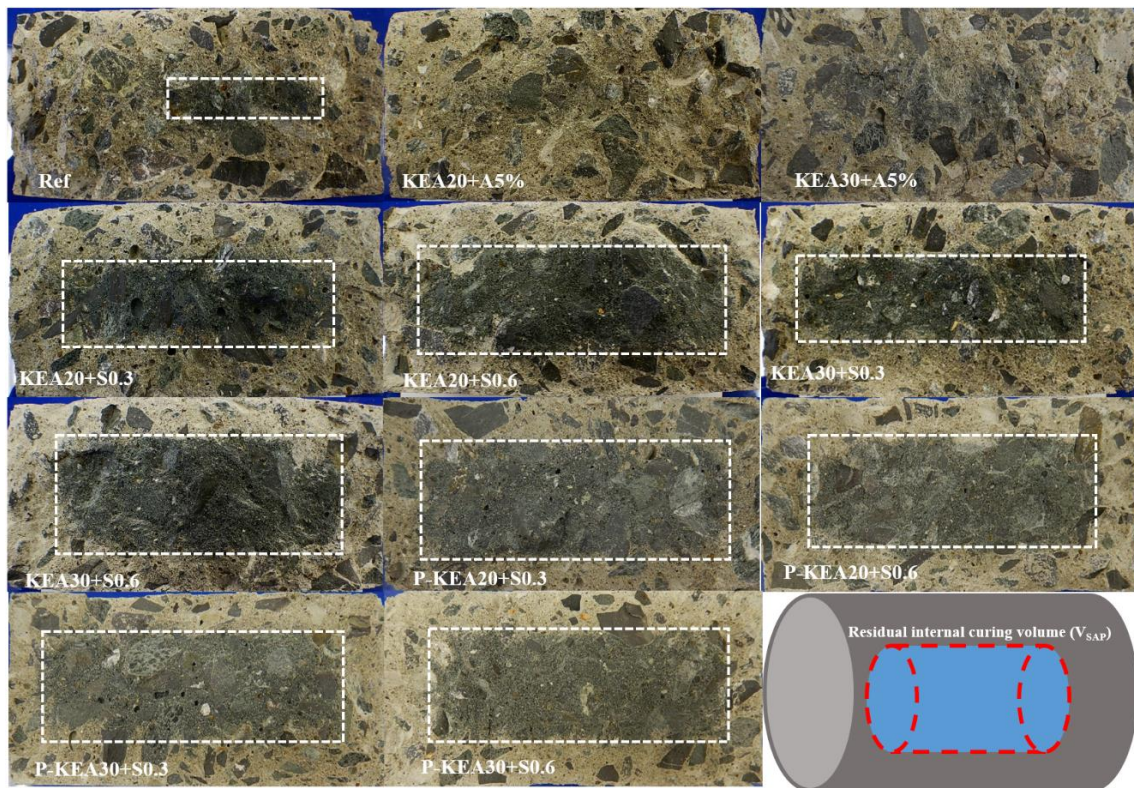


Figure 5.17. Range of concrete affected by internal curing.

Figure 5.17 shows the range of concrete affected by internal curing after 91 days (Demolding after 1 day, water curing 6 days, sheet curing for 21 days, and cured for 63 days under drying conditions (RH 60%, temperature 20°C)). For the Ref, KEA20 + 5% and KEA30 + A5%, it can be found that after 63 days of curing under drying conditions, the concrete seems to be completely dry or has a smaller range of influence. On the contrary, for the concrete specimens with SAP, due to the continuous effect of the internal curing (SAP continuously releases moisture), which slows down the loss of moisture inside the concrete, so the residual wetting range is relatively large. Therefore, assuming that the influence range of the residual wetting inside the concrete is a cylinder, the volume of the cylinder is calculated, and the influence volume is shown in Figure 5.18. From this figure, it can be noticed that compared with the concrete mixed with dry SAP powder, the pre-soaked SAP has a larger wet residual volume. This may be related to the absorption capacity of SAP in tap water and cement extract (see Figure 5.2(b), the absorption capacity in tap water is approximately 4 times that in cement extract). Accordingly, the pre-soaked SAP may store more moisture than the addition of dry SAP powder, so it is possible to maintain the internal curing state for longer under the same drying conditions.

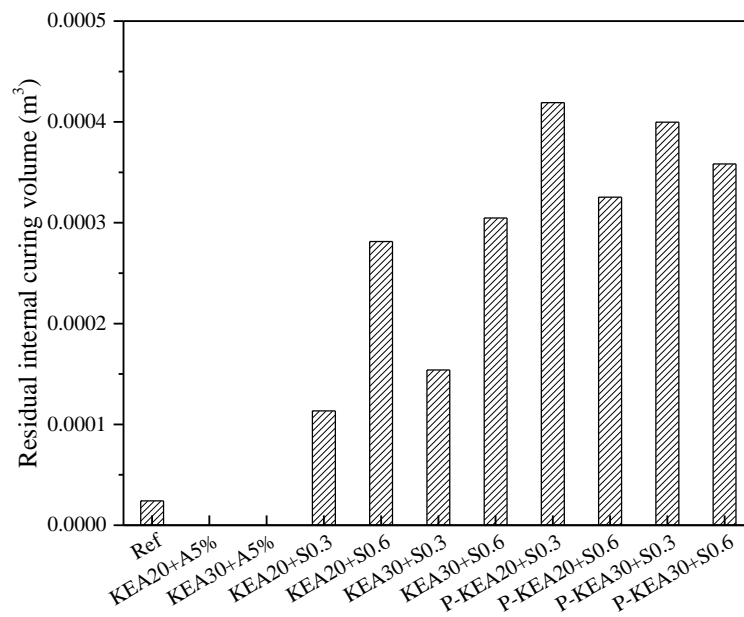


Figure 5.18. Estimate the residual internal curing volume.

5.5.4 Effect of incorporation methods of SAP on length and mass change

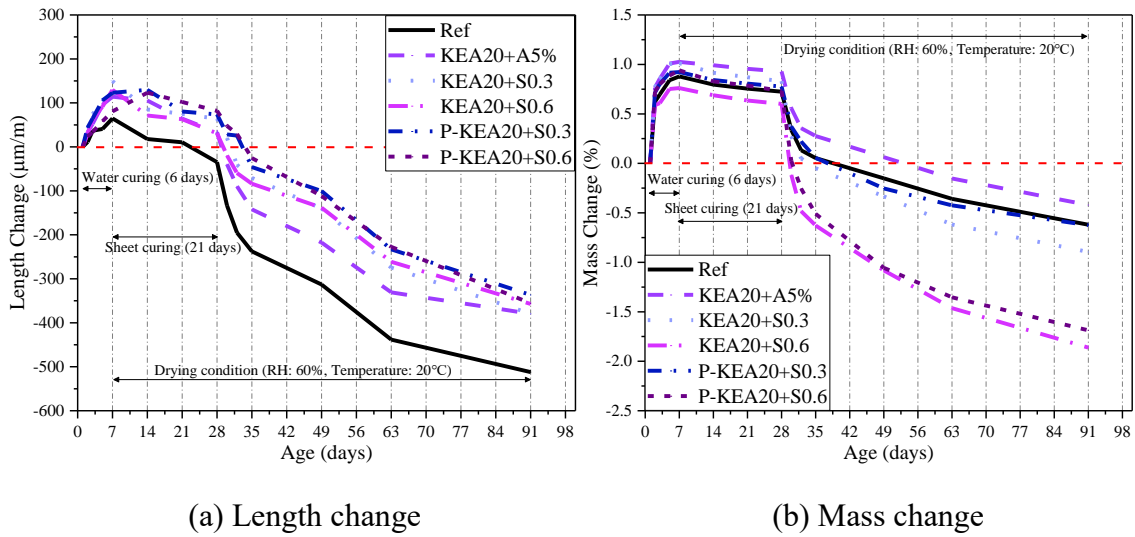


Figure 5.19. Effect of the incorporation methods of SAP on length and mass (KEA20).

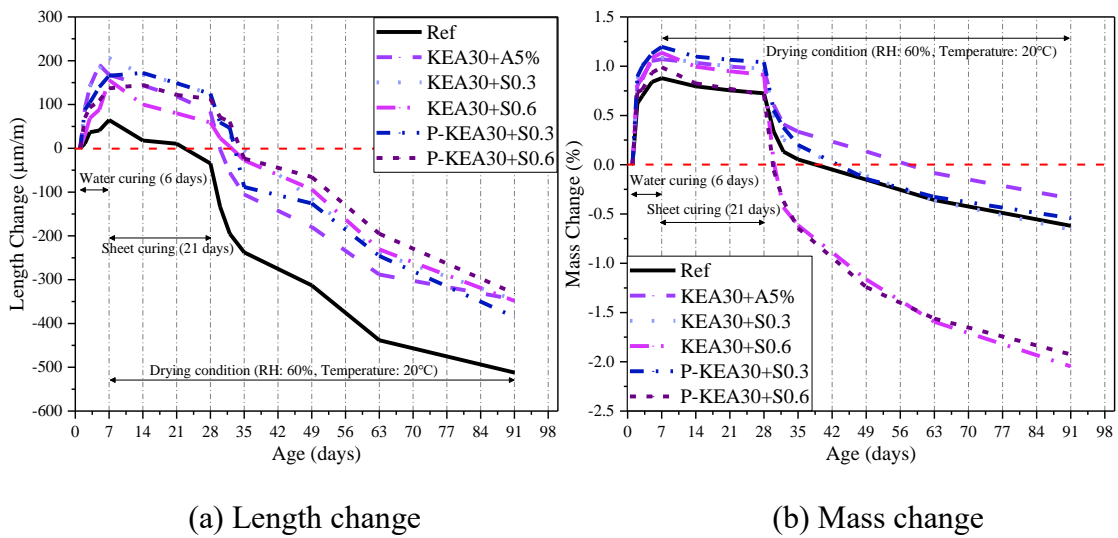


Figure 5.20. Effect of the incorporation methods of SAP on length and mass (KEA30).

Figure 5.19 and 5.20 show the effect of incorporation methods of SAP on length and mass change. Overall, the early expansion of concrete increases with the increase of expansion agent, regardless of incorporation methods and contents of SAP. Compared with Ref, the addition of KEA causes early concrete expansion, thereby compensating for concrete

drying shrinkage. In terms of the duration of the initial expansion, compared with the addition of dry SAP powder, the concrete with pre-soaked SAP has a longer expansion time (up to 14 days). However, the maximum expansion value of specimens with pre-soaked SAP is slightly lower than that of concrete with dry SAP powder. In addition, compared with Ref, KEA20 + 5%, and KEA30 + 5% samples, the addition of SAP slows down the accelerated shrinkage of concrete after the film is cured (after 28 days), regardless of the incorporation methods. Also, it can be noticed that the shrinkage of the concrete samples with SAP before 63 days is less than that of the KEA20 + 5% and KEA30 + 5% samples. This result is different from the test result of the mortar sample (before 49 days) and the 91-day shrinkage of the concrete samples was smaller than that of the mortar samples, which may be mainly related to the size effect of the samples and the use of coarse aggregate. Furthermore, it can be observed that the mass loss of the concrete cured by the film in 7 to 28 days is negligible (see Figures 5.19(b) and 5.20(b)). Therefore, it can be considered that in this period, the shrinkage behavior of concrete is mainly autogenous shrinkage. It can be found that compared with Ref, the addition of KEA and SAP seems to improve the autogenous shrinkage behavior of concrete. However, for concrete with dry SAP powder, when compared with KEA20 + A5% and KEA30 + A5%, it seems that the addition of KEA plays a major role in the autogenous shrinkage of concrete. On the contrary, for the concrete with pre-soaked SAP, the combination of pre-soaked SAP and KEA presents a significant synergistic effect on the autogenous shrinkage of the concrete, which not only extends the expansion period but also reduces the autogenous shrinkage of the concrete. To sum up, the addition of SAP delayed the drying shrinkage of concrete, regardless of the incorporation methods. At the same time, the synergistic effect of KEA and SAP reduces the autogenous shrinkage of concrete, especially for concrete with pre-soaked SAP.

### **5.5.5 Pores distribution characteristics**

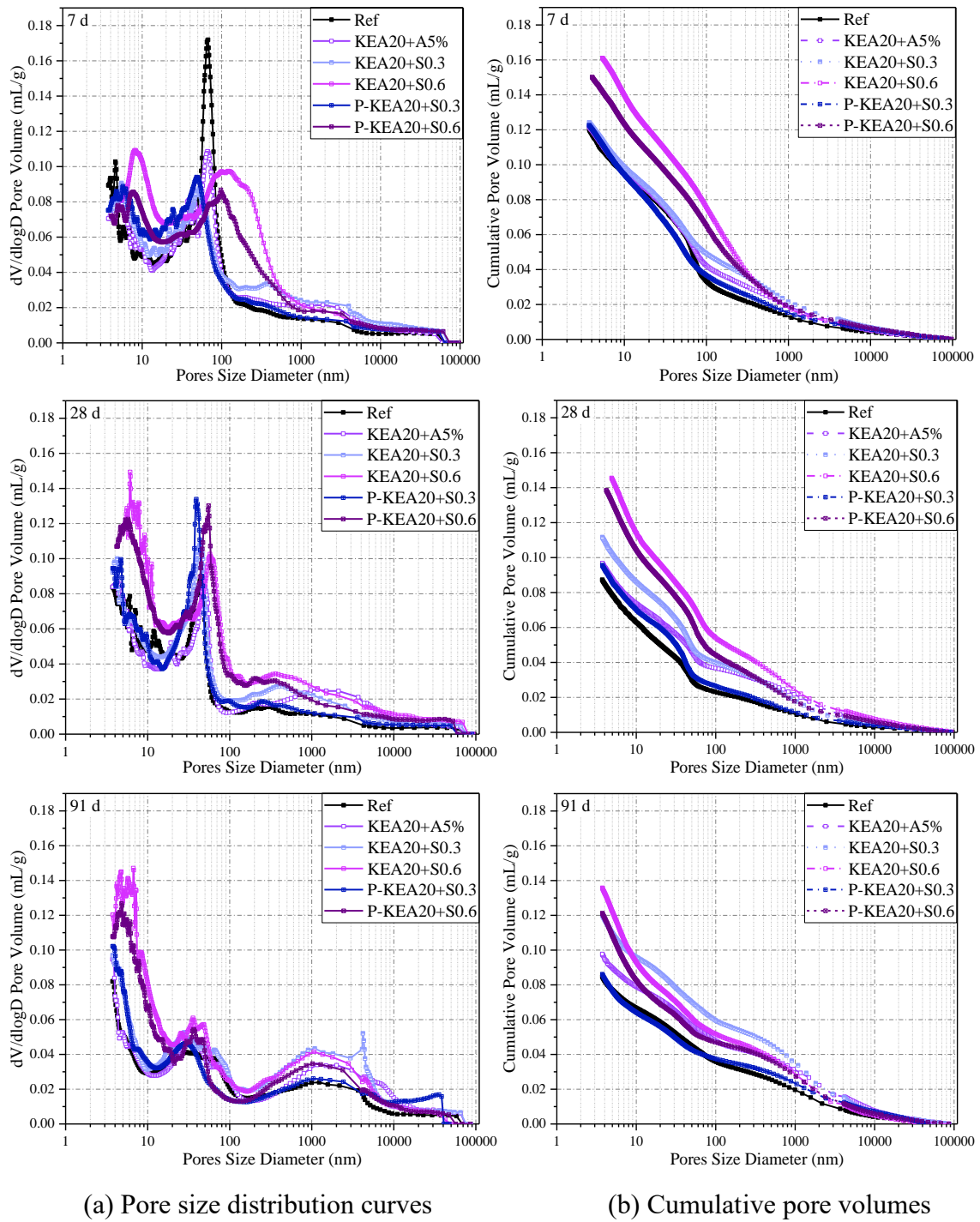


Figure 5.21. Effect of incorporation methods and contents of SAP on the pore distribution characteristics. (KEA20)

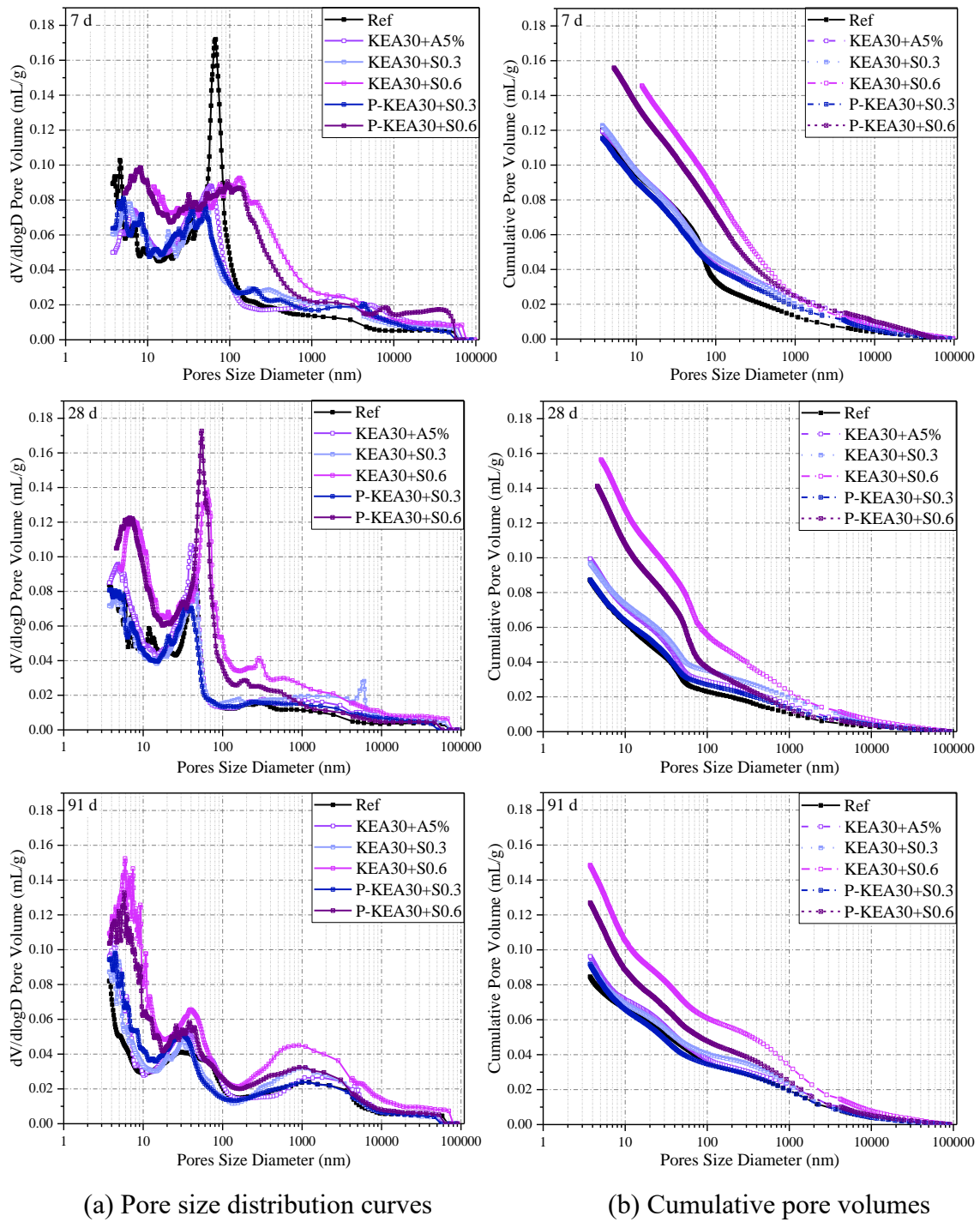
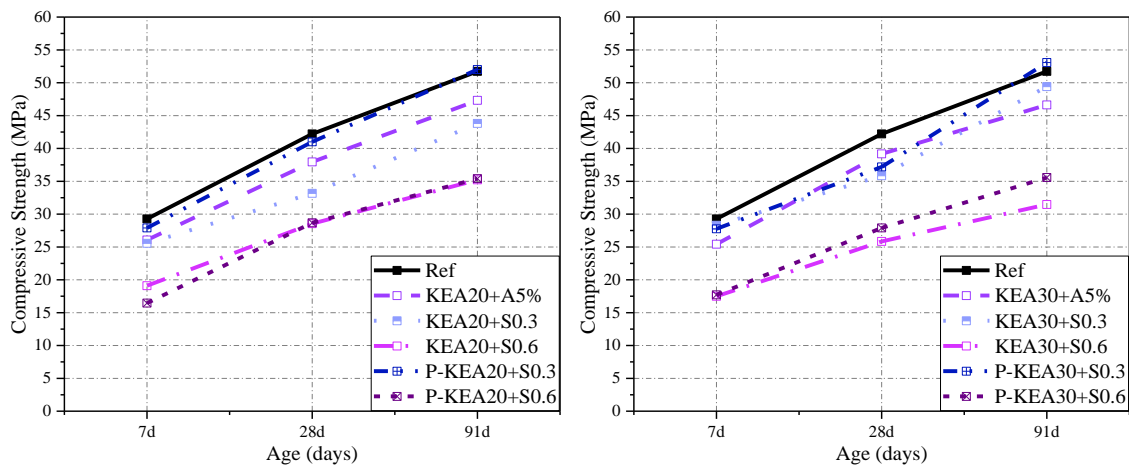


Figure 5.22. Effect of incorporation methods and contents of SAP on the pore distribution characteristics. (KEA30)

Figures 5.21 and 5.22 show the effect of SAP incorporation methods and the contents of SAP and KEA on the pore distribution characteristics. Overall, the cumulative pore volume decreases with increasing age, while the pore size distribution curves shift to the left and downward. As can be seen from Figures, compared with the concrete sample with dry SAP powder, the pore volume of the pre-soaked SAP sample is smaller, regardless of the concrete age and the contents of KEA and SAP. This may be related to the SAP cluster phenomenon mentioned earlier. In fact, due to the SAP cluster phenomenon in fresh concrete, the dispersion of independent SAP particles in the concrete is reduced, thereby the pore volume in the hardened concrete measured by MIP slightly lowered. Besides, for concrete samples with SAP, it can be noticed that when the age is between 7 and 28 days, the transition from large pore diameter to small pore diameter is more significant, especially for the concrete samples with the SAP content of 0.6%. For the effect of the contents of KEA on the pore distribution characteristics, it can be found that when the SAP same dosage, the pore volume of the pore sizes within the range of 0 - 100 nm in the order of descending were KEA30 > KEA20 > Ref. This may be related to the expansion agent (KEA) promoting pore refinement.

**5.5.6 Effect of incorporation methods of SAP on compressive strength**



(a) Concrete specimens with KEA20

(b) Concrete specimens with KEA30

Figure 5.23. Compressive strength of concrete with different incorporation methods, SAP

and KEA contents.

Figure 5.23 shows the compressive strength of concrete with different SAP and KEA contents. It can be found that the content of KEA has little effect on the compressive strength of concrete. It also can be seen that the addition of SAP and the introduction of air bubbles by air-entraining agent reduce the compressive strength of concrete compared with Ref. Moreover, by comparing the compressive strength of concrete of different ages, it is found that when SAP content is 0.3%, its compressive strength is closer to that of concrete with 5% air content. This seems to be related to the relatively close air content of the fresh concrete. Also, for the samples with 0.3% SAP content, it can be seen that the slope of the compressive strength curve from 7 to 28 days is smaller than the slope of the curve from 28 to 91 days, which indicates that the strength develops rapidly after 28 days. In contrast, for other samples, the compressive strength develops slowly after 28 days. Furthermore, comparing concrete samples with the same age and SAP content, it is found that the compressive strength of the concrete with pre-soaked SAP is slightly greater than that of the concrete sample with dry SAP powder. This may be mainly due to the fact that the pore volume of the concrete sample with pre-soaked SAP is slightly lower than the sample with dry SAP powder as shown by the distribution of pore characteristics in Figures 5.21 and 5.22. Although the addition of pre-soaked SAP leads to the formation of larger pores in concrete as shown in Figure 5.16, it is not present in large amounts. Most of the SAP in the concrete matrix (excluding the clustered SAP) is still in a uniform and dispersed state.

## 5.6 Summary

- The incorporation of SAP can effectively mitigate its autogenous shrinkage and the length change value of the mortar with SAP is smaller than Ref until 49 d, regardless of with/without KEA. Moreover, the hybrid addition of SAP and KEA increases the initial expansion of the specimens as compared with the individual addition of KEA, which has a beneficial effect on compensating for the shrinkage of the mortar under drying conditions.

- The addition of SAP seems to be negative for relative shrinkage (equivalent to drying shrinkage), whereas, the addition of KEA seems to improve the adverse effects, in particular, when the SAP content is greater than or equal to 0.2%, the combined effect of SAP and KEA is more prominent. It is because KEA improves the early expansion of the mortar. In addition, the length change vs. mass change has a good linear correlation under the drying environment.
- The addition of SAP seems to delay cement hydration and increase the volume of macropores (greater than 100 nm), thereby reducing the compressive strength of the mortars. In contrast, the introduction of KEA slightly promoted the formation of micropores, resulting in a slight increase in compressive strength compared to the samples without KEA.
- The addition of SAP and KEA resulted in an increase in pore volume with pore diameter in the range of 0 - 100 nm at 28 d, especially for samples with KEA, and this result ultimately increased the drying shrinkage. However, for samples with KEA, in view of it promoting pore refinement so as to reduce moisture evaporation.
- From the regression analysis, the relation between macropore volume (pore diameter > 50 nm) vs. compressive strength follows a power function with a relatively high correlation regardless of SAP content and with/without KEA. Therefore, a pore volume greater than 50 nm can characterize the compressive strength regardless of the presence of SAP and KEA.
- For the concrete with pre-soaked SAP, due to the clustering of pre-soaked SAP in the fresh concrete, it is difficult to uniformly distribute in the concrete matrix, resulting in the formation of larger pores in the hardened concrete. However, the existence of these larger pores did not adversely affect the compressive strength of concrete. In addition, when the surface of concrete was exposed for 63 days under drying conditions, the wet residue range of the concrete samples with pre-soaked SAP was larger than that of the concrete samples with dry SAP powder.

- For the length and mass change, the combined effect of SAP and KEA is beneficial to mitigate the autogenous shrinkage of concrete and delay the drying shrinkage, regardless of the incorporation methods of SAP. Moreover, SAP maintains the relative humidity inside the concrete by continuously releasing water, which causes an increase in the loss of concrete mass.
- The voids created by SAP and air-entraining agent have a negative impact on the compressive strength of concrete. The compressive strength decreases with the increase of SAP contents, regardless of the incorporation methods of SAP. In addition, when the SAP content is 0.3%, its compressive strength is greater than or close to the concrete samples with 5% air content.

## 5.7 Reference

- 308, A. C. (2001). *Guide to Curing Concrete (ACI 308R-01)*. Retrieved from Farmington Hills:
- Aligizaki, K. K. (2005). *Pore structure of cement-based materials: testing, interpretation and requirements*: Crc Press.
- Almeida, F. C. R., & Klemm, A. J. (2018). Efficiency of internal curing by superabsorbent polymers (SAP) in PC-GGBS mortars. *Cement and Concrete Composites*, 88, 41-51. doi:10.1016/j.cemconcomp.2018.01.002
- Bentz, D. P., & Jensen, O. M. (2004). Mitigation strategies for autogenous shrinkage cracking. *Cement and Concrete Composites*, 26(6), 677-685. doi:10.1016/s0958-9465(03)00045-3
- Cabrera, J. J. C., & composites, c. (1996). Deterioration of concrete due to reinforcement steel corrosion. 18(1), 47-59.
- Chatterji, S. J. C., & Research, C. (1995). Mechanism of expansion of concrete due to the presence of dead-burnt CaO and MgO. 25(1), 51-56.
- Chen, B., Ding, J., Cai, Y., Bai, Y., & Zhang, W. (2016). Influence of internal curing and expansive agent on concrete complex Internal curing agent crack resistance *Journal*

- of the Chinese Ceramic Society*, 44(2), 189-195 (in Chinese).
- Chen, W., Qian, J., He, B., Liu, J., Zhang, L., & Jia, X. (2013). Effects of expansive agent and shale pottery on shrinkage reduction of lower water-cement ratio mortar. *Journal of the Chinese Ceramic Society*, 41(4), 505-510 (in Chinese).
- Chol, H., Lee, J., Lee, B., & Nam, J. (2019). Shrinkage properties of concretes using blast furnace slag and frost-resistant accelerator. *Construction and Building Materials*, 220, 1-9. doi:10.1016/j.conbuildmat.2019.05.003
- Cohen, M. D., Olek, J., Dolch, W. L. J. C., & Research, C. (1990). Mechanism of plastic shrinkage cracking in portland cement and portland cement-silica fume paste and mortar. 20(1), 103-119.
- Collins, F., Sanjayan, J. G. J. C., & Research, C. (2000). Cracking tendency of alkali-activated slag concrete subjected to restrained shrinkage. 30(5), 791-798.
- Corinaldesi, V., & Nardinocchi, A. (2016). Mechanical characterization of Engineered Cement-based Composites prepared with hybrid fibres and expansive agent. *Composites Part B: Engineering*, 98, 389-396. doi:10.1016/j.compositesb.2016.05.051
- Cusson, D., & Hoogeveen, T. (2008). Internal curing of high-performance concrete with pre-soaked fine lightweight aggregate for prevention of autogenous shrinkage cracking. *Cement and Concrete Research*, 38(6), 757-765. doi:10.1016/j.cemconres.2008.02.001
- Gagné, R. (2016). Expansive agents. In *Science and Technology of Concrete Admixtures* (pp. 441-456).
- Gruyaert, E., Debbaut, B., Snoeck, D., Díaz, P., Arizo, A., Tziviloglou, E., . . . De Belie, N. (2016). Self-healing mortar with pH-sensitive superabsorbent polymers: testing of the sealing efficiency by water flow tests. *Smart Materials and Structures*, 25(8). doi:10.1088/0964-1726/25/8/084007
- Gupta, S. (2018). Effect of presoaked superabsorbent polymer on strength and permeability of cement mortar. *Magazine of Concrete Research*, 70(9), 473-486. doi:10.1680/jmacr.17.00120
- Hasholt, M. T., Jensen, O. M., Kovler, K., & Zhutovsky, S. (2012). Can superabsorbent polymers mitigate autogenous shrinkage of internally cured concrete without compromising the strength? *Construction and Building Materials*, 31, 226-230.

- doi:10.1016/j.conbuildmat.2011.12.062
- Jensen, O. M., Hansen, P. F. J. C., & research, c. (2001). Water-entrained cement-based materials: I. Principles and theoretical background. *31*(4), 647-654.
- Jensen, O. M., Hansen, P. F. J. C., & Research, C. (2002). Water-entrained cement-based materials: II. Experimental observations. *32*(6), 973-978.
- Jin, S., Zhang, J., & Han, S. (2017). Fractal analysis of relation between strength and pore structure of hardened mortar. *Construction and Building Materials*, *135*, 1-7. doi:10.1016/j.conbuildmat.2016.12.152
- Kong, X.-m., Zhang, Z.-l., & Lu, Z.-c. (2014). Effect of pre-soaked superabsorbent polymer on shrinkage of high-strength concrete. *Materials and Structures*, *48*(9), 2741-2758. doi:10.1617/s11527-014-0351-2
- Kovler, K., & Zhutovsky, S. (2006). Overview and Future Trends of Shrinkage Research. *Materials and Structures*, *39*(9), 827-847. doi:10.1617/s11527-006-9114-z
- Laustsen, S., Hasholt, M. T., & Jensen, O. M. (2013). Void structure of concrete with superabsorbent polymers and its relation to frost resistance of concrete. *Materials and Structures*, *48*(1-2), 357-368. doi:10.1617/s11527-013-0188-0
- Lee, H. X. D., Wong, H. S., & Buenfeld, N. R. (2016). Self-sealing of cracks in concrete using superabsorbent polymers. *Cement and Concrete Research*, *79*, 194-208. doi:10.1016/j.cemconres.2015.09.008
- Li, M., Liu, J., Tian, Q., Wang, Y., & Xu, W. (2017). Efficacy of internal curing combined with expansive agent in mitigating shrinkage deformation of concrete under variable temperature condition. *Construction and Building Materials*, *145*, 354-360. doi:10.1016/j.conbuildmat.2017.04.021
- Liu, J., Farzadnia, N., Shi, C., & Ma, X. (2019a). Effects of superabsorbent polymer on shrinkage properties of ultra-high strength concrete under drying condition. *Construction and Building Materials*, *215*, 799-811. doi:10.1016/j.conbuildmat.2019.04.237
- Liu, J., Farzadnia, N., Shi, C., & Ma, X. (2019b). Shrinkage and strength development of UHSC incorporating a hybrid system of SAP and SRA. *Cement and Concrete Composites*, *97*, 175-189. doi:10.1016/j.cemconcomp.2018.12.029
- Liu, J., Shi, C., Ma, X., Khayat, K. H., Zhang, J., & Wang, D. (2017). An overview on the

- effect of internal curing on shrinkage of high performance cement-based materials. *Construction and Building Materials*, 146, 702-712. doi:10.1016/j.conbuildmat.2017.04.154
- Lura, P. (2003). Autogenous deformation and internal curing of concrete.
- Lyu, Z., Guo, Y., Chen, Z., Shen, A., Qin, X., Yang, J., Wang, Z. (2019). Research on shrinkage development and fracture properties of internal curing pavement concrete based on humidity compensation. *Construction and Building Materials*, 203, 417-431. doi:10.1016/j.conbuildmat.2019.01.115
- Ma, X., Liu, J., Wu, Z., & Shi, C. (2017). Effects of SAP on the properties and pore structure of high performance cement-based materials. *Construction and Building Materials*, 131, 476-484. doi:10.1016/j.conbuildmat.2016.11.090
- Mechtcherine, V., Gorges, M., Schroefl, C., Assmann, A., Brameshuber, W., Ribeiro, A. B., . . . Zhutovsky, S. (2013). Effect of internal curing by using superabsorbent polymers (SAP) on autogenous shrinkage and other properties of a high-performance fine-grained concrete: results of a RILEM round-robin test. *Materials and Structures*, 47(3), 541-562. doi:10.1617/s11527-013-0078-5
- Mechtcherine, V., & Reinhardt, H.-W. (2012). *Application of super absorbent polymers (SAP) in concrete construction: state-of-the-art report prepared by Technical Committee 225-SAP* (Vol. 2): Springer Science & Business Media.
- Mechtcherine, V., Schröfl, C., Reichardt, M., Klemm, A. J., Khayat, K. H. J. M., & Structures. (2019). Recommendations of RILEM TC 260-RSC for using superabsorbent polymers (SAP) for improving freeze–thaw resistance of cement-based materials. 52(4), 75.
- Mechtcherine, V., Schröfl, C., Wyrzykowski, M., Gorges, M., Lura, P., Cusson, D., . . . Weiss, J. (2016). Effect of superabsorbent polymers (SAP) on the freeze–thaw resistance of concrete: results of a RILEM interlaboratory study. *Materials and Structures*, 50(1). doi:10.1617/s11527-016-0868-7
- Mechtcherine, V., Snoeck, D., Schröfl, C., De Belie, N., Klemm, A. J., Ichimiya, K., . . . Falikman, V. (2018). Testing superabsorbent polymer (SAP) sorption properties prior to implementation in concrete: results of a RILEM Round-Robin Test. *Materials and Structures*, 51(1). doi:10.1617/s11527-018-1149-4
- Monteiro, P. (2006). *Concrete: microstructure, properties, and materials*: McGraw-Hill Publishing.

- Oh, S., & Choi, Y. C. (2018). Superabsorbent polymers as internal curing agents in alkali activated slag mortars. *Construction and Building Materials*, 159, 1-8. doi:10.1016/j.conbuildmat.2017.10.121
- Otieno, M., Beushausen, H., & Alexander, M. (2016). Chloride-induced corrosion of steel in cracked concrete – Part I: Experimental studies under accelerated and natural marine environments. *Cement and Concrete Research*, 79, 373-385. doi:10.1016/j.cemconres.2015.08.009
- Philleo, R. J. M. S. o. C. (1991). Concrete science and reality. 1-8.
- Schroefl, C., Mechtcherine, V., Vontobel, P., Hovind, J., & Lehmann, E. (2015). Sorption kinetics of superabsorbent polymers (SAPs) in fresh Portland cement-based pastes visualized and quantified by neutron radiography and correlated to the progress of cement hydration. *Cement and Concrete Research*, 75, 1-13. doi:10.1016/j.cemconres.2015.05.001
- Schröfl, C., Snoeck, D., & Mechtcherine, V. (2017). A review of characterisation methods for superabsorbent polymer (SAP) samples to be used in cement-based construction materials: report of the RILEM TC 260-RSC. *Materials and Structures*, 50(4). doi:10.1617/s11527-017-1060-4
- Shen, D., Wang, T., Chen, Y., Wang, M., & Jiang, G. (2015). Effect of internal curing with super absorbent polymers on the relative humidity of early-age concrete. *Construction and Building Materials*, 99, 246-253. doi:10.1016/j.conbuildmat.2015.08.042
- Snoeck, D., Dewanckele, J., Cnudde, V., & De Belie, N. (2016). X-ray computed microtomography to study autogenous healing of cementitious materials promoted by superabsorbent polymers. *Cement and Concrete Composites*, 65, 83-93. doi:10.1016/j.cemconcomp.2015.10.016
- Snoeck, D., Jensen, O. M., & De Belie, N. (2015). The influence of superabsorbent polymers on the autogenous shrinkage properties of cement pastes with supplementary cementitious materials. *Cement and Concrete Research*, 74, 59-67. doi:10.1016/j.cemconres.2015.03.020
- Snoeck, D., Pel, L., & De Belie, N. (2018). Superabsorbent polymers to mitigate plastic drying shrinkage in a cement paste as studied by NMR. *Cement and Concrete Composites*, 93, 54-62. doi:10.1016/j.cemconcomp.2018.06.019
- Snoeck, D., Steuperaert, S., Van Tittelboom, K., Dubruel, P., & De Belie, N. (2012).

- Visualization of water penetration in cementitious materials with superabsorbent polymers by means of neutron radiography. *Cement and Concrete Research*, 42(8), 1113-1121. doi:10.1016/j.cemconres.2012.05.005
- Snoeck, D., Van den Heede, P., Van Mullem, T., & De Belie, N. (2018). Water penetration through cracks in self-healing cementitious materials with superabsorbent polymers studied by neutron radiography. *Cement and Concrete Research*, 113, 86-98. doi:10.1016/j.cemconres.2018.07.002
- Snoeck, D., Van Tittelboom, K., Steuperaert, S., Dubruel, P., & De Belie, N. (2012). Self-healing cementitious materials by the combination of microfibres and superabsorbent polymers. *Journal of Intelligent Material Systems and Structures*, 25(1), 13-24. doi:10.1177/1045389x12438623
- Soliman, A. M., & Nehdi, M. L. (2010). Effect of drying conditions on autogenous shrinkage in ultra-high performance concrete at early-age. *Materials and Structures*, 44(5), 879-899. doi:10.1617/s11527-010-9670-0
- Song, C., Choi, Y. C., & Choi, S. (2016). Effect of internal curing by superabsorbent polymers – Internal relative humidity and autogenous shrinkage of alkali-activated slag mortars. *Construction and Building Materials*, 123, 198-206. doi:10.1016/j.conbuildmat.2016.07.007
- Wang, X. F., Fang, C., Kuang, W. Q., Li, D. W., Han, N. X., & Xing, F. (2017). Experimental investigation on the compressive strength and shrinkage of concrete with pre-wetted lightweight aggregates. *Construction and Building Materials*, 155, 867-879. doi:10.1016/j.conbuildmat.2017.07.224
- Wehbe, Y., & Ghahremaninezhad, A. (2017). Combined effect of shrinkage reducing admixtures (SRA) and superabsorbent polymers (SAP) on the autogenous shrinkage, hydration and properties of cementitious materials. *Construction and Building Materials*, 138, 151-162. doi:10.1016/j.conbuildmat.2016.12.206
- Weyers, R., Conway Jr, J., Cady, P. J. C., & Research, C. (1982). Photoelastic analysis of rigid inclusions in fresh concrete. *12*(4), 475-484.
- Wittmann, F. J. C., & research, c. (1976). On the action of capillary pressure in fresh concrete. *6*(1), 49-56.
- Yang, H., He, Z., Shao, Y., & Li, L. (2018). Improving Freeze-Thaw Resistance and Strength Gain of Roller Compacted Fly Ash Concretes with Modified Absorbent Polymer. *Journal of Materials in Civil Engineering*, 30(3). doi:10.1061/(asce)mt.1943-

5533.0002159

- Yu, P., Mo, L., & Deng, M. (2019). Synergetic effect of MEA and SAP on the deformation and mechanical properties of concrete. *Magazine of Concrete Research*, 1-24. doi:10.1680/jmacr.19.00202
- Zhang, M., Sakoi, Y., Aba, M., & Tsukinaga, Y. J. J. o. A. C. F. (2019). Effect of initial curing conditions on air permeability and de-icing salt scaling resistance of surface concrete. 5(1), 56-64.
- Zhang, W., Hama, Y., & Na, S. H. (2015). Drying shrinkage and microstructure characteristics of mortar incorporating ground granulated blast furnace slag and shrinkage reducing admixture. *Construction and Building Materials*, 93, 267-277. doi:10.1016/j.conbuildmat.2015.05.103
- Zhutovsky, S., Kovler, K., Bentur, A. J. M., & Structures. (2002). Efficiency of lightweight aggregates for internal curing of high strength concrete to eliminate autogenous shrinkage. 35(2), 97-101.

## CHAPTER 6 RECOMMENDATION OF FABRICATING DURABLE BRIDGES

### CONCRETE IN COLD CLIMATE

This study has provided significant investigation of promising on fabricating durable concrete suitable for the cold climate. In this section, some recommendations against the deterioration of concrete in cold climates are proposed.

#### Frost damage

Frost damage is the most important factor and source for the deterioration of concrete bridge structures in cold climate. Using additional curing or prolonging the curing period can effectively improve the deicing salt scaling resistance of concrete surface (At least three weeks of additional curing is recommended). It is well known that the introduction of air bubbles into concrete has a positive effect on the deicing salt scaling resistance. However, the degradation of air voids quality during the actual construction stage of concrete and the process from fresh to maturity is a practical issue. For example, the escape of air bubbles caused by the concrete transportation, pumping and vibration compaction process. Although increasing the air content of fresh concrete is an effective way to improve the air bubbles quality of mature concrete, it is still difficult to accurately and quantitatively control the air voids quality of hardened concrete through the air content of fresh concrete. In addition, air void distribution characteristics in hardened concrete is an extremely complex issue. Even though the same execution process, materials, chemical admixtures, and climate environment were employed for fabricating the same concrete, it is difficult to ensure a stability void distribution characteristics. Therefore, the difference in the air content of each batch of hardened concrete can only be reduced by increasing the initial target air content and ensuring

the same initial target air content. Thereby improving the deicing salt scaling resistance of concrete.

In addition, the introduction of superabsorbent polymers (SAP) seems to be promising in improving the deicing salt scaling resistance of concrete. The voids created by the swelled SAP particles seems to replace the air voids in air-entrained and some studies have shown that the addition of SAP improves the deicing salt scaling resistance of concrete. The addition of SAP can improve the deicing salt scaling resistance of mortar, whereas, in terms of the efficiency of improving the deicing salt resistance is slightly insufficient as compared with the mortar inclusion of 5% air content.

### **Chloride attack**

In general, the attack of chloride ions is mainly the damage to the steel bars in the RC structures. Therefore, blocking the contact of chloride ions with steel bars is an effective way to resist the attack of chloride ions. Using the blended cements to reduce the permeability of concrete, such as fly ash cement or blast furnace slag cement. The use of blended cements increase the resistivity and hinders the penetration of chloride ions. Another way is to use anticorrosion steel bar to directly block the connection between the steel bars and the outside. These two methods need to be appropriately selected through the harshness of the climate environment. For example, compared with Shinyanagibuchi Bridge, Mount Aobuna No. 1 Bridge is in a harsher climate, so the blast furnace slag cement and anticorrosion steel bars were employed on the Mount Aobuna No. 1 Bridge at the same time (see Figure 4.2).

### **Alkali-silica reaction**

Alkali silica reaction (ASR) is a chemical reaction between alkali hydroxide (usually derived from Portland cement) in concrete pore solution and reactive silica ( $\text{SiO}_2$ ) in sili-

ceous aggregate to generate hygroscopic alkali-silica gel (ASR gel). ASR gel itself is harmless to concrete, however when it absorbs moisture in the environment and swells, it will exert pressure on the surrounding concrete. Therefore, controlling or reducing the formation of ASR gel may reduce the risk of ASR. Aggregates with less silica content and Supplementary cementitious materials (SCMs) such as fly ash (FA), slag cement (GGBFS), or silica fume were employed for reducing the risk of ASR. Among them SCMs can reduce porosity and bind alkalis and calcium within hydration products. Therefore, it is necessary to use SCMs in cold regions, which can not only control the risk of ASR, but also improve the frost resistance of concrete.

### **Early-age shrinkage cracking**

Early-age shrinkage cracking of concrete is a persistent problem that arises from rapid complex volume changes such as autogenous shrinkage, drying shrinkage and thermal deformation. In this work, the lime-type expansive agent (KEA) and superabsorbent polymers (SAP) were used for improving the early-age shrinkage of concrete, the incorporation of SAP can effectively mitigate its autogenous shrinkage and the length change value of the mortar with SAP smaller than Ref until 49 d, regardless of the presence of KEA. It is well known that KEA is beneficial for compensating for shrinkage of RC structures, especially when the W/B is relatively low. The hybrid addition of SAP and KEA increase the initial expansion of the specimens as compared with individual addition of SAP, which is a beneficial effect on compensating for the shrinkage of the mortar under drying conditions. However, it also be noted that excessive addition of SAP will cause a decrease in compressive strength.

Indeed, the expectation for SAP to improve the durability of concrete is not limited to the improvement of the early shrinkage behavior of shrinkage, but also the long-term protection of concrete through its own water absorption/release performance. Research such as self-healing and self-sealing properties.

### Considerations on the durability of concrete in the super- and sub-structures of the bridge

Firstly, for the concrete of superstructure of bridge (bridge slab), it may subject to severe deterioration from deicing salt, fatigue damage, and bending stress. Therefore, for RC bridge slabs, in cold climate, the following countermeasures should be recommended:

(1) **Low W/B ratio ( $W/B \leq 0.45$ )** ensures that the low porosity (compactness) of concrete is formed by cement hydration.

(2) **Additional curing** is used to increase the density of the concrete surface to decrease the air permeability and resist deicing salt scaling.

(3) By increasing the **air content** ( $6\% \pm 1$ ) of fresh concrete, the loss of air content in concrete due to transportation, finishing and vibration is compensated.

(4) **SCMs** (Fly ash and Blast furnace slag) should be used to reduced carbon dioxide emissions, ASR, and drying shrinkage.

(5) **Anti-corrosion steel bars** are used to prevent corrosion of steel bars.

(6) **Expansive agent** and **Superabsorbent Polymers (SAP)** are employed to mitigate the autogenous shrinkage.

Secondly, for the concrete of substructures of bridge (pier, abutment and box culvert), compared with the bridge superstructure, the deicing salt freeze-thaw damage is lighter. The thermal expansion due to cement hydration in mass concrete has become the main factor leading to concrete deterioration. Therefore, for the substructures, the following countermeasures should be recommended:

(1) Properly increase the W/B ratio to reduce the influence of the heat of hydration on the **thermal expansion** of concrete (for example,  $W/B = 0.5$ ).

(2) Use mineral admixtures (Fly ash or Blast furnace slag) to replace ordinary Portland cement to reduce the heat of hydration and **thermal expansion**.

(3) **Additional curing, prolonging the initial curing period** and using **permeability formwork** may effectively improve the surface quality of concrete and make up for the defects of mass concrete caused by bleeding.

(4) In cold climates, proper **air content** is introduced into concrete to resist frost damage, however, the air content (**approximately 4.5%**) can be slightly lower than the air content (**approximately 6%**) in the bridge slab. Reducing the air content in the concrete can appropriately improve the bearing capacity of the bridge substructures.

### **How to apply Superabsorbent Polymers (SAP) internal curing concrete in practical construction?**

Superabsorbent polymers (SAP), a potential internal curing material for concrete, not only shows a positive effect on mitigating the autogenous shrinkage of concrete but is also a promising material in resisting frost damage. Moreover, ready-mixed concrete as the mainstream of engineering construction is widely used in infrastructure construction. Thus, the use of SAP for ready-mixed concrete may be an issue that needs to be considered for the improvement of high-performance concrete in the future. However, for practical construction, before using SAP for concrete serving in cold regions, the following recommendations should be noted:

(1) Recommendations on the method and content of using SAP as an admixture into concrete: Compared with adding pre-soaked SAP, incorporating SAP in a dry powder state is easy to handle and can ensure its uniform distribution in the concrete (The cluster phenomenon will not appear). In terms of compressive strength, it decreases with the increase of SAP content. Accordingly, the SAP content of 0.3% is more appropriate.

(2) In this work, the voids created by SAP were used to replace the air voids introduced by the air-entraining agent to resist deicing salt scaling, which did not achieve the expected effect. Figure 6.1 shows the results of the cumulative scaled materials of concrete with/without SAP after 60 cycles of freeze-thaw. It can be noticed that the void created by SAP does

not improve the effect of concrete against salt freezing scale, but increases the amount of accumulated scale. The reason may be attributed to the large size of SAP particles ( $476.6 \pm 52.9 \mu\text{m}$ ), so it is recommended to use SAP with smaller size particles, preferably with a size less than  $100 \mu\text{m}$ . As can be seen from Figure 6.2, the addition of large-size SAP powder causes the large-size scales to peel off after being damaged by salt freezing.

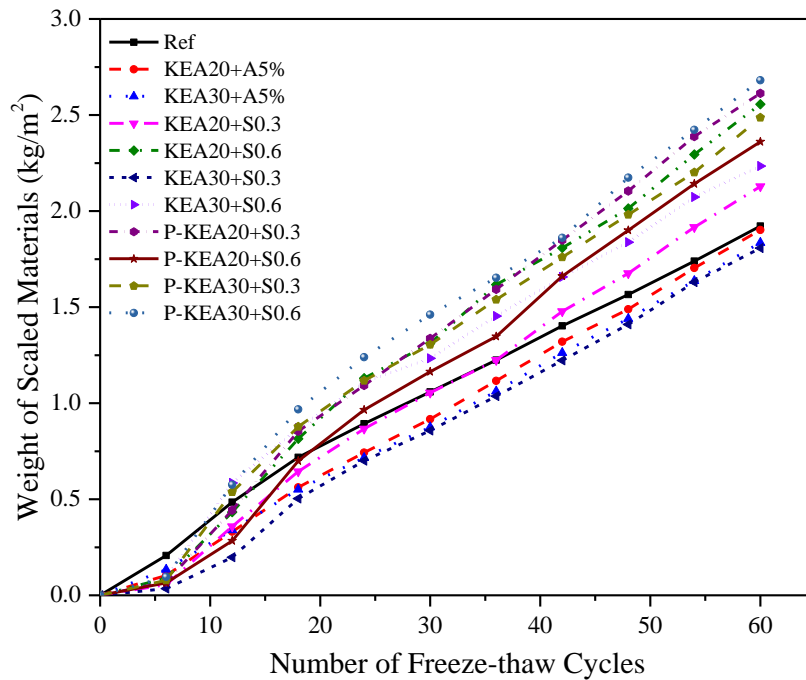


Figure 6.1. Cumulative scaled materials of concrete surface after 60 cycles of freeze-thaw.



(a) Ref

(b) A5% Sample

(c) SAP Sample

Figure 6.2. Comparison of the size of the peeled scales of various samples after salt freezing damage.

(3) For the ready-mixed concrete that is widely used in infrastructure construction. Transportation distance, transportation time, and the choice of the way to store and use SAP powder in the ready-mix plant are quite critical issues. SAP powder should avoid contact with humid environment (sealed storage). The SAP powder, aggregate and binder are fully stirred under dry conditions to ensure the uniform distribution of the SAP powder in the mixture. After adding water, ensure sufficient mixing time so that the extra water is fully absorbed by the SAP powder.

## CHAPTER 7 CONCLUSIONS

### 7.1 General

This work is mainly aimed at investigating the durability of concrete structures in cold climates. It mainly covers field surveys and laboratory tests, including not only the RC substructures of the existing bridges, but also the RC slabs under construction. The field investigation mainly uses non-destructive testing to investigate the influence of the initial curing period of the existing RC bridge substructures on the deicing salt scaling resistance of the concrete. For the concrete durability of the RC bridge slab under construction, laboratory and field tests were carried out. In this chapter, the findings and conclusions of the main research chapters are summarized, respectively.

### 7.2 Major conclusions

#### CHAPTER 2

- The additional curing after demolding or extending the initial curing period can effectively improve the surface quality of concrete, and the surface air permeability coefficient was decreased with the increase of the curing period. When the curing period was greater than about 14 days, there was less variation of the surface air permeability, and the variation trend and speed of the decrease of surface air permeability coefficient will reduce.
- The results of the visual rating of surface micro cracks show the relationship between the micro-cracks and the surface air permeability that the visual rating increases with the decrease of the surface air permeability coefficient. Thus, it is possible that the assessment of the surface quality of concrete through the visual rating of surface micro cracks.

- By using the permeability formwork, the surface air permeability was greatly reduced. In particular, using the permeability formwork was effective for the concrete that has a great amount of bleeding.
- It is helpful for the decision-makers in construction to consider an appropriate initial curing period based on the relationship between the surface air permeability coefficient with the scaling amount after 60 freezing-thawing cycles and the curing period.

### CHAPTER 3

- Concrete with FB cement has a better deicing salt scaling resistance than that of N and BB. Nevertheless, when the air content of fresh concrete reaches 6%, it has little difference in terms of deicing salt scaling resistance regardless of cement types and W/B ratios. In addition, the use of mineral admixtures (fly ash or blast furnace slag) or blended cements can effectively inhibit ASR expansion, especially for BB cement (replacement rate is 42.5%).
- The use of mineral admixtures and reducing the W/B ratio are beneficial to reduce the drying shrinkage of concrete. Moreover, concerning uniaxial restrained and free shrinkage, it can be found that BB - KEA (W/B=0.40) shows good resistance to cracking, autogenous shrinkage, and drying shrinkage.
- The reduction in deicing salt scaling resistance after vibration of the concrete. However, in terms of vibration time, there is little difference in the effect of concrete on the deicing salt scaling resistance. This may be related to the secondary random escape of bubbles caused by the secondary vibration when the concrete sample is loaded into the mold on site.
- Concerning the restrained shrinkage of actual RC slab on construction site, the use of BB40 - KEA has a better effect of early compensation for shrinkage. In addition, through the observation of the cracking of the RC slab 1 year later, it was found

that the cracks appeared at the bottom of the RC slab and were almost mainly concentrated around the spacer blocks (the maximum crack width was 0.14 mm).

#### CHAPTER 4

- By comparing the distribution characteristics of air void of hardened concrete with different mix proportions, it is confirmed that a large number of air void was presented in the diameter of 50 – 300  $\mu\text{m}$ . Especially for the fine air voids, the air void frequency of W/B 35% are greater than that of W/B 50%, regardless of different cement type. It would depend on retention of air void due to increasing viscosity of concrete as unit powder content (W/B), and on the dosage of AE agent.
- In case of the range of diameter 0 – 200  $\mu\text{m}$  which is entrained by AE agent, the percent of air void frequency was greater than 50%, compare to the range of other diameter, regardless of different mixture proportions and execution process. From this point of view, the value of fine air void frequency than that of air content will be promising as important factor to evaluate the effect of air entrainment.
- Excessive vibration is lowered the quality of air void as the range of diameter 0-200  $\mu\text{m}$ . However, influence of pumping process is relatively small.
- The spacing factor fits better with the air void frequency than with the air content in linear condition. Especially, while the range of diameter 0 – 200  $\mu\text{m}$ , the correlation co-efficient of the regression curve is 0.94. This result is illustrated that the spacing factor can be reflected indirectly through the number of air void, regardless of different mix proportions and execution on RC slab. In addition, the diameter less than 200  $\mu\text{m}$  is one of the significant factors to evaluate the distribution of air void and the spacing factor.
- Using PP fiber and wet-curing can improve the deicing salt scaling resistance of concrete surfaces. In addition, the curing methods of fiber concrete would be one of the significant factors to determine the surface scaling resistance of the concrete

under the severe environment. The dosage of EA has little influence on deicing salt scaling resistance of concrete.

- Air void distribution characteristics in hardened concrete is an extremely complex issue. Even though the same execution process, materials and chemical admixtures both on mock slab and actual slab, it is difficult to ensure a stability void distribution characteristics. Furthermore, the spacing factor fits better with the air void frequency in a linear condition regardless of the mock slab and actual slab. Void frequency is one of the significant factors for evaluating the spacing factor of concrete.
- The results of the NDT test in-situ show that the actual RC slab has fine compactness. However, it also can be noticed that the unevenness of concrete quality on the same RC bridge slab due to the micro-cracks of the concrete surface. Therefore, the issue of how to meet the requirement of concrete quality needs further consideration through the usage of the environmental condition after initial curing of concrete structures.

To sum up, the considerable results in this study can be provided by tasking the mock RC slab for the practical improvement of the actual RC slab, for instance, slump, the air content of fresh concrete, vibration time and admixture dosage. However, it is probably not enough to make a clear judgment on the stability of air void distribution of the actual RC slab by the mock RC slab, which the attribute of many important variables impact on the air void quality of concrete, such as pumping condition, temperature changes, handling and transporting. Although, the rise of target air content, the using PPF and the adequate wet curing period would be contributed to make durable concrete for deicing salt scaling resistance of concrete.

## CHAPTER 5

- The incorporation of SAP can effectively mitigate its autogenous shrinkage and the

length change value of the mortar with SAP is smaller than Ref until 49 d, regardless of with/without KEA. Moreover, the hybrid addition of SAP and KEA increase the initial expansion of the specimens as compared with the individual addition of KEA, which has a beneficial effect on compensating for the shrinkage of the mortar under drying conditions.

- The addition of SAP seems to be negative for relative shrinkage (equivalent to drying shrinkage), whereas, the addition of KEA seems to improve the adverse effects, in particular, when the SAP content is greater than or equal to 0.2%, the combined effect of SAP and KEA is more prominent. It is because KEA improves the early expansion of the mortar. In addition, the length change vs. mass change has a good linear correlation under the drying environment.
- The addition of SAP seems to delay cement hydration and increase the volume of macropores (greater than 100 nm), thereby reducing the compressive strength of the mortars. In contrast, the introduction of KEA slightly promoted the formation of micropores, resulting in a slight increase in compressive strength compared to the samples without KEA.
- The addition of SAP and KEA resulted in an increase in pore volume with pore diameter in the range of 0 - 100 nm at 28 d, especially for samples with KEA, and this result ultimately increased the drying shrinkage. However, for samples with KEA, in view of it promoting pore refinement so as to reduce moisture evaporation.
- From the regression analysis, the relation between macropore volume (pore diameter > 50 nm) vs. compressive strength follows a power function with a relatively high correlation regardless of SAP content and with/without KEA. Therefore, a pore volume greater than 50 nm can characterize the compressive strength regardless of the presence of SAP and KEA.
- For the concrete with pre-soaked SAP, due to the clustering of pre-soaked SAP in the fresh concrete, it is difficult to uniformly distribute in the concrete matrix, re-

sulting in the formation of larger pores in the hardened concrete. However, the existence of these larger pores did not adversely affect the compressive strength of concrete. In addition, when the surface of concrete was exposed for 63 days under drying conditions, the wet residue range of the concrete samples with pre-soaked SAP was larger than that of the concrete samples with dry SAP powder.

- For the length and mass change, the combined effect of SAP and KEA is beneficial to mitigate the autogenous shrinkage of concrete and delay the drying shrinkage, regardless of the incorporation methods of SAP. Moreover, SAP maintains the relative humidity inside the concrete by continuously releasing water, which causes an increase in the loss of concrete mass.
- The voids created by SAP and air-entraining agent have a negative impact on the compressive strength of concrete. The compressive strength decreases with the increase of SAP contents, regardless of the incorporation methods of SAP. In addition, when the SAP content is 0.3%, its compressive strength is greater than or close to the concrete samples with 5% air content.